

UNIVERSITÀ  
DEGLI STUDI  
DI PADOVA

UNIVERSITA' DEGLI STUDI DI PADOVA

Dipartimento di Ingegneria Industriale DII

Corso di Laurea Magistrale in Ingegneria dell'Energia Elettrica

# Development of a Bidirectional Charger for Electric Vehicles

**Relatore:**

Prof. Roberto Turri

**Correlatore:**

Prof. Ghanim Putrus, Northumbria University

**Candidato:**

Ridoy Das

Anno Accademico 2015/2016



# Index

## Summary

<b>1. Introduction</b>	<b>5</b>
<b>2. Overview of the current technologies for electric vehicles</b>	<b>10</b>
2.1 Current technologies	10
2.2 Smart Charging	11
2.2.1 Centralized Control	12
2.2.2 Decentralized Control	13
2.2.3 A brief comparison	15
2.3 Batteries for Electric Vehicles	15
<b>3. Economical and functional feasibility of a bidirectional charger</b>	<b>19</b>
3.1 Approach to the problem	19
3.2 Practical considerations	20
3.2.1 Economic considerations	21
3.3 Profitability of V2G	22
3.3.1 Frequency response	22
3.3.2 Reserve	23
3.3.3 Short Time Operating Reserve (STOR)	24
3.3.4 BM Start Up	24
3.3.5 Black start	24
3.3.6 Reactive Power	24
3.3.6.1 Obligatory reactive power service	24
3.3.6.2 Enhanced reactive power service	25
<b>4. Topology of the converters</b>	<b>26</b>
4.1 AC/DC Converter's scheme	26
4.1.1 Pulse Width Modulation	27
4.1.2 Bipolar and Unipolar PWM	30
4.1.3 Three-Phase converter	31
4.2 DC/DC converter	33
4.2.1 Buck converter	34
4.2.2 Boost converter	35
4.2.3 The chosen converter: a combination of both	36
4.3 LC filter and interfacing	36

<b>5. Control approach and Regulator</b>	<b>38</b>
5.1 Active and reactive power control	38
5.1.1 Drop Control	39
5.2 DC/DC Control	42
5.3 The practical approach	43
5.3.1 The system	44
5.3.2 System's parameters	45
5.4 PID controllers	45
5.4.1 P controller	46
5.4.2 PI controller	46
5.4.3 PD controller	47
<b>6. Simulink model</b>	<b>48</b>
6.1 The complete system	48
6.2 AC/DC Controller	52
6.2.1 PWM Generator	54
6.3 DC/DC Controller	57
<b>7. Simulations</b>	<b>60</b>
7.1 G2V Simulations	60
7.2 V2G Simulations	72
<b>8. Physical bidirectional charger</b>	<b>75</b>
8.1 The dSPACE platform	75
8.2 The Simulink model	76
8.3 The dSPACE layout	79
8.4 The physical system	80
8.4.1 The converter	83
8.4.2 The Driver circuit	83
8.4.3 DC Bus capacitor and DC filter	85
8.4.4 Other components	87
<b>9. Relevant tests</b>	<b>89</b>
9.1 Tests without a delay circuit and high resistance	89
9.2 Tests with a delay circuit	92
9.2.1 Test with high resistance	92
9.2.2 Test with low resistance	98
<b>10. Conclusions</b>	<b>100</b>

References

## Summary

Many years ago the electrification phenomenon had boosted the modernization of several countries. In some others this process is still going on, and in the modern world the electricity is essential for our lives. There is a tendency to bring any application that employs energy in the electrical context because this is a form of energy that is known and efficient. The same has been done with transportation nowadays and because of this, Electric Vehicles (EVs) have become popular. However, with the increasing deployment of EVs, the main issue that has arisen, is their management and big part of this is the uncontrolled charging problem.

When EVs are randomly deployed and charged, in the worst case all together, the lack of smartness in the EVSE (Electric Vehicle Supply Equipment) makes them a burden for the grid. Instability of the grid, local losses, congestion are among the consequences that this issue implies.

Some solutions have been proposed for this matter and they are the G2V and V2G technologies. In the G2V (Grid to Vehicle) approach the charger employs a unidirectional power flow between grid and vehicle that can be, in case, regulated according to the necessities. This technology can be implemented to decrease the stress for the grid in peak hours by asking less power instead of the maximum.

An improvement of the G2V technology is the V2G (Vehicle to Grid) approach that requires a bidirectional power flow between grid and vehicle. This concept includes the G2V operation and moreover allows the battery to discharge in favour of the grid, so that instead of acting as a simple load, the EV behaves as a local generator supplying the grid. An additional task is the PFC (Power factor Correction) which means, the charger is providing also reactive power along with the active power.

In this work a bidirectional charger that implements V2G has been designed as well as the control approach. By using a SPWM (Sinusoidal Pulse Width Modulation) technique, the charger has been controlled against variable references in Simulink. A physical charger has been built and interfaced with the model through the dSPACE platform and bidirectional power exchange has been proven.

# 1 Introduction

Transportation is among the sectors that allow huge variety of products and additional features in order to tailor the goods according to the tastes of the customers. However, nowadays the most useful and desired feature is the eco compatibility, where the internal combustion engines (ICEs) struggle to excel. This is why **Electric vehicles (EVs)** are becoming popular and their deployment is increasing day by day, but this makes us facing some major challenges. Initially the shifting towards a more eco-friendly transportation device led to **Hybrid Electric Vehicles (HEV)** that use for the propulsion a part of the energy coming from an ICE and the remaining from a battery that is on board. The battery allows bidirectional power flow whereas the ICE only unidirectional. The scheme of the power train is represented in *Fig1.1*. HEVs are more efficient than common thermal vehicles because the engine is cut off when the vehicle stops, the kinetic energy is recovered when breaking and the ICE is more efficiently used and all these result in a reduced fuel consumption. As can already be perceived, the battery in this case is charged and discharged by the internal system according to the external condition such as speed, required power, torque etc. This will be a differentiating factor compared to **PHEV (Plug-in Hybrid Electric Vehicle)** and **BEV (Battery Electric Vehicle)**.

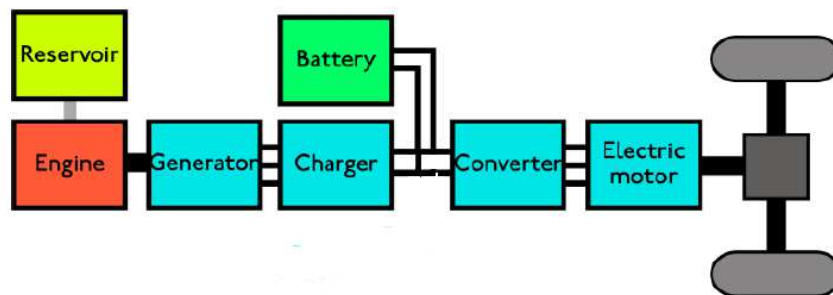


Figure 1.1 Schematic of the power train of a HEV [6]

With PHEVs the vehicle can be connected to an outlet in order to charge the battery. The latest upgrade form this technology is a completely electrified propulsion where the required energy is provided by a battery: BEVs. No ICE are required in this system, where the electric motors that move the wheels are supplied with a static energy supplier, which is usually a battery. This system allows a complete detachment from fossil fuels, hence fosters emission reduction by using only electricity without chemical reactions that produce residues. These are great achievements but require significant commitments both in terms of technological improvements and a social acceptance. The latter is becoming more and more consolidated because of the common will to prevent climate disasters. But as far as the technology aspect is considered, the deployment of this new form of transportation challenges us in new scopes.

Huge deployment of EVs means more energy asked to the grid, which results in an increase of electricity production if no other choice is available, and this is already a burden. An uncontrolled charging of EVs is even more dangerous because it creates serious instability in the grid due to an unbalance between production and demand. This causes frequency and voltage deviations, faults due to local congestions, losses, less efficiency of the grid etc. Since electric vehicles are mobile and unplanned loads, in the first instance there is an incapability to predict their demands, their location and all the consequences. EVs are equipped with on board slow chargers: chargers that allow to fill the battery with relatively small power rates and can be connected to domestic outlets. Usually these are connected during nights in residential areas or during office time in office car parks. Charging with these devices require hours and involve small power absorption, thus maybe for now, that EVs have just started to be deployed, these chargers don't represent a big deal but in the next future they will represent a serious threat to the stability of the grid because EVs are expected to be highly deployed, hence an increased energy demand from them is predicted. But this is not even the worst of the scenarios: in order to reduce the charging time Fast charging technology has been developed and usually it requires roughly half an hour. Yet it's not comparable with the fuel filling in ICE vehicle. The new technology provides energy in DC and high power. This means, these chargers absorb large powers from the grid in order to charge the batter quicker. Because EVs have to compete with ICE vehicles, charging has to be done with ease so these chargers are more and more installed in streets. They are used during daytime and can be placed in the car

parks of any shopping center. In these hours the electricity demand is at its highest point and if a bunch of street chargers start charging at the same time this could cause serious troubles in the local grid. Congestion, voltage drop and unbalances will occur and other local loads will also be affected. Though huge deployment of EVs is the key for an increased feasibility of smart systems, if no control is applied, it will cause serious problems to the grid. Currently the chargers that are made available, only charge the battery with an on-off system, supplying the maximum power and they are not equipped with any kind of “smartness”. If it was possible to modulate the power absorbed from the grid, and subsequently delivered to the EV, then it would have been possible to control the level of the loads that has to be applied to the grid in that moment. This is the kind of operation that **G2V (Grid to Vehicle)** technologies want to approach. First of all, it only requires a unidirectional power flow and limited information exchange. The power flow can be controlled according to references that are decided in accordance to control directives. With this system is possible, for instance, to decrease the power absorption when the grid is busy and this reduces losses, prevents congestions, increase the efficiencies of the transformers, prevents voltage distortion and voltage drop. It's understandable that in order to implement this technology a minimum level of information exchange between charger and the grid is required. For instance, a reference signal that communicates the voltage level at the nearest node can be used to identify whether it's convenient or not charging at the full power, and consequently calculate the power that has to be absorbed from the grid in order to optimize the operations in a local framework. Another reference signal could be represented by the electricity price of the nearest node that will tell if the power level has to be kept as high as it is or decreased, or in case if the absorption has to be stopped if the price is too high. This system can also help to buffer the intermittent generations of Renewable Energies (RE). For instance, if during the night the wind generation increases whereas the electricity demand is low as usual, the charging of EVs can be increased in order to consume that surplus of energy that won't be poured in the grid causing instability. With this much upgrades, already significant improvements can be obtained and one of the most important is that no new generation plant has to be installed in order to satisfy the extra power absorbed by the charging of EVs. This obviously has a cost, because an upgrade of the current chargers is required and an information link has to be installed; however, comparing pro and cons this doesn't represent a disadvantage because G2V doesn't require huge extra investments.

The upgrade of the G2V approach is the **V2G (Vehicle to Grid)** technology that allows bidirectional power flow between grid and EVs. With this approach a control over the level of power exchange and the direction of the power exchange is obtainable. In other words, the EV can behave both as a load or as a local generator. If considered convenient, while charging the battery, the smart charger can decide to reverse the power flow and sell power to the grid. Not only the price of the electricity at the nearest node has to be evaluated, but also other aspects like the nearest loads and generators, the congestion level, the voltage at the nearest node but most importantly the user's necessities. Since the EV is a vehicle before anything else, it has to serve the user first of all and then take care of other requirements. In order to implement V2G, different level of control are required that goes from smarter control to less smart control. **High level control** deals with a larger framework then a **low level control** whose ultimate goal is to ensure an efficient power exchange between the EV and the nearest node. The high level control has to consider the necessities of all the entities involved that are **the grid, the user and the battery**. The grid's necessities include a reasonable load level, low losses, no voltage or frequency deviation, no congestion, low harmonic level and an efficient distribution of the RE production. The user needs the EV to travel between a point A and a point B in a given time, therefore needs a minimum charge level for the battery within a prefixed charging time. Also the battery has requirements, such as low degradation, reasonable current rate and given charging-discharging cycles. **The Smart Charger** has to consider all these necessities and combine them in the most useful way by weighing them properly. This means, if for instance, the user needs a fast charging, this has to be privileged over the other necessities of the grid or the battery. Or if the battery has reached a high number of charging-discharging cycles, the current provided to charge the battery has to be adequately contained. Whether the grid is seriously busy, the absorbed power has to be reduced and if required, the power flow has to be reversed in order to supply the grid. An example of this kind of architecture is shown in *Fig1.2* where the controller considers inputs from different subjects and elaborates them in order to control the low level charger.

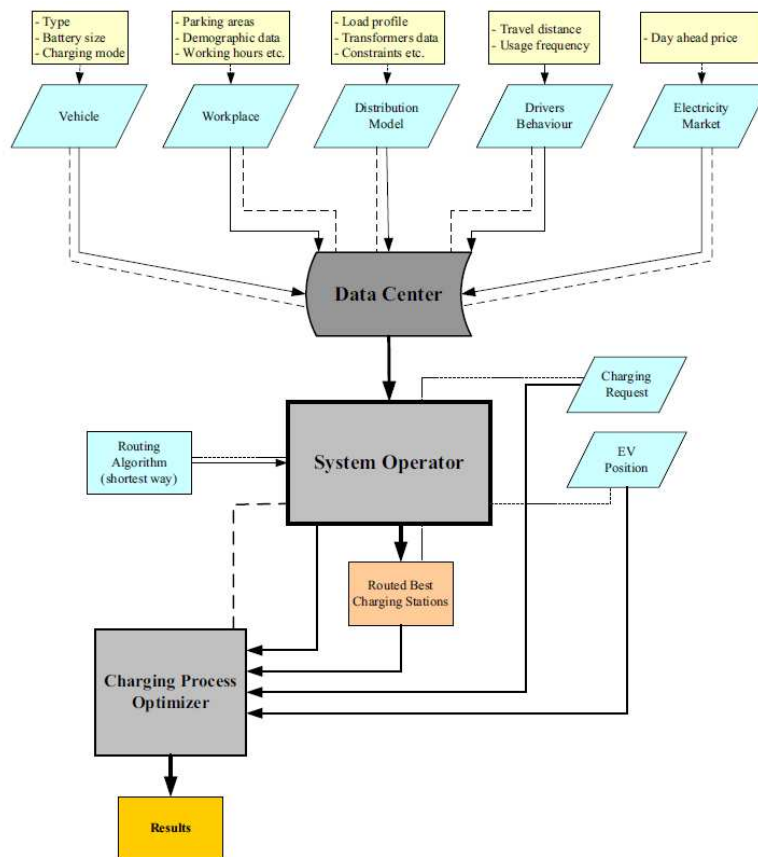


Figure 1.2 High level controller of V2G application [7]

In this controller several variables are considered from different actors: also the workplace has to be taken in consideration because it is different to charge in some place or others according to the local loads deployment. If the zone is characterized by a high electricity demand maybe due to offices, this has to be taken in account as well as the working hours that could be more or less busy in terms of congestion. The driver's behaviour represents a key factor in deciding the correct charging approach because of the fortuity regarding EVs movements. Being a mobile load implies advantages and disadvantages for the control: an advantage is represented by the possibility to have local and mobile generators that makes the process more flexible. A big disadvantage is the fortuity of their participation in the V2G regulation. One further optimization level can be considered by calculating the best route and the most convenient charging station, according to the EVs position and the local grid's condition. As can be seen the main technological challenge surges is the information exchange. High density information exchange is required in order to implement this architecture and because of this a dedicated network has to be built. The Fig1.2 shows that all the information is handled by a Data Center, so also the capacity of this center is a matter of concern. Local information has to be collected by these data centers and shared with elaborators of a higher level that decide the optimization process for a wider area, and the same up to the national level control. The whole control system is layered and every layer establishes an optimization process for that level. At the end, the total optimization is obtained by connecting the single optimizations and processing them for the sake of the whole system. The need of entities that collect and process the information are immediately perceived and these are called **Aggregators**. These external entities connect the EVs that are willing to participate to V2G in their zone, collect the information and do the optimization. They are also economical entities as well as technical entities. This is because the price of the electricity is involved and participating to V2G represents a cost both in term of battery degradation and vehicle engagement for a given time. The convenience to participate to V2G has to be carefully evaluated, calculating the cost of the battery wear and the user's necessities and comparing the result with the current electricity price in the market. If a real profit is perceived that it's profitable to participate to V2G. In the Fig 1.3 an example of the whole system including EV, grid, Aggregator and all the power and communication links is represented.



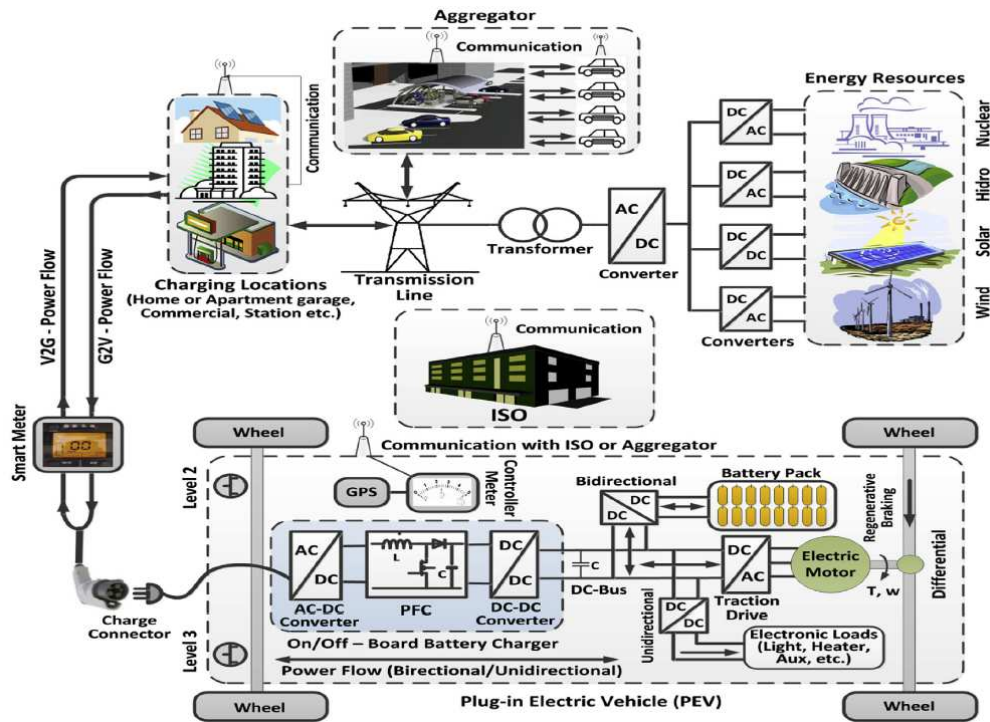


Figure 1.3 Whole electrical system for the power and information flow [8]

As said before, information plays an important role in V2G operation, in fact the EV is communicating with either the Aggregator or the system operator. In this figure the energy resources are represented as well, and specifically solar and wind generation, because their intermittent production can be buffered with the V2G system.

But not everything is convenient both in monetary terms and from the complications point of view. The immediately perceivable damage is done to the battery. In fact, V2G accelerates the battery wear because of the high number of charging-discharging cycles. Another important issue is the lack of privacy where Aggregators are handling all the information specially the driver's behaviour. The high level of intelligence that Aggregators need to have and that has to be installed on board represents another major hurdle for the implementation of V2G. The large information network that is required, a part from the existing network, needs huge investments. Something that is not a technical obstacle but is as serious, is the social acceptance. People have just started to appreciate EVs as a transportation tool but giving up the right to own the vehicle for the sake of the grid and hopefully a profit, even it is for a limited time, is something that will need time to be accepted. So despite the high potential benefits, V2G hasn't been practically employed, though several studies have been conducted on this matter.

In the initial part of this dissertation the state of art of V2G has been presented. The most innovative technologies in terms of smart charging approach, the control scheme and batteries have been explained. The meaning of smart charging, the required entities and the interaction between them have been considered. The role of aggregators that changes if the control is centralized or decentralized is analysed. A special focus on the current technologies in regards of batteries for EV concludes the second chapter: important parameters, types of batteries, models and costs have been studied.

In order to implement V2G some economical and practical considerations need to be done and this is what the third chapter aims to do. Since it has been perceived that V2G is not always profitable, a series of profitable applications for V2G focusing on the price payed and the costs and some practical considerations regarding the usage are done.

The topology of the charger is explained in the fourth chapter: the available topologies, the firing of the switches using the SPWM control, the harmonic content and over-modulation are studied. Relevant schemes for AC/DC and DC/DC converters and Unipolar and Bipolar SPWM are explained. The necessity and the composition of a DC filter are presented.

The fifth chapter explains the control of active and reactive power in three-phase systems and the drop control in single-phase systems. Moreover, the DC/DC control is explained as well as the selected approach. The system and its parameters, the controller and the different types of controller are also studied.

The sixth chapter presents the complete Simulink model that has been designed which consists of the AC/DC controller, PWM generator, DC/DC controller, grid model, battery model and the LC filter. The designing process of these components are also highlighted.

Simulations of the model against fixed references are undertaken in the seventh chapter. Initially the behaviour of the model against a fixed reference of active power with nil reactive power reference is simulated and improvements are done. The behaviour with a reactive power reference and a nil active power reference is simulated. The chasing of a variable power reference in both G2V and V2G operations are analysed and considerations are made.

The physical system is described along with the dSPACE platform. The Simulink model used to interface with dSPACE, the board and the workspace are shown and described. The physical system which consists of the AC/DC converter, the DC Bus capacitor, the LC filter, the battery, the single-phase transformer that supplies the system and the measuring instruments are presented in the eighth chapter.

Practical tests with no delay circuit and after with delay circuit and high or low resistance are done and the results presented in the ninth chapter.

Conclusions over the presented project and the future work are done.

## 2 Overview of the current technologies for electric vehicles

### 2.1 Current technologies

Despite the limited time that electric vehicles have been used for, they have received significant technological improvements such as better performing batteries, much more deployed infrastructure and better performance of the vehicles.

Initially let's define what an electric vehicle or otherwise called **Plug-in Electric vehicle** is: for the U.S. Department of Energy, it's a light vehicle that draws electricity from a battery with a capacity of at least 4kWh and is capable of being charged from an external source. The current commercial PEVs are listed below:

Model	Type	Battery capacity (kWh)	Electric range (EPA) (km)	Charge characteristics	
				Time (h)	Power (kW)
Mitsubishi iMiEV	BEV	16	100	7	3.1
Nissan Leaf	BEV	24	118	8	3.3
Tesla model S	BEV	60/85	335/425	8.5 <sup>a</sup>	11 <sup>a</sup>
Chevrolet volt	PHEV	16.5	61	3 <sup>b</sup>	3.3
Toyota Prius	PHEV	5.2	18	1.5	3.3
Ford fusion energy	PHEV	7.5	34	2.5	3.3

<sup>a</sup> For 85 kWh battery.

<sup>b</sup> Battery final state of charge limited.

Table 2.1 Current EVs and their specifications [9]

But for the charger there has always been a lack in “smartness” in the sense that EVs have always been considered as pure loads, and therefore sometimes burdens for the grid, and not as potential supportive generators. Aim of this chapter is to give an overview of the recent technologies available or not in the market for EVs (Electric Vehicle). We will also provide here after, examples of smart charging systems where this bidirectional charger could be used at their ultimate stage, where they interface with the vehicle. These systems consider different aspects and variables in order to optimize various processes but their common target is to reduce losses and costs. Depending on the complexity of the algorithms they can consider the user's necessities, the load level of the grid, the battery's status, the electricity price in the nearest node, losses, the most convenient route for the closest charging station and user's driving behaviour. All these variables are collected and carefully evaluated by a **Central control system** that gives them different priorities and formulates an **optimization algorithm** whose outcome is a charging pattern; this is **high level control**. According to this charging procedure, that is **low level control**, an appropriate converter is instructed to charge or discharge the battery. This means that there are two types of connection:

- the **power connections** transfers energy from the grid to the battery or vice versa;
- the **control and communication connections** collect information about those involved and provides commands to the active parts;

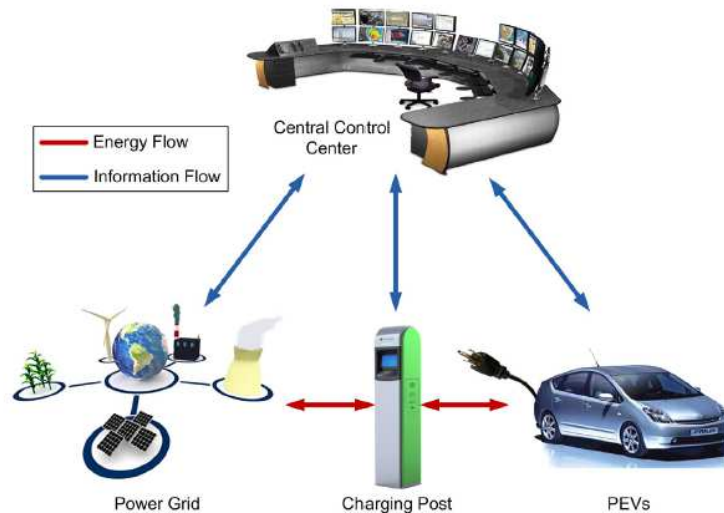


Figure 2.1 A general scheme for the control system and the relevant flows[14]

In the literature four types of charging method can be found:

- **Controlled charging;**
- **Un-controlled charging;**
- **Delayed charging;**
- **Off-peak charging.**

If uncontrolled charging is adopted, and therefore the charging starts as the car is connected, with large deployment of electric vehicles, the grid is put under serious stress. In fact, components of the grid like transformers and cables face high load that results in a decrease of the reliability. In order to prevent this issues, an intelligent scheduling of the charging process has to be done, which means that an appropriate amount of power has to be drawn from the grid with controlled charging. This will prevent congestion, decrease the losses, the cost of the electricity, the voltage deviation, the line current, increase the reliability, less impact on peak capacity, balance of the load profile, stability of the grid and at the same time it's possible to have high penetration of electric vehicles without violating any limit. However, there are drawbacks: in order to implement V2G services bidirectional power flow has to be available and communication between EVs and an independent central system operator is fundamental. The off-peak charging is a passive strategy and no control is required: this consists of charging the EVs during night because its economically profitable.

## 2.2 Smart Charging

Smart charging means that the charging profiles of EVs are controlled in order to obtain improvements for the user, for the grid or economic benefits. Algorithms used for these purposes can be programmed in order to pursue multiple objectives as the minimization of losses, reduction of the overall operative costs, minimization of the generation costs, elimination of transformer's and line's overloading, maximization of profit for the users and reduction of Green House Gasses (GHG) emissions. Essentially, smart charging levels the loads of EVs in order to meet these targets and therefore it applies **Demand Side Management** while the EV is charging; the so called **Grid to Vehicle (G2V)** mode. This requires just unidirectional power flow. An addition to the smart charging is the **Vehicle to Grid (V2G)** mode that implies the injection of power into the grid. In this mode EVs operate as reserve and distributed generators and given that they are parked 96% of the time, this is reasonable. They can perform frequency regulation, spinning reserve and load balancing by participating to the ancillary services market. Besides, they can be used for valley filling<sup>1</sup> and peak shaving<sup>2</sup>. In order to implement V2G there has to be an interfacing electronic converter that allows bidirectional power flow though this causes a rapid degradation of the battery; this is the principal drawback of V2G.

<sup>1</sup> Charging during the off-peak periods

<sup>2</sup> Discharging during peak periods

Power flow	Power level	Control	Cost	Effect on battery	Distribution system	Requirements and challenges	Benefits
Unidirectional Power Flow	Levels 1, 2 and 3	Easy. Active control of charging current. Time-sensitive energy-pricing helps to manage basic control.	Less price. Additional cost is not required	No discharging degradation	Update or investment is not Required. Many utility objectives can be met with high penetrations of PEVs	Requirement of power connection	<ul style="list-style-type: none"> <li>- Easy control and simple handling</li> <li>- Reactive power and dynamic adjustment of charge rate's services are provided, even without reversal.</li> <li>- simpler interconnection issues</li> <li>- Reactive power is supplied or absorbed, without discharging a battery, by means of current phase-angle control</li> <li>- Control of voltage and frequency</li> </ul>
Bidirectional Power Flow	Expected only for Level 2	Difficult. Extra drive control circuits. Extensive measures.	High price	High degradation of battery because of repeated cycling	Investment costs and updates are needed	<ul style="list-style-type: none"> <li>- Two-way power connection and communication</li> <li>- Appropriate smart metering/ sensors</li> <li>- Significant change of information</li> <li>- Cost and investment are higher</li> <li>- Losses of energy</li> <li>- Device stress</li> </ul>	<ul style="list-style-type: none"> <li>- Ancillary services</li> <li>- Support to renewable energy sources</li> <li>- Support to Reactive power</li> <li>- Valley filling</li> <li>- Regulation and stabilization of Active Power</li> <li>- Voltage regulation</li> <li>- Frequency regulation (down-up)</li> <li>- Spinning reserves</li> <li>- Load balancing</li> <li>- Power management</li> <li>- Filtering of current harmonic</li> </ul>

Table 2.2 Advantages and disadvantages of unidirectional and bidirectional power flow [8]

Let's now explore the idea of an **Aggregator**: it's a body that binds more EVs making them interact with the other actors of an electric system like they were a single entity. This allows better technical management and much more visibility in the electricity market. The flexibility and control capability of aggregators depends roughly on the number of EVs that are under their control. More in detail it depends on the initial and final charge level and the charging time. Thus, aggregators are technical and more importantly economic characters that allow better organization of EV fleets.

There are two ways of smart charging: **centralized control** and **decentralized control**. The function of the aggregator, the information exchange intensity and the whole architecture varies according to the kind of control.

### 2.2.1 Centralized control

The aggregator directly controls all the EVs in its area which means that it provides them all the charging/discharging schedules and takes care about all charging phases. Besides, the aggregator bids in the electricity market. In order to do that it has to forecast the demand<sup>3</sup> of each EV daily, and once the demand profile of the fleet has been forecasted it's communicated to the Distribution System Operator (DSO). The DSO will check if there is any violation of limits regarding the load level of transformers and lines or other safety requirements and in case will request changes in the demand profile before approving it. Once the schedule has been approved the aggregator bids and buys the electricity from the market. The aggregator can also participate to the ancillary service market: the EVs of a fleet can carry out the secondary or tertiary frequency regulation. When an abnormal behaviour of the grid occurs the DSO requests the aggregator for regulation and charging/discharging schedules of EVs are modified according to the necessities. Whenever the aggregator is participating in a regulation of this kind it expects a payment from the DSO.

It's clear that in order to apply this kind of control an intense information exchange between EV/aggregator and aggregator/DSO is vital and hence databases have to be used: data like EV's ID, Charging Point's (CP) ID, state of charge of the batteries (SOC) and user's necessities are exchanged. The aggregators will provide the **set-points** to their respective CPs according to algorithms whose aim is to optimize different targets. After that, CPs will control

<sup>3</sup> By historical data, user's preferences etc.

their chargers establishing the desired power-flow. In this exact point our work is required, because the proposed charger will implement the set-points that have been imposed and charge/discharge the battery.

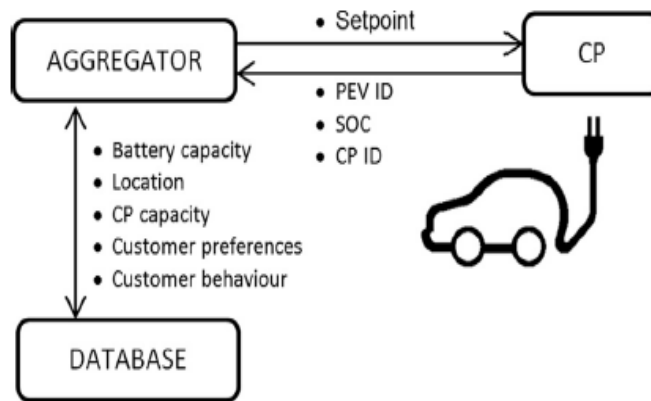


Figure 2.2 Data exchanged in Centralized control [9]

Algorithms that are appointed to optimize different objectives can be found in the literature: maximizing aggregator profit, reducing costs for users, limit grid impacts, minimizing generation costs, improving overall system costs, avoiding transformers and lines overload and improve voltage profiles.

One of these algorithms periodically computes load flows and checks whether the operating conditions are safe. In case it notices any anomaly like a deviation of a node voltage or an overload of a transformer stops the charging of some EVs by putting them in a waiting list and if allowed by the DSO further, the charging of these EVs restart.

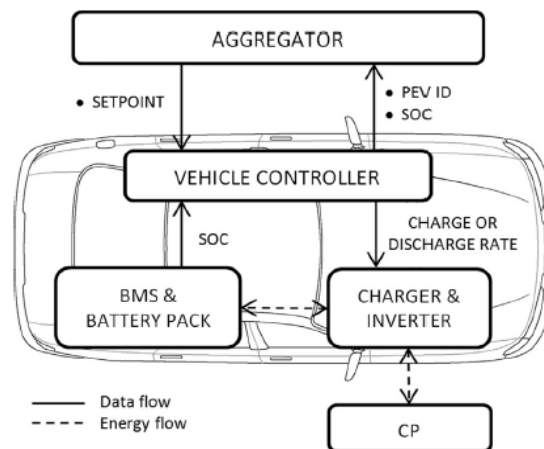


Figure 2.3 Architecture and information exchanges in Centralized control [9]

If we want to implement real time solutions, fast computing algorithms are required even though by increasing the penetration rate of EVs and the accuracy of these programs, the processes become slower. A major drawback of the centralized control is the conflict with the user's preferences: because low voltage grids are characterised by low X/R ratio, voltage regulations is influenced only by active power control. The coordinated voltage control requires time and might delay the charging procedure. In this architecture the aggregators handle a huge amount of data and as the penetration ratio of EVs increases it becomes harder controlling this information and it requires expensive communication system. Not only that, to prevent a system failure a back-up system is necessary for the safe operation.

### 2.2.2 Decentralized control

In this architecture the decision-making capability belongs to each EV owner rather than an external aggregator and thus the EVs need to be smart. Anyway, aggregators can influence the decision of EV owners regarding the

charging/discharging schedules by providing them prices or control signals and from there each EV tries to optimize their own charging cost keeping in mind the user's necessities and without communicating private information to aggregators. It's easy to understand that because the intelligence is singular and not shared this will try to look at its own interest and hence the aim of most of the algorithms is to minimize the charging costs. As an example, a solution that tries to minimize the charging cost of single vehicles in a building and the load variance is presented. Each vehicle receives information regarding the total load of the building and individually optimizes the charging profile in order to pay the least. The individual profiles are sent to the building controller that calculates the total load profile of the building and transmits it to a higher entity.

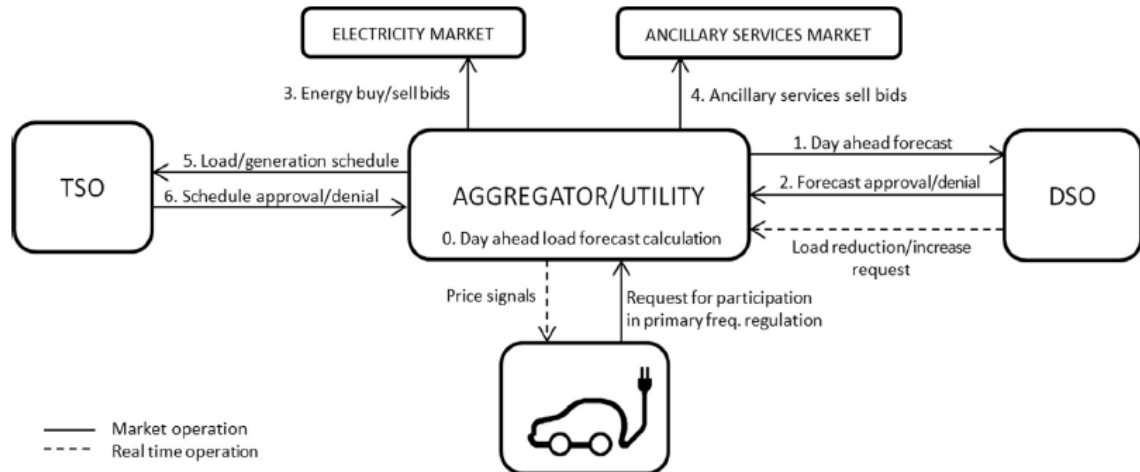


Figure 2.4 Architecture and information exchanges of the Decentralized control [9]

Being aimed only at the minimization of costs through price signals makes these algorithms insensitive to other issues like losses, congestions and voltage deviations. Thus, the DSO has to change the set-points given to the EVs in order to fix these issues; the price signals will also consider these aspects. Secondary and tertiary frequency regulation are impractical due to the lack of a central system to schedule the charging/discharging patterns. The primary frequency regulation is rather approachable through droop control method. In these schemes there is a dead-band in order to prevent frequent battery degradation. Whenever the frequency exceeds the limits of this dead-band the controller acts to take back the frequency in its normal region. If frequency is decreasing, then initially the battery charging will be reduced but whether it's not enough the battery will start supplying the grid. If frequency is increasing the controller will drain more power from the grid to charge the battery. A drawback that is immediately noticeable is the dependency of the gains of the droop controllers on the number of EVs participating to the procedure. These gains need to be changed according to the variations of the number of regulating vehicles.

A common method for the decentralized architecture is the **multi-agent system (MAS)**: this is a set of two or more intelligent entities, agents, that interact in an environment. In literature it can be found that an agent is a virtual or physical entity located in an environment that is able to react autonomously to the changes in that environment. Here, each EV has its own agent which will have different targets, like charging at the minimum cost or to have a minimum SOC available even if it's expensive. Usually there are two level of algorithm: the local algorithm aims to minimize the costs whereas the second algorithm has to avoid avalanche due to sudden increase on charging or discharging caused by low/high prices. This can be solved with a feedback signal of the transformer load. Within this architecture is possible to perform decentralized voltage control and an example is proposed here after: each EV sends their charging profile to the aggregator that calculates the nodal voltages for every node. This information is sent back to the EVs and then they try to minimize their objective function which can either be the minimization of all pilot nodes or minimization of only pilot nodes of its neighbourhood.

Given that EVs are moving, the computing capacity and the intelligence that is required for the decentralized control has to be movable along with the vehicle as well. Computing power, knowledge and intelligence have to be on-board of EVs. A possibility is to adopt a mobile agent concept: the agent that contains all the required information and intelligence regarding an EV migrates from one charging post to another whenever the related

EV plugs in. Once the EV is connected a message is sent to the aggregator that connects with the stationary agent which is cloned and migrated to the new CP. When the charging/discharging process is completed the agent goes back to the stationary CP and reports all the data.

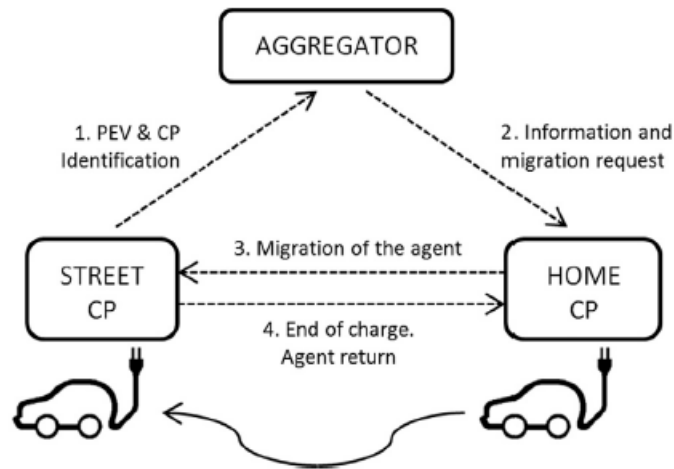


Figure 2.5 Multi-Agent system and migration [9]

### 2.2.3 A brief comparison

Both of these architectures have advantages and drawbacks and depending on the priorities, one among them is better than the other. Generally speaking, optimization in centralized control is easier due to the availability of all required information but, in turn the huge amount of data is difficult to handle and most of the time some information are unknown in advance; this will affect the optimization. In the decentralized scheme the decisions of EVs can be influenced by price signals or control signals but because it's the EV who takes the final decision there is uncertainty and there might be the avalanche phenomenon. As already said, in the centralized architecture all the information is collected and processed from a central entity and hence it implies large databases and high computational power; on the other hand, the decentralized solution doesn't face these issues but an intelligence has to be present on board of each EV. Since the information are locally elaborated in the decentralized scheme, privacy is guaranteed as opposed to the centralized architecture. If new EVs are willing to participate to the control, this will slightly change the centralized scheme while the decentralized control won't be affected at all, due to its high modularity. If a fault occurs in the centralized control, in order to ensure the correct operation there has to be a back-up system.

## 2.3 Batteries for Electric Vehicles

It's obvious that the most important and essential part of an electric vehicle is the battery, thus, if the battery is performant and efficiently charged then the whole vehicle will be efficient. This is why so much concern and a continuous need of improvements for this topic. The life cycle of batteries consists of seven steps: component production, cell production, module production, building of battery packs by assembling the modules and including an electronic control system and a cooling system, integration with the vehicle, use of the battery as long as the vehicle is operating and finally re-use and recycling. The most competitive and efficient batteries nowadays are the **Lithium-ion**; they have high efficiency (85-95%), high energy density and high number of life cycles (3000-5000). In this family there are variations: the most important in terms of automotive use are lithium-nickel-cobalt-aluminum (NCA), lithium-nickel-manganese-cobalt (NMC), lithium-manganese-spinel (LMO), lithium titanate (LTO) and lithium-iron phosphate (LFP). In order to ensure good life span, a correct release of energy and prevent thermal runaway these batteries need to be carefully monitored, cooled and balanced. In order to figure out which one is the most appropriate technology for automotive use they have to be compare along six parameters: **safety**, **life span** (in terms of charging/discharging cycles and the whole life), **performances** (peak



power at low temperature, SOC, thermal behaviour), **specific energy** (energy stored/kg), **specific power** (power stored/kg) and **cost**.

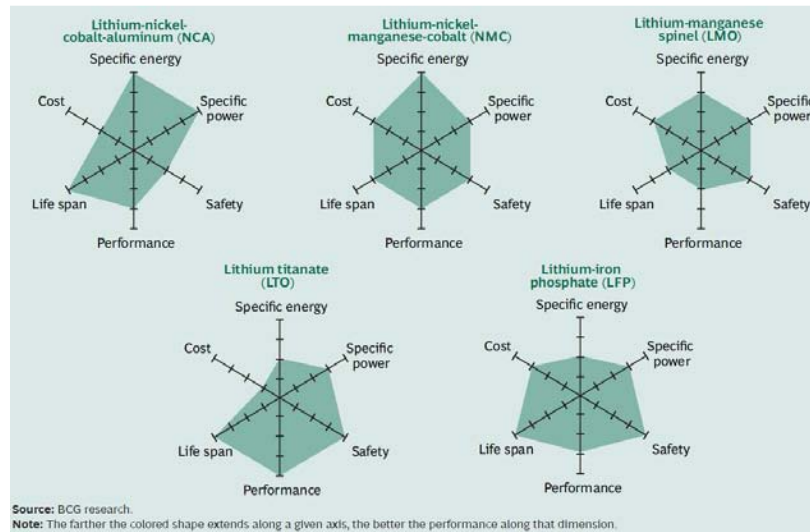


Figure 2.6 Characteristics comparison among different types of battery [10]

None of the chemistries presented dominates over all the six dimension, hence, favouring one feature will penalize the others. For instance, NCA is highly performing in terms of specific energy and power but is the least safe, on the other hand LTOs and LFPs are the safest but struggle in terms of specific energy.

As far as safety is concerned, the main challenge is to avoid thermal runaway, that is a positive feedback loop where chemical reactions happening in the cells exacerbate heat release causing a fire. This is mainly due to a short-circuit, overcharged battery or a high discharge rate. To prevent thermal runaway strict safety measures like a performant cooling system, SOC monitoring system, cell discharge balancing need to be undertaken.

Life cycle is calculated either in number on full charging/discharging cycles before the battery degrades at 80% of its nominal capacity at full charge or the overall age that the battery is useful for. Point to be noted is that, aging is accelerated by high ambient temperature. A common life span of electric vehicle's batteries is ten years and producers tend to install larger batteries then required so that after ten years of degradation, the battery still has enough energy to run the vehicle.

Performances have to guaranteed in either high and low temperatures though performance degradation occurs when a wide range of temperatures is expected.

Specific energy and power of current batteries are still much low then those of gasoline, thus the driving range will continue to be limited to 250-300 km between charges in the near future.

One of the major issues for EVs is the charging time. Currently it takes ten hours to charge a battery of 15 kWh with a standard 120V outlet. Huge improvements in this sector are expected, like the fast charging with a 240V outlet with much more power, 40A, which is going to take two hours or three phase commercial charging stations that takes just 20 min. Extra safety measures like improved cooling systems need to be accounted which means extra cost for the manufacturers. An innovative method is the battery swapping that can charge the whole capacity in less than three minutes but it implies high standardization and serious logistic complexity.

The ultimate parameter that will make a user chose an EV over an Internal Combustion Engine Vehicle (ICEV) is the cost. The biggest part of the cost of an EV is represented by its battery, therefore, improvements of battery costs means great reductions of EVs cost. Nowadays Tesla models have a battery pack cost of 260\$/kWh; the costs have fallen significantly in the past few years and are expected to fall further reaching 100\$/kWh. This means that very soon EVs will be competitive in terms of price with common vehicles.

In order to work with the battery without harming its health the charging/discharging process has to be carefully controlled and monitored. For this purpose, clever charging/discharging patterns have been developed like the

Constant Current (CC)/ Constant Voltage (CC) etc. However, these solutions focus only on how to regulate the power flow without any information of the battery whereas it's the ultimate knowledge that allows a correct operation. For instance, with a weak battery, that means either with low charge or with many charging/discharging cycles, it's better charging with small currents because otherwise it will result in an increase of the internal resistance and a decrease of the usable capacity. Another important factor is the temperature that accelerates battery aging. All these parameters have to be considered by the high level controller which is the one that considers the necessities of all the parts involved and gives them priorities. Therefore, there has to be another device that calculates and provides these parameters to the controller: the **Battery Management System (BMS)**. Then, let's define these parameters:

- **State Of Health (SOH)**, represents the general health of the battery and its capacity compared to a new battery; it's the difference between the usable capacity and the capacity at the end of life (80% of the rated capacity);  $SOH=100\%-80\%-f(\text{cycle})$ ; the usable capacity of the new battery is 100%,  $0\% \leq SOH \leq 20\%$  and the SOH depends and varies according to a function of the charging/discharging cycle;
- **State Of Charge (SOC)**, is the percentage of the maximum usable capacity of the battery;  $SOC = \frac{\int i dt}{C_{usable}}$  where  $C_{usable}$  is defined in Ampere hours and is the maximum usable capacity;  $0 \leq SOC \leq 1$ ;
- **Charging current rate ( $C_{rate}$ )**,  $C_{rate} = \frac{\Delta SOC}{T_{plugged}} = \frac{SOC_{final} - SOC_{remain}}{T_{plugged}}$ ;  $\frac{1}{8}C \leq C \leq 1C$ .

The internal chemical processes of a battery are really complicated and impractical if we want to work in a controlled system. Therefore, usually a battery model that represents its behaviour is considered and simplified as possible. From previous studies the following battery model is presented:

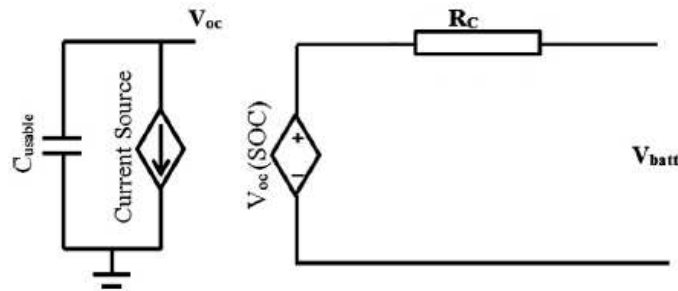


Figure 2.7 Battery equivalent model [2]

The open voltage of the cell OCV, is a function of the SOC as can be seen, and it's obtained experimentally whereas  $R_c$  represents the resistive loss due to both the internal resistance and the polarization voltage drop.  $V_{batt} = V_{OC} \pm iR_c$ .

The resistive factor is influenced by SOC, charging/discharging current and temperature. However, the effect of current is small and if a temperature control is adopted, the temperature's effect can be neglected as well, hence only SOC is considered influencing  $R_c$ .

$$R_c = R_1 + R_2 = 0.006 + 0.01378 + 0.000023 SOC^{-2.517};$$

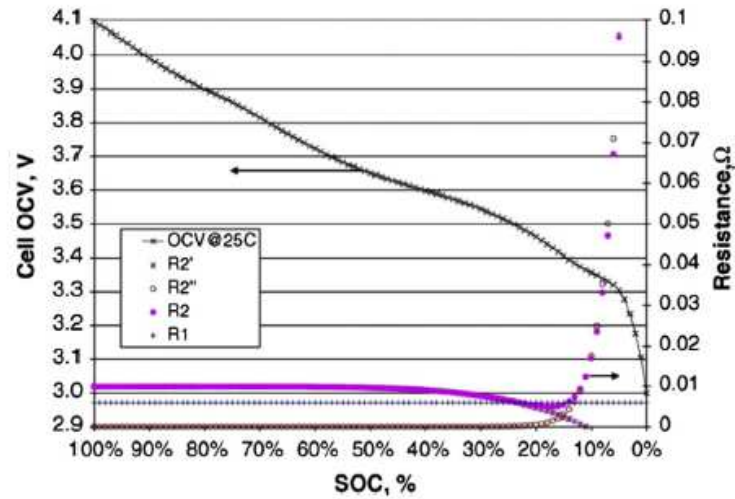


Figure 2.7 Cell voltage and internal resistances of the battery [2]

A battery pack for an EV consists of modules connected and assembled together; the modules are obtained by connecting in series or in parallel several battery cells. The parameters of a pack are therefore:

$$C_{pack} = N_p N_s C_{cell}; \quad (2.1)$$

$$V_{pack} = N_s V_{cell}; \quad (2.2)$$

$$R_{pack} = \frac{N_s R_{cell}}{N_p}; \quad (2.3)$$

High SOC, temperature, Depth of Discharge (DOD) and current rates accelerate the degradation of the battery: the internal resistance increases and the usable capacity decreases. For an operation with low degradation, as far as the temperature is concerned, working at 20° ensures the best results. Since the other factors need to be minimized, the controller, once has received this information from the BMS, has to consider the route that the user is going to travel and calculate the minimum SOC required for the journey. Moreover, by knowing the time that the EV is going to be plugged for, it will compute, according also to the current situation of the grid, the available time and decide the minimum current rate. If the grid needs support, then according to the seriousness of the demand it will compute the minimum DOD for the discharging. Otherwise, with high charging rate, SOC and DOD degradation occurs and the voltage is notched as can be seen from the following image.

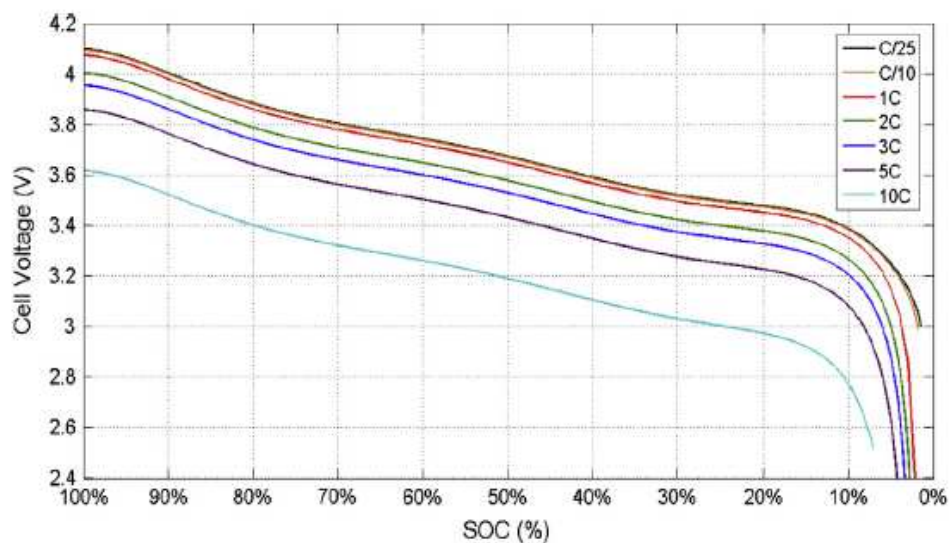


Figure 2.8 Cell voltage for different SOC and C rates [2]

## 3 Economical and functional feasibility

### 3.1 Approach to the problem

When it comes to consider whether the *electrical vehicles*(EV) might be a promising step for our next, green future the chargers of these EVs have an important role in order to make the decision. With the latest huge deployment of EVs it's becoming more clear that this will be a big option for implementing environmental friendly policies.

But like any other technology that is not industrially-ready, it has to be verified if it is also economically feasible. We know that EVs, specially *Battery Electrical Vehicles*(BEV) have low almost nil operational cost. But this is only if we don't consider the battery degradation cost, that in this kind of application is extremely usual because it's a direct consequence of the charging and discharging cycle. Considering also that the biggest part of the vehicle's cost is due to the battery, this makes not convenient the usage of EVs as a support for the grid because it will require frequent charging and discharging. However, nowadays safe charging-discharging modes have been experimented and proven successful. We are talking about the *Constant Current Mode*(CC), *Constant Voltage Mode*(CV), *Constant Power Mode*(CP) and the *Trickle Current Charging Mode* which is used to maintain the battery fully charged without any risk to harm its health, due to overcharging. Thanks to these charging modes the battery degradation has become more acceptable and controllable.

What we'll consider in this report is whether the adoption of EVs to support the grid is economically and practically convenient for the users. Let's start saying that there are two ways to provide support for the grid with an EV.

The first is the ***Grid to Vehicle(G2V)*** technology that means, there is a unidirectional connection between the EV and the grid and not so much communication and intelligence is involved. Anyway, also in this mode is possible to support the grid by charging the battery when the grid is relatively free or in rest and not charging when it is under stress. What we need in order to decide whether it's convenient or not charging the battery in a certain moment is a ***reference signal*** that lets us know how busy the grid is. It could be the grid frequency like they use to do in primary frequency regulation; in a highly inductive connection the active power exchange depends on the load angle between the grid voltage phasor and the charger's voltage phasor which depends in turn on the frequency. Or it could be the electricity market price; when the price is high it's better not charging the EV, whereas when the price is low we can charge the battery. By charging in the low-demand hours is also possible to support those plants that can't stop the production during the night, when the electricity demand is low, because of their high inertia and because it would cause damages to the machines, like in thermal power plants. Moreover, by increasing the magnitude of the charger's voltage it is possible to provide reactive power to the grid thanks to the DC BUS capacitor. This is due to the relationship between the magnitude of the voltage drop, at the terminals of the grid-charger connecting inductance and the reactive power in a highly inductive link. This is the easiest way to support the grid and also the cheapest due to little communication between grid and charger. However, this mode doesn't allow to provide active power to the grid as much as we need, because a significant part of the apparent power is engaged by the reactive power, so the EV can't act as rotatory reserve.

Another mode is the ***Vehicle to Home(V2H)***; this one is used if there are smart houses where along with the electric loads there are also photovoltaic(PV) panels to produce energy and a park of EVs. Whenever needed the available EVs could satisfy the electricity demand of a part of the loads if the PV panels are not working.

***Vehicle to Vehicle(V2V)*** allows the power exchange between EVs in order to charge those vehicles that have to leave earlier by discharging those that can stay for longer. These two modes need more communication between the vehicles or vehicle and home but the infrastructure required to implement them is still not massive.

The last and more effective mode is the ***Vehicle to Grid(V2G)***. With this mode there is the full power exchange capability between charger and battery. It means that if the charger considers convenient discharging part of

the capacity to support the grid then it can do so. Hence, a bidirectional link is required but that's not all. A big number of measurements are also necessary like the grid voltage, the current coming towards the charger, the battery's voltage and current. Because of these measurements and others like the reference signal and the huge amount of communication the infrastructure required is massive and this obviously has a cost. In V2G the EV can participate to a lot of ancillary services: frequency regulation, reserve, black start, reactive power etc. We will try to understand which are economically and practically convenient further on. But because it can be a potential alternative to new reserve and because of its proven benefits to the grid we'll consider and investigate on the V2G mode in this work.

There are 4 charging levels according to IEC 61851:

- **Level 1**; *slow charging* from a *house-hold type socket-outlet* in AC; the charger is passive with no control, the voltage is 230/400 and the current doesn't have to exceed 16A;
- **Level 2**; *slow charging* from a *house-hold type socket-outlet* with an *in-cable protection* device in AC; it's again a passive connection but ensures earth protection, residual current, overcurrent protection etc. and the voltage is 230/400 with the current not exceeding 32A;
- **Level 3**; *slow or fast charging* using a *specific EV socket-outlet* with *control* and *protection* function installed in AC; the connection can be active with proper communication pins, it provides earth protection and the voltage is 230/400 whereas the current doesn't have to exceed 250A;
- **Level 4**; *fast charging* using an *external charger* in DC; it can be divided in two sublevels:
  - **level 1** where the  $V < 500V$ ,  $I < 80A$  and  $P_{max} = 40kW$ ;
  - **level 2** where the  $V < 500V$ ,  $I < 80A$  and  $P_{max} = 100kW$ .

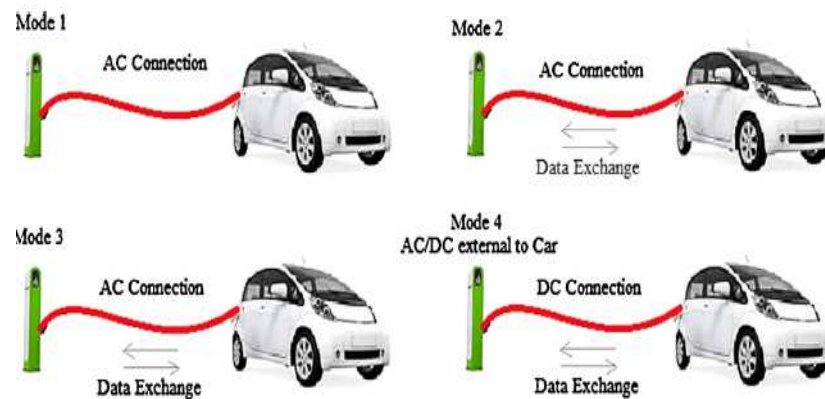


Figure 3.1 Different charging levels and types of connections [11]

Usually in the first three levels the charger is inboard while in the fourth level the charger is off board. This is due to the rating of the charger: in the first three levels the power exchanged with the EV is relatively small whereas in the DC charging mode, since it does first charging, the power exchanged is bigger and therefore it's safer and space-friendly having an external charger. The fourth level of IEC 61851 follows the guidelines of the **CHAdEMO** protocol: it's a fast charging method for BEVs which delivers up to 62.5 kW and takes maximum a half an hour to fully charge a low-range EV. The maximum recognized voltage is 500V and the maximum current is 125A. These chargers are supposed to use the JARI DC fast charge connector.

Also the places where this charger might be located are different: slow chargers are likely to be located in residential areas because of their small power rating while fast chargers are usually located in public places.

### 3.2 Practical considerations

In order to build the charger, we need to choose one between this two families and to do so we need to do further considerations. What we need to consider is an *economical and practical feasibility study*.

Installing chargers at home requires less infrastructure for the mass deployment of electric mobility whereas installing a big amount of fast chargers in the streets needs big investments. This is because nowadays there are already a lot of smart-houses with an EV charger annexed. On the other hand, still today a fast charger is rare.

Our aim is to support the grid effectively so in order to bring significant variations to the grid we need to supply or absorb big amounts of power. So if we want to be “seen” from the grid the number of chargers, and consequently EVs, interacting with the grid is really important. In case of slow chargers, big number of EVs are required to give enough support to the grid but since fast chargers involve bigger powers there could be less of them. It’s clear that in order to cause great impact on the grid it’s necessary to have a big number of EVs charging/discharging at the same time. Therefore we need EV parking systems in public places or private places like big residential buildings. Fast charging is required mostly during the day whereas slow charging is required during the night. Due to these different approaches their function towards the grid is different. During the day, the grid needs to be protected from overloads and from frequency deviations. During the night the basic need for the grid is the distribution of excess energy due to renewable energies production. From this point of view fast chargers could do V2G during the day when necessary while slow chargers could do G2V control during the night.

### 3.2.1 Economic considerations

Installing fast chargers would mean new infrastructure installation and hence big investments are required. In order to recover the investment, the investors need a guaranteed revenue so we need to setup a return plan. To do that we need to know how many EVs are going to participate to V2G at a well-known time. So there is the need to stipulate contracts with EV owners in order to guarantee a minimum threshold. But that’s not all: an EV owner is willing to participate to V2G only if receives a sufficient revenue from it. What decides if V2G will have good revenues is the electricity price in the market, but it’s volatile. In order to archive great returns the “*fleet manager*” has to bid in the electricity market. So there is the need of this external individual who runs the EV fleet and try to seek revenues for the EV owners and for itself to justify its existence. In spite of all these efforts to group a big number of EVs to archive the minimum unit of measure of 1MW, the amount of power that can be supplied would not be competitive against big/medium producers because of the high production cost. All these considerations suggest to start **local actions**. However, the **Aggregators** could participate to ancillary services which will be explained later.

What is the marginal cost for an Aggregator? What is the cost of producing one more kW? It’s really high if we consider that, given an amount on EVs parked at a certain time it’s hard to know if any other EV is coming. On the other hand, it’s sure that EVs will get back home or will leave home so the availability of a residential charger is more predictable. Anyway, this hurdle could be overcome by stipulating contracts with EV owners as said before and also by statistic data from the past. The latter will require years because this system hasn’t been developed yet.

It’s better considering an EV fleet more like a given amount of power that can be switched on if necessary but can’t produce more. Again this suggests to take part to ancillary services. Stored energy in idle vehicle could be used to quickly replace a loss of supply in the short term: fault. From this point of view fast chargers are more useful because they provide a big amount of energy in short time.

Another thing we need to consider is that, fast charging takes approximately half an hour whereas slow charging takes several hours, so different time scale. They should be assigned to different duties in term of grid support. As said before fast chargers could be fast reserve and slow chargers could be used as long time reserve. Moreover, in fast chargers the discharge will be deep but rare while in slow chargers the discharge will be shallow but frequent. Further investigations on batteries characteristics need to be done to know which is less harmful for the battery’s health. From now we can say deep discharges are more harmful.

We have seen that this mechanism won’t be competitive in the electricity market against medium/big producers. This is why it has to be *subsidised* by, for instance a **capacity payment**. So, there has to be a **smart meter** to ensure effective communication between vehicle and grid and these devices are common in smart houses nowadays so slow chargers won’t require further investments. From the final use point of view, the amount of power supplied from an EV is large in term of household demand but its small compared with the demand of the grid. Again, this points out the value of local power exchanges rather than long-distance exchanges which would also cause losses.

If V2G is available only during the night, then it’s not useful since there are conventional generators which can provide the required energy. Then G2V could be done by recharging the EVs during off-peak time. Or V2G could be done during office time when EVs are parked in a certain company’s parking.

Now some considerations on the  $feasibility = \frac{n^{\circ} \text{ of } BEV}{n^{\circ} \text{ of } vehicles}$ : (3.1)

More charging locations implies more operational cost reduction but not the infrastructure cost reduction. For Plug-in Hybrid electrical vehicles (PHEV) this will mean more gasoline reduction and hence lower cost so more feasibility. Either larger capacity batteries or higher power charging is necessary to increase feasibility. However, we should consider that most of the non-home charging infrastructure isn't used, because it's demonstrated that most of the time EVs are charged either at home or at work, though it's necessary to increase the feasibility. Since this involves a cost factor we should rather know that home charging alone can meet the needs of most drivers given that for long range EVs the chargers in the street become poorly utilized. From the infrastructural point of view, a study demonstrates that in order to minimize the cost the *Electric Vehicle Supply Equipments*(EVSE) should be placed for the 80% at home and 9.6% at work. It all depends on the deployment of these EVs since if they aren't sufficiently deployed more non-home EVSE are required.

Going back to the choice between home chargers and street chargers, EV charging increases the amount of power flow and cause system losses. Supplying EV loads with nearby distributed generation and V2G are among the possible approaches to lower the system losses. Again, local actions are suggested. EV charging causes also phase unbalance; by using an appropriate load managing system, such as distributing the EV loads evenly across all the three phases or using three phase chargers, we can prevent this problem. This seems to favour street chargers because usually they are three phase for the relatively huge amount of power drained. But studies show that EV's fast charging injects significant harmonics into the power grid.

The considerations done so far doesn't seem to favour significantly one type or the other because both have their advantages and disadvantages. What has been put clear is that local actions should be favoured rather than long-distance exchanges, there is a need of an aggregator in order to deal with the grid and that there has to be a subsidy system to be sufficiently competitive. Our aim is to prove the concept that an EV provided with a bidirectional smart charger can be a support for the grid since it can supply active power when necessary and meanwhile exchange reactive power to do power factor correction. In order to archive our purpose both the chargers are valid because both are able to do V2G, and the design we'll do can be adapted to both. In this case to prove the concept we'll develop a single phase charger in laboratory and we'll verify the power exchanges with the "grid" and the proper control system.

### 3.3 Profitability of V2G

What we need to do now is to consider the ancillary services that our charger can participate to and to evaluate the economic revenue that an EV owner can expect. There are a lot of ancillary services required from the National Grid among which we have **Frequency response, Reserve, Black Start** and **Reactive power**.

#### 3.3.1 Frequency response

**Mandatory frequency response** means that the appointed generator must automatically change the active power output in response to a frequency change. This service has to be provided by all the generators connected to the transmission system. The statutory frequency limit is 49.5-50.5 Hz and the operational limit is 49.8-50.2Hz. This service is divided in **Primary Response, Secondary Response and High Frequency Response**; Primary Response needs the provision of extra active power or a decrease in demand in 10s after requested and for a further 20s. The Secondary Response needs the active power in 30s and for a further 30 minutes whereas the High Frequency Response needs the provision in 10s and for indefinite time. Obviously EVs can't participate to the latter. The technical requirements for the participation are the following:

- necessity to maintain a minimum level of active power in the range 47-50.5Hz;
- stable frequency control in the range 47-52Hz;
- ability to control the frequency on an islanded network to below 52Hz;
- capable of a frequency drop between 3-5%;
- necessity to frequency control in a target set in the range 49.9-50.1Hz;
- frequency control dead band of less than  $\pm 0.015\text{Hz}$ ;
- necessity to deliver a minimum level of frequency response.

A delay of maximum 2 seconds before measurable response is seen from a generating unit in response to a frequency deviation is accepted.

There are two operating modes:

- **Limited Frequency Sensitive Mode** where if the frequency is below 50Hz generator has to maintain power output and whether above 50.4Hz it has to reduce the output by a minimum of 2% for every 0.1Hz rise. If the output goes below the Designed Minimum Operating Level, then the park has to be disconnected;
- **Frequency Sensitive Mode** where the generators have to respond to any frequency change by adjusting the output. Above 50.5Hz the limits are the same of Limited Frequency Sensitive Mode.

Before considering the payment for these services we should have an idea about how can the **battery wear** of EV's be evaluated. Some studies give us this values:

- 25c/kWh with 80% DOD;
- 17c/kWh with 70% DOD.

**DOD** is **Depth of Discharge** which is the complement of State of Charge(SOC) and therefore means how much we are discharging the battery. It can be expressed in Ah or in percent points.

Going back to the frequency regulation's payment, let's consider, for instance, the payment and the amount of MWh exchanged in few days of October 2015. For instance, in one day the quantity exchanged was 1053.5MWh with a payment of 4099.06£ having an average payment of 3.89£/MWh which is definitely not affordable for aggregators considering that with a DOD of 70% the battery wear is 13.41£/MWh.

There is also the **Firm Frequency Response (FFR)** which has the following requirements:

- Providers must have suitable operational metering;
- There is a test that has to be passed;
- To deliver minimum 10MW Response Energy;
- Must have the capacity to operate in frequency sensitive mode for dynamic response or change their MW level via automatic relay for non-dynamic response;

The payment is composed by the following elements:

- *Availability fee*; hours for which the service is made available by the provider;
- *Window Initiation fee*; for each FFR nominated window that National Grid instructs within the Tendered frames;
- *Nomination fee*; for each hour utilised in FFR nominated windows there is a holding fee;
- *Tendered Window Revision fee*; National Grid notifies providers of window nominations in advance and, if the provider allows, the payment is payable if National Grid subsequently revise the nomination;
- *Response Energy fee*; payment for the energy provided.

For instance, in a generic month the Availability fee was 946£/h and the Nomination fee was 131£/h so this type of service is affordable for EV owners.

### 3.3.2 Reserve

#### Fast Reserve

This is used with other energy balancing services in order to control frequency deviation that arise from sudden and unpredictable changes in generation or demand. Rapid and reliable delivery of active power from generation or reduction in consumption from demand sources is provided. It starts within two minutes after receiving instructions with 25MW or greater per minute rate and a minimum of 50MW provided. The delivery has to be sustained for minimum 15 minutes. The appointed provider makes the service available for a pre-agreed period and keeps the relevant units ready if National Grid needs it. The requirements are the following:

- Act within 2 minutes or less;
- Minimum volume of 50MW;



- Minimum run up/run down rate of 25MW/minute;
- Delivery sustainable for at least 15 minutes;
- Should be repeatable;
- Maximum commitment time of 5 minutes;
- Reliable delivery; time tolerance of  $\pm 30$ s and always volume more than 90% of the contracted amount.

Providers must submit *tenders* so if high prices are tendered then there is the possibility to lose the contract. The payment is composed by the following elements: Availability Payment £/h, Positional Payment £/h, Window Initiation £/per Firm Window and the Utilisation Payment £/MWh. In January the Availability Payment has been 263-445 £/h, Positional Payment 335/445 £/h and the Utilisation Payment 125/140 £/MWh. This range of payment make this service affordable for aggregators.

### **3.3.3 Short Time Operating Reserve (STOR)**

Involves a minimum of 3MW of generation or demand reduction. The delivery has to happen within 240 minutes or less and when instructed full MW have to be provided for at least 2 hours. The payment is composed by the following elements: availability payment [£/MWh] and utilisation payment [£/MWh]. We have observed that in a certain period the minimum and maximum threshold for these payment voices have been the following:

- Availability 0/12 £/MWh;
- Utilisation 70/250 £/MWh.

This makes this service practically feasible for EV owners.

### **3.3.4 BM Start Up**

This is additional generation balancing mechanism and the units that take part in it would not otherwise been accepted in other balancing mechanism due to their technical characteristics and associated lead-times. Requirements for providers are that they have to prepare the generator in 89 minutes from instruction and the hot standby which means that the unit has to be kept in a state of readiness for an agreed period of time. The payment for this service is composed by a BM start up payment [£/h], and there are three rates for this, and the hot standby payment [£/h]. However, the requirements and the ambiguity of the payment make this service not convenient for aggregators.

### **3.3.5 Black start**

When there is a total or a partial shutdown of the grid in order to recover from this situation there is the necessity of DC sources. Isolated power stations are started individually and gradually connected to each other in order to form an interconnected system again. If there is an emergency, then black start stations are powered by small auxiliary generation plant but not all power plants have this capability. The requirements are:

- Ability to start up the main generation plant or at least one module and be ready to energise part of the Network;
- Accept instantaneous loading or demand blocks of 35-50 MW and controlling frequency and voltage levels.;
- Provide at least three sequential Black start;
- High service availability.

There is an agreed availability fee per settlement period and a utilisation payment. These are stipulated through bilateral contracts. Anyway these kind of service require high reliability and availability. Also the size of the unit is a matter of consideration because it has to be big enough to start a big plant. In future, with a huge deployment of EVs and EVSE this service might be provided.

### **3.3.6 Reactive Power**

#### **3.3.6.1 Obligatory reactive power service**

This is the provision of varying reactive power: at any given output the generators could be requested to provide or absorb reactive power to regulate the voltage close to its connection point; so it's a local basis service. All

generators have to have the capability to provide reactive power and over 50 MW all generators have to provide this service. Requirements:

- Ability to supply the rated power output (MW) at any point between the limits 0.85 and 0.95 power factor;
- Short circuit ratio less than 0.5;
- Keep the reactive power output under steady state conditions fully available within the voltage range  $\pm 5\%$  at 400kV, 255kV, 132kV and lower voltages;
- Stability over the entire operating range.

There are Default Payment Arrangements and according to the utilisation factor it can be 2.32-3.17 £/MVarh. Since the provision of reactive power doesn't cost anything to the charger, except the reduction of the active power exchangeable, it's worth to take part to this service.

### **3.3.6.2 Enhanced reactive power service**

This service is for those generators that aren't required to supply the obligatory reactive power service. The payment is composed by the Available Capacity Price [£/MVarh] and/or a Synchronised Capability Price [£/MVarh] and/or a Utilisation Price [£/MVarh]. The commitment is given through tenders. A price between 2.7-2.9 £/MVarh is payed.

These considerations have been made in order to try to define an economical revenue that EV owners can expect if they take part to V2G. A part from the battery wear another cost should be considered: keeping the vehicle available for V2G makes it unavailable for the user. This is why in most of the payment structures seen so far an availability fee was included. However, most of the services seen till now aren't economically affordable due to the low deployment of EVs and EVSE. In a near future with a high EV density these services will be a great option for further developments in the smart grid area.

## 4 Topology of the converters

In order to ensure a correct power transfer between the grid and the battery, the correct topology for the charger has to be chosen. There is a big number of schemes available for static converters but they have their proper applications. For instance, since we have to exchange power between AC and DC we can take a simple half bridge diode rectifier but we don't have to forget the aim of the charger. We need to change the power exchange between grid and battery so we have to vary the output of the charger. Plus, it has to be bidirectional, so already, diode bridges aren't suitable for our use, because they don't give any possibility to reverse the power flow by introducing a delay in the switching. In order to control the output, and to be able to reverse the power flow we need semi-active switch converters: these ones allow us to delay the switching of the device, that is not left to the conditions of the external circuit but to the user, once the component is directly polarized. So by introducing a delay we can control the shape and therefore the mean value of the output voltage and the delay between this and the output current if an inductance is involved, and usually it is. Commonly IGBTs and MOSFETs are the most used for these applications due to their ability to bear high voltages and current. For this project IGBTs with 600V of maximum voltage and 30A of maximum current have been used.

Both IGBTs and MOSFETs are voltage controlled semiconductor devices. They assemble the structure of a transistor but they are controlled with a gate voltage signal instead of a current signal. This is because there is an insulation between gate and the device, and in order to have current conduction, there is a threshold voltage for the gate that has to be exceeded. Another merit of these devices is the high operating frequency that is absolutely fundamental for these applications because the grid doesn't allow a high quantity of harmonics; MOSFETs can go up to 1MHz whereas IGBTs 100kHz. By increasing the frequency as much as possible, thanks to the Unipolar PWM is possible to have a few harmonics in the output and even at very high frequencies. A flaw for MOSFETs is the relatively high conduction loss due to the conduction resistance which grows with the reverse voltage; reverse voltage is the highest voltage that the device can bear when switched off. For IGBTs the **flaw** is the **commutation** which takes time and involves losses.

### 4.1 AC/DC converter's scheme

Since what we are designing is a single phase charger then its scheme involves a single phase bridge built with IGBTs and its controlled with Unipolar PWM.

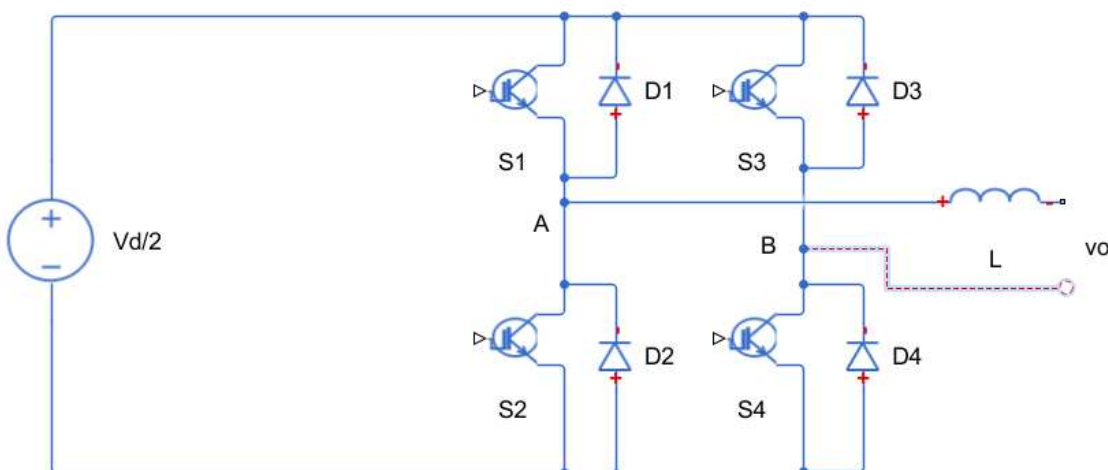


Figure 4.1 Single-Phase Full Bridge converter

### 4.1.1 Pulse Width Modulation

For now, let's consider just one leg of the bridge which consists of two switches not activated at the same time, because it would cause a short circuit. Almost always the switches include a biased against diode. This is because in order to ensure the four-quadrant operation we have to allow every combination of voltages and currents signs. So for instance when the voltage is positive, the current can either be positive or negative depending on if the battery is charging or discharging. So, because the switches allow the current flow in only one direction, and when they are switched off they are open circuits, these diodes are necessary to let the current pass.

Let's suppose that the current is going out from node A; if  $S_1$  is switched on then the voltage of node A is  $V_d/2$ ,  $S_2$  is obviously switched off, and the current will pass through  $S_1$ , whereas if  $S_2$  is switched on, the voltage of node A is 0 and the current will pass through  $D_2$ . When the current is going in the node A then if  $S_1$  is switched on then the current will pass through  $D_1$  and if  $S_2$  is switched on then the current will pass through  $S_2$ .

This switching of these IGBTs is done with the **Sinusoidal Pulse Width Modulation (SPWM)** technique: what we do, is to compare a triangular **carrier** signal with a **modulating sinusoidal signal**. These signals are provided at the gate terminal of the switches; without any kind of signal at the gate the devices are open circuits. When the amplitude of the modulating signal is higher than the amplitude of the carrier, the output is high otherwise is low. This signal is used to control the switching of the IGBTs. By studying the harmonic content of  $v_o$  we'll spot a fundamental that has the same amplitude and frequency of the modulating signal. In other words, by properly switching the IGBTs between the high and low values of a DC source we can have a sinusoid at the output. It's true that there are other harmonics but they are at high frequencies. They're located at the multiples of the carrier's frequency and around it, considering that odd harmonics are absent because of the odd symmetry.

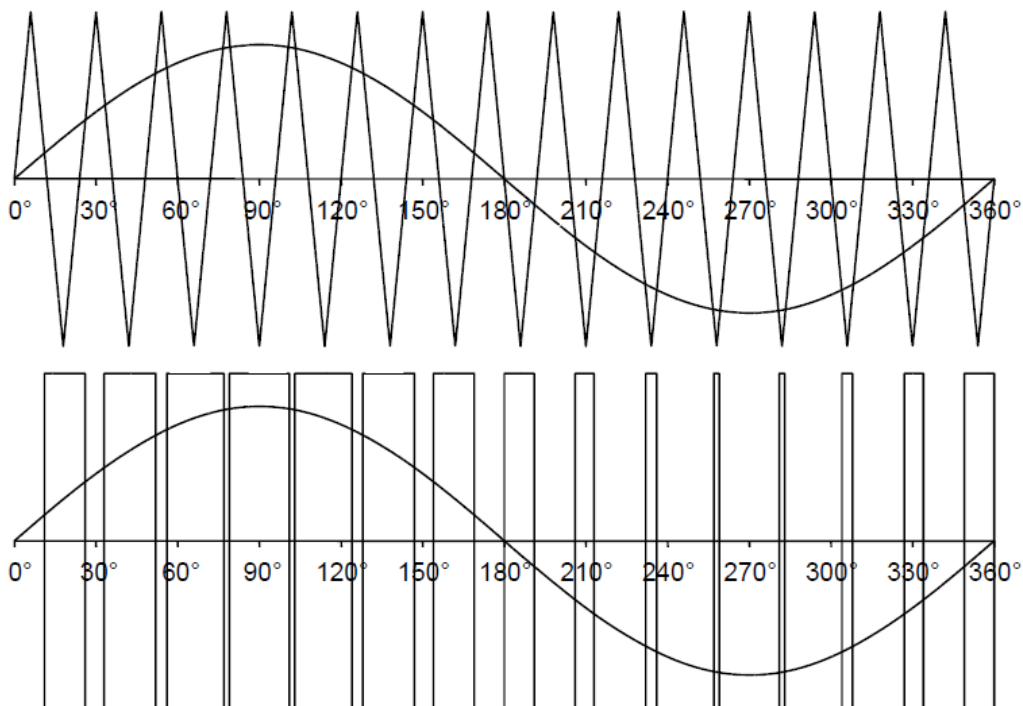


Figure 4.2 Sinusoidal Pulse Width Modulation for inverters [3]

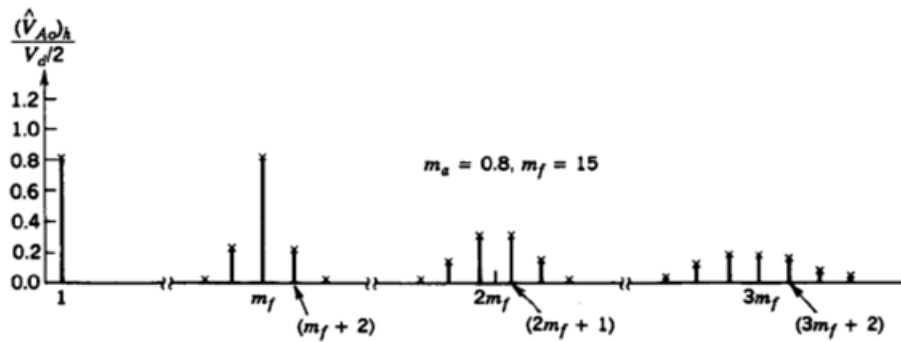


Figure 4.3 Harmonic content of SPWM [3]

Now we'll define two fundamental parameters:

$$\text{Amplitude Modulation ratio: } m_a = \frac{V_{control}}{V_{tri}}; \quad (4.1)$$

$$\text{Frequency Modulation ratio: } m_f = \frac{f_c}{f_1}; \quad (4.2)$$

The former is the ratio between the amplitude of the modulating signal and the carrier signal whereas the latter is the ratio between the carrier signal's frequency and the fundamental frequency. By changing these parameters it's possible to vary the amplitude and the harmonic content of the output signal. If we analyse the harmonic content of  $v_o$  we'll see that it has the fundamental, as said before, but also multiple harmonics at the frequencies  $k \cdot f_s \pm n$ . The amplitude of these multiple harmonics goes down with increasing  $k$  and  $n$ , so the highest harmonic is the one at  $f_s$ . If the modulating signal is:

$$v_{control} = V_{control} \sin \omega_1 t; \quad (4.3)$$

and if  $V_{control} \leq V_{tri}$  then:

$$(v_o)_1 = \frac{V_{control}}{V_{tri}} \sin \omega_1 t \frac{V_d}{2} = m_a \frac{V_d}{2}; \quad (4.4)$$

where  $\omega_1$  is the fundamental pulsation. So by controlling  $m_a$  we can change the amplitude of the output voltage. Talking about  $m_f$ , if we choose it as odd and integer we'll profit by the odd symmetry which means that the output voltage waveform won't have even harmonics. If  $m_f \leq 21$  then we have synchronous PWM which means that carrier and the modulating signal are synchronised and it requires integer  $m_f$ . This technique is used mainly because with the asynchronous PWM we have sub-harmonics that cause core saturations in electric motors. So if  $m_f \geq 21$  we have asynchronous PWM which means that the carrier and modulating signals don't have the same frequency. Usually in this case the carrier frequency is kept constant while the modulating frequency varies:  $m_f$  won't be integer. One of our conditions was  $V_{control} \leq V_{tri}$ . What if it's not verified? In this case we would be in **over-modulation** that means  $V_{control} \geq V_{tri}$  and  $m_a \geq 1$ . Since the amplitude of the modulating signal is greater than the amplitude of the carrier signal then the output signal will saturate to the high condition for some time. This makes the amplitude of the fundamental, contained in the output voltage, higher than in the linear condition but the waveform has much more harmonics. Moreover, the amplitude of the fundamental doesn't vary linearly with  $m_a$ . If  $m_a$  is high enough then the waveform becomes a square wave and also here we have all the odd harmonics. It's not possible to increase the amplitude of the fundamental more than this.

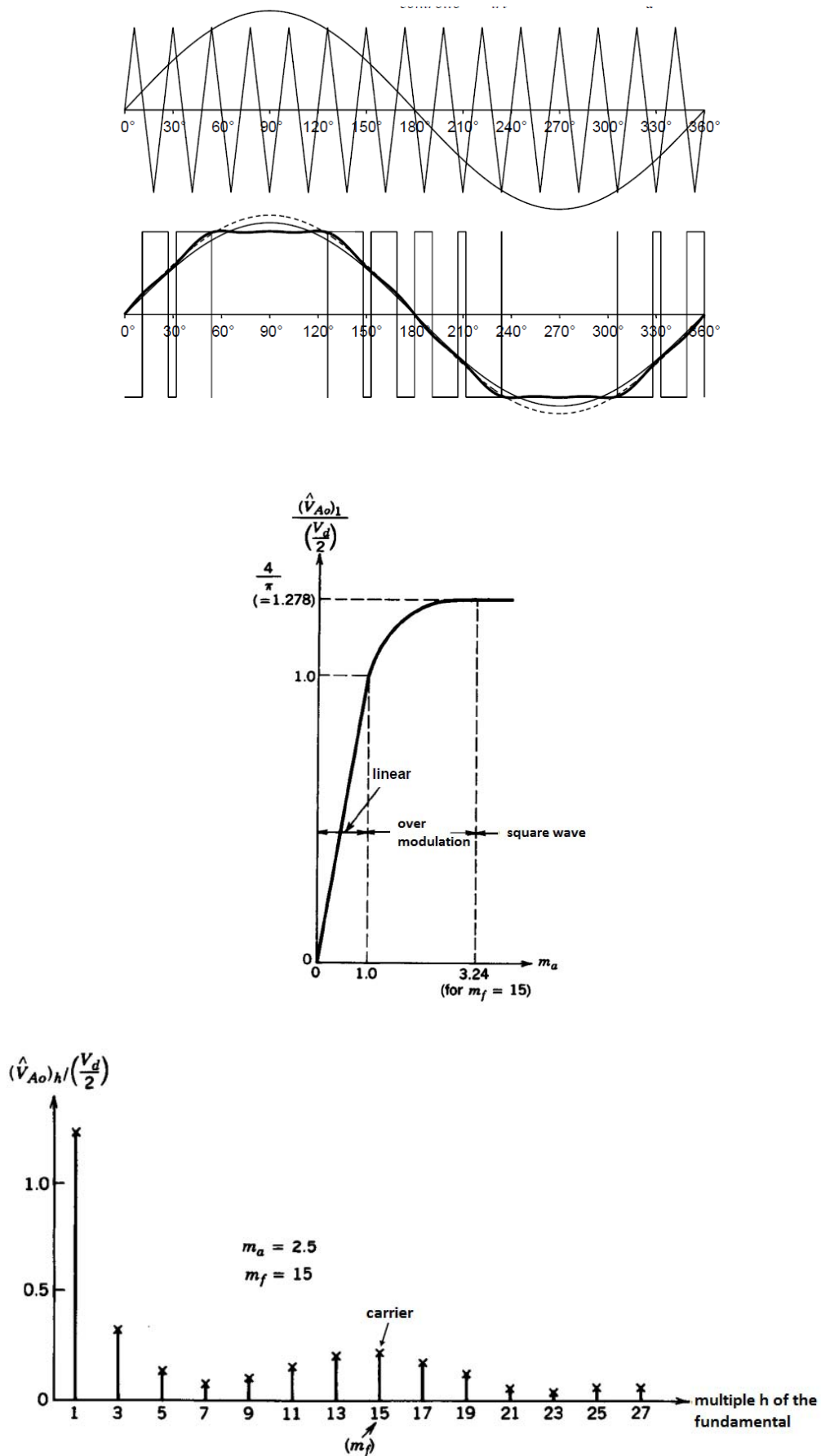


Figure 4.4 (a) Over-modulation in SPWM; (b) Voltage ratio and amplitude modulation ratio; (c) Harmonic content in square wave operation [3]

### 4.1.2 Unipolar and Bipolar PWM

Now it's time to consider the *single phase full bridge*.

There are two PWM techniques that can be used to control this device: **Bipolar PWM** and **Unipolar PWM**.

In the **Bipolar PWM**  $T_{A+}$  and  $T_{B-}$  and  $T_{A-}$  and  $T_{B+}$  are switched in couple. So, when the amplitude of the sinusoid is greater than the amplitude of the carrier  $T_{A+}$  and  $T_{B-}$  are switched on and  $T_{A-}$  and  $T_{B+}$  are switched off and vice versa.

So:  $v_{B0}(t) = -v_{A0}(t)$  (4.5)

$$v_0 = v_{A0}(t) - v_{B0}(t) = 2v_{A0}(t); \quad (4.6)$$

$$V_{o1} = m_a V_d \text{ if } m_a \leq 1 \quad (4.7)$$

$$V_d < V_{o1} < \frac{4}{\pi} V_d \text{ if } m_a \geq 1 \quad (4.8)$$

The harmonic content is the same as explained above.

In the **Unipolar PWM**, the legs of the bridge aren't switched at the same time as the Bipolar PWM. In this case the legs are controlled separately by comparing  $v_{tri}$  with  $v_{control}$  and  $-v_{control}$ . If  $v_{control} > v_{tri}$   $T_{A+}$  on and  $v_{AN} = V_d$

$$v_{control} < v_{tri} \quad T_{A-} \text{ on and } v_{AN} = 0$$

$$-v_{control} > v_{tri} \quad T_{B+} \text{ on and } v_{BN} = V_d$$

$$-v_{control} < v_{tri} \quad T_{B-} \text{ on and } v_{BN} = 0.$$

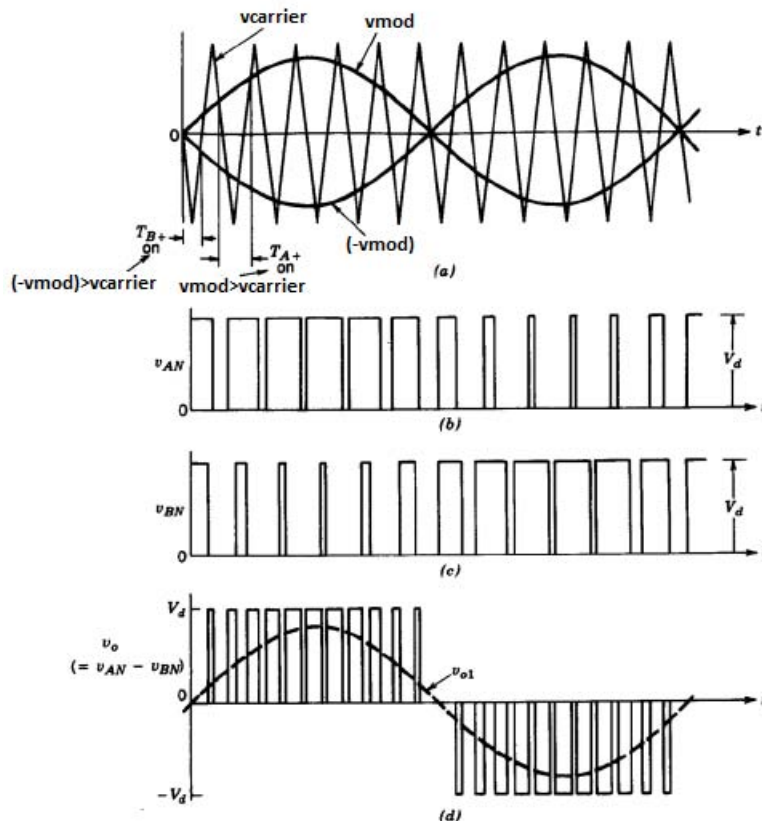


Figure 4.5 (a) Unipolar PWM; (b) Firing signal of leg a; (c) Firing signal of leg b; (d) Voltage between the two legs [3]

The output waveform has double frequency and therefore the greatest harmonic is at  $2f_s$ . If we have chosen an odd  $m_f$ , then  $2f_s$  is absent and the greatest are  $2f_s \pm 1$ .

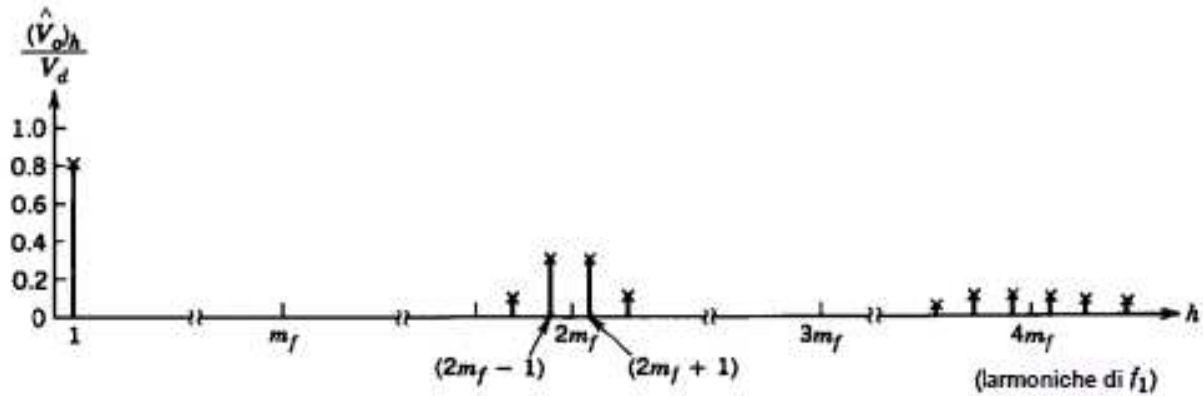


Figure 4.6 Harmonic content of Unipolar PWM [3]

If we choose  $m_f$  as odd and multiple of 3 then the harmonic at  $m_f \cdot f_1$  isn't present, third harmonics (multiple of three) are absent,  $2 \cdot m_f \cdot f_1$  isn't present so the greatest are  $2f_s \pm 1$ . Also here is possible to employ the over-modulation, but again, going beyond a certain value of  $m_a$  we'll have the square wave mode, and then the amplitude of the fundamental of the output waveform won't increase anymore.

### 4.1.3 Three-Phase Converter

There is also the three phase PWM: three modulating signals with  $120^\circ$  of phase shift between them are compared with a single carrier;

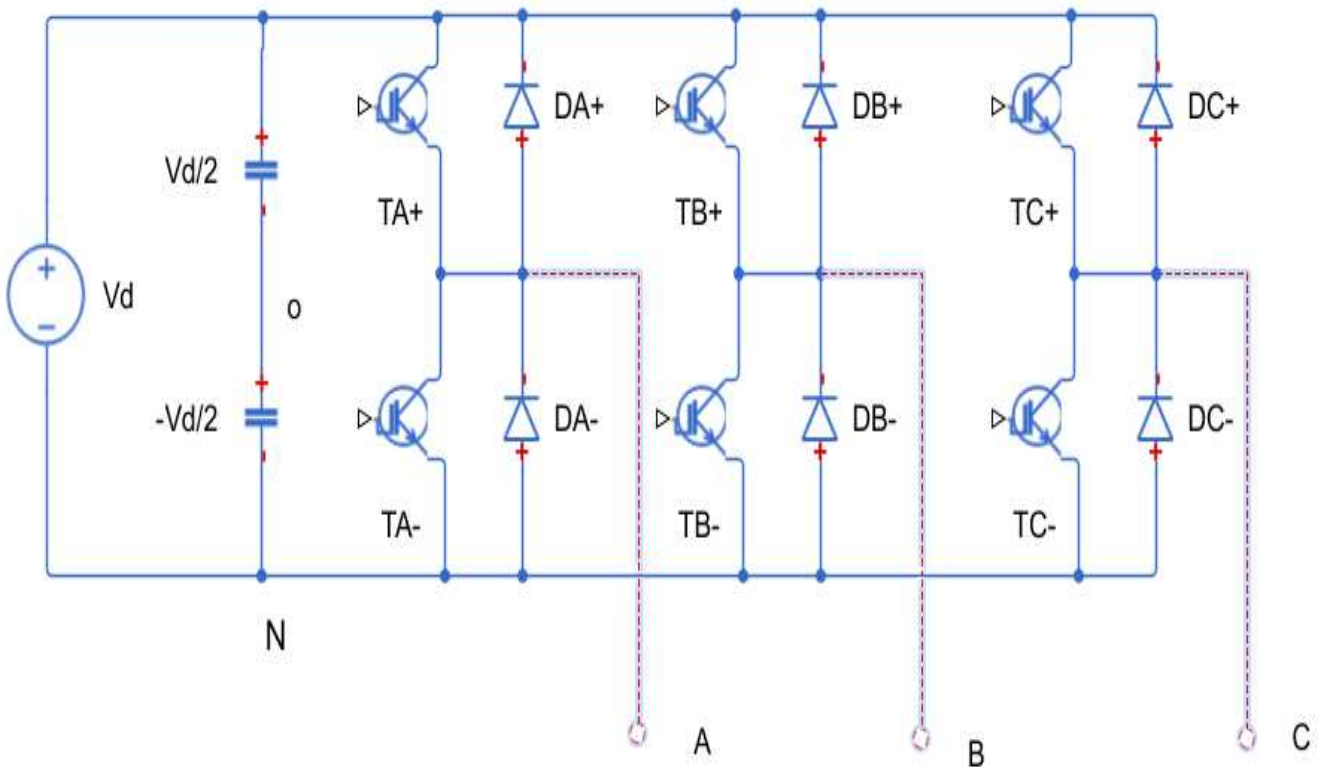


Figure 4.7 Three-Phase converter



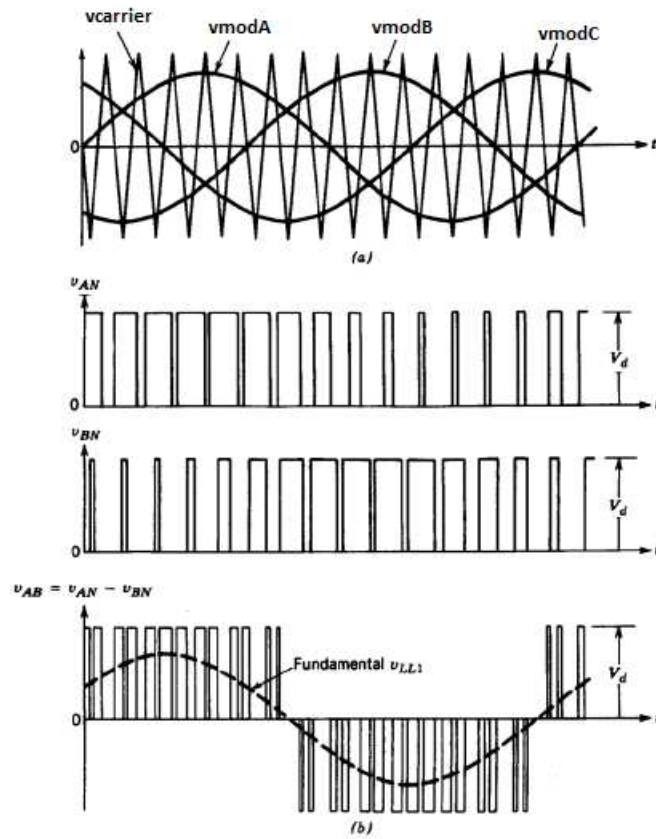


Figure 4.8 PWM in a three-phase converter [3]

$v_{AN}$ ,  $v_{BN}$ , and  $v_{CN}$  are compared with  $v_c$  and the line to line voltage between two phases oscillates between 0 and  $V_d$  in the positive half wave, and between  $-V_d$  and 0 in the negative half wave and has double frequency. If the frequency modulation ratio  $m_f$  is odd, and multiple of 3, then the harmonics multiple of three are absent, the  $m_f$  harmonic is absent,  $2m_f$  is absent since it's even and therefore the biggest harmonics are  $2m_f \pm 1$ .

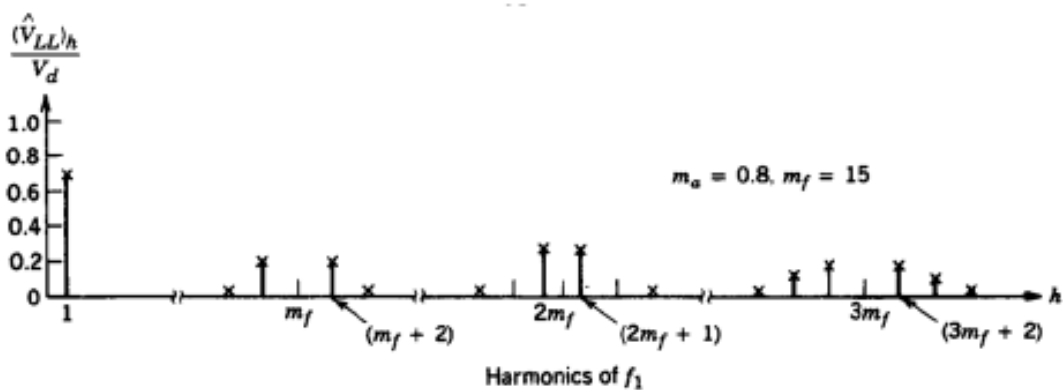


Figure 4.9 Harmonic content in three phase PWM [3]

### 4.3 DC/DC Converter

Once designed the AC-DC converter we could interface the grid and the battery just with that. Since an IGBT switched bridge allows bidirectional power flow, discharges of the battery towards the grid would be allowed. But its better including another part to the whole system for the following reasons: the interface voltage is a problem because it affects the power flow; in fact, having a certain power exchange between grid and battery through just the AC/DC converter, if we increase this, the voltage will fall and the power exchange with it. Not only that, if we are charging or discharging the battery, its voltage varies so again it will affect the power flow and the health of the battery. Besides, more specifically, if we want to exchange and regulate the reactive power, then the voltage of the DC Bus is involved. If we want to supply reactive power to the grid, the DC Bus voltage has to be increased, whereas if we want to absorb reactive power from the grid this voltage has to decrease. And if the voltage of the DC Bus is changing, in the case we have just the AC/DC converter, the output voltage is changing. If we consider the internal resistance of the battery constant for a reasonable time, this means that, if the supplying voltage is changing, the current provided to the battery is changing and since we are at the DC part of the converter, the power changes along with the current. What happens is that, it's not possible to have independent active and reactive power controls. So there has to be something in between that conciliates the two parts by changing the voltage ratio, thus, the DC bus voltage becomes independent from the voltage at the battery. This is what a DC/DC converter does: the inputs of these converters are DC as well as their outputs, but with different amplitudes of the mean value. These converters use a Pulse Width Modulation (PWM) regulation: a triangular wave carrier is compared with a constant signal, which is the desired output, and the result is the controlling signal for the switches.

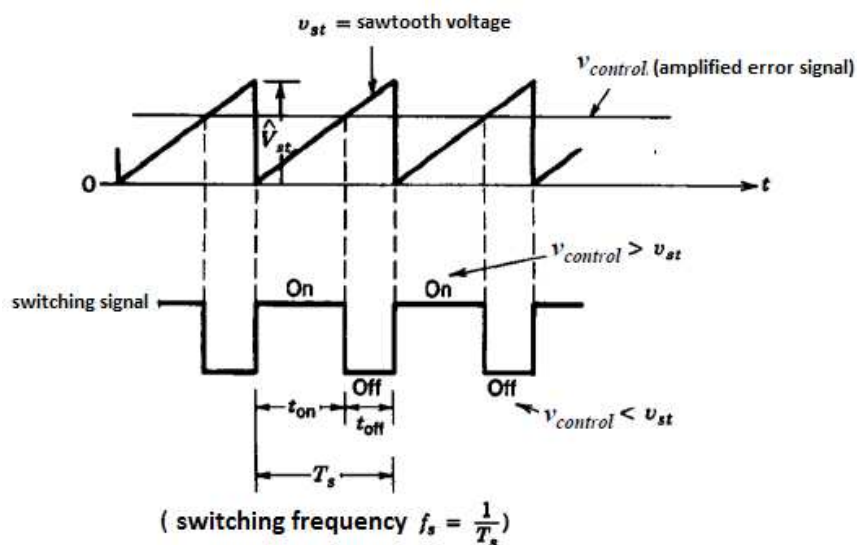


Figure 4.9 Pulse Widthe Modulation [4]

There are different schemes for these converters, but mainly they increase or decrease the amplitude of the mean value of the output waveform. It's useful to study the operation of the **Buck** and the **Boost** converters though we won't use them but rather a combination of them.

### 4.3.1 Buck converter

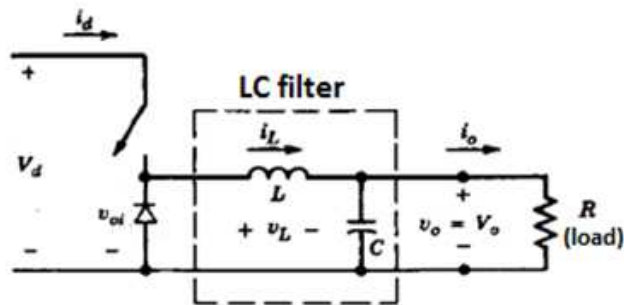


Figure 4.10 Buck converter [4]

In this scheme the resistor represents the load. By switching T we'll have the following waveform  $V_{oi}$  which has the mean value  $V_o$ .

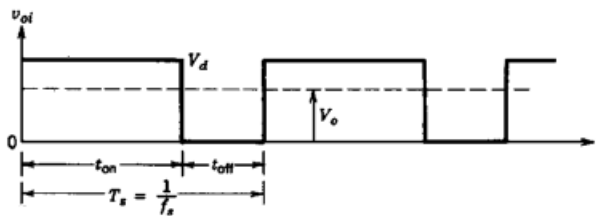


Figure 4.11 Input voltage of the LC filter [4]

By computing the integral of this waveform over the integration period, so by looking at its mean value we'll notice a relationship between  $V_d$  and  $V_o$ .

$$V_o = \frac{1}{T_s} \int_0^{T_s} v_o(t) dt = \frac{1}{T_s} \int_0^{t_{on}} V_d dt = \frac{t_{on}}{T_s} V_d = D V_d \quad (4.9)$$

where  $D$  is the **duty cycle**, that is the percentage of the period in which the output is high. So as we can see, by changing  $D$  is possible to vary the mean value of the output voltage. Since  $D$  is between 0 and 1 this converter can only reduce the amplitude, so it has to be  $V_o < V_d$ . Naturally, the output waveform has harmonics, but if high frequency is adopted then these are positioned at high frequencies, like multiples of the switching frequency.

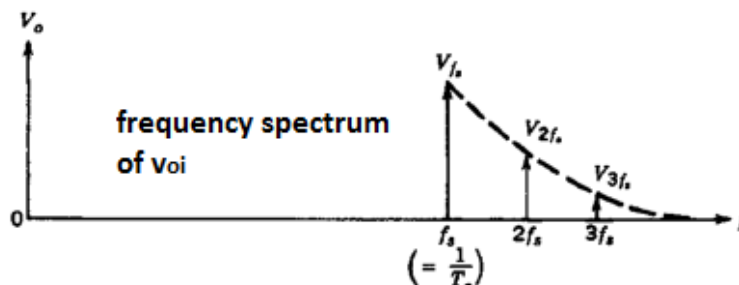


Figure 4.12 Harmonic content of the output voltage [4]

In this scheme there is a LC filter which is used to knock down the harmonics. By choosing a high switching frequency is possible to have small and hence cheap components.

### 4.3.2 Boost converter

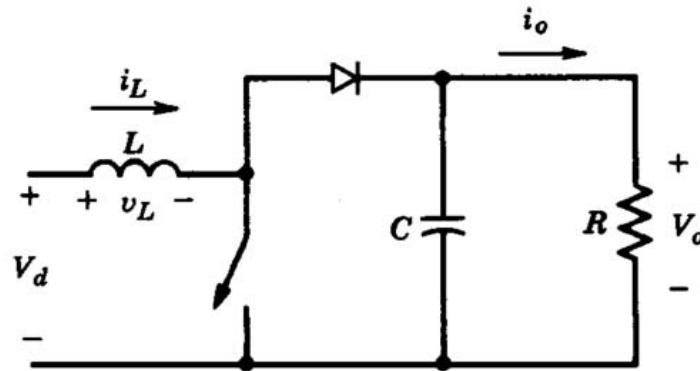


Figure 4.13 Boost converter [4]

In this case by switching T we are charging and discharging the inductor towards the load, so the current is going up and down. When the switch is turned on the load is isolated.

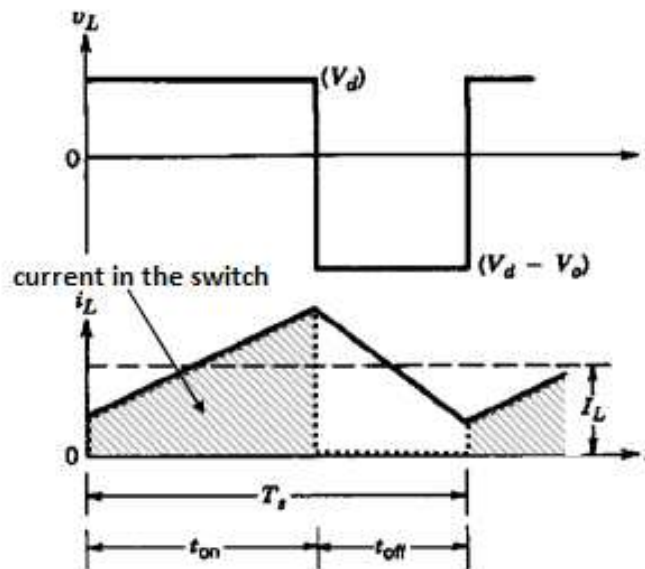


Figure 4.14 (a) Voltage supplied to the inductor; (b) current in the inductor [4]

Since there is an inductor that is charging and discharging, the energy discharged has to be the same of the energy charged. This means the integral of the inductor's voltage over the period has to be zero:

$$V_d t_{on} + (V_d - V_o) t_{off} = 0; \quad (4.10)$$

$$\frac{V_o}{V_d} = \frac{T_s}{t_{off}} = \frac{1}{1-D} \quad (4.11)$$

As we can see, by changing D we can vary the mean value of the output waveform between  $V_d$  and ideally infinite, so this converter can only increase the output: it has to be  $V_o > V_d$ .

### 4.3.3 The chosen converter: a combination of both

Now that the operations of these converters are clear we introduce the chosen topology for this project. It's a single leg DC-DC converter.

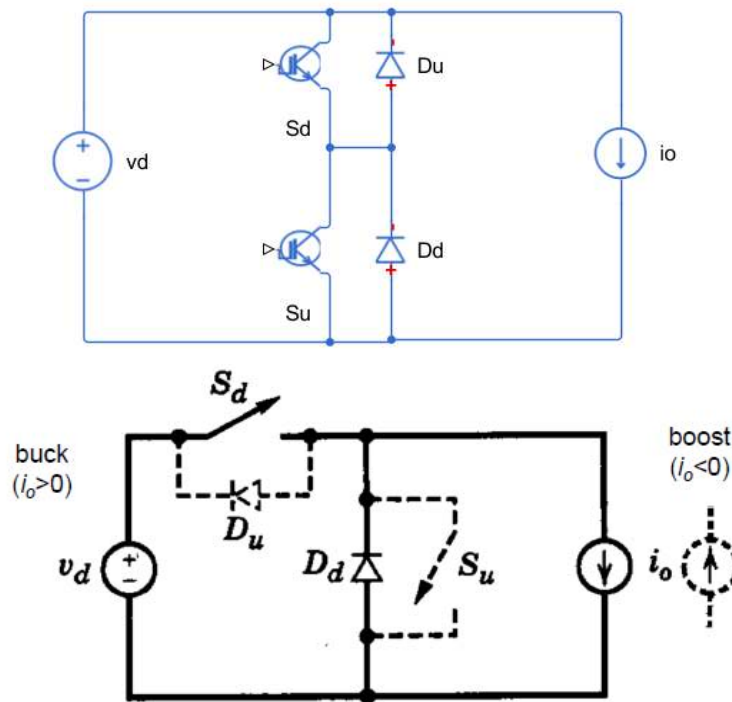


Figure 4.15 (a) Single leg converter; (b) Single leg converter, Buck-Boost differentiation [4]

If we observe carefully, we'll notice that this converter can be seen as a Buck and Boost converter put together depending on the function. If charging,  $S_d$  and  $D_d$  are active so there is a Buck converter whereas if discharging,  $S_u$  and  $D_u$  are active so there is a Boost converter.

## 4.4 LC Filter and interfacing

Since we are interfacing the charger with the battery, and one of the operating modes is charging, the DC-DC converter will decrease the output voltage of the charger in order to match the battery's necessity. Because the waveform required from the battery is a constant one whereas the output waveform of the DC-DC converter will be oscillating we need to use a filter that kills some harmonics in order to not damage the battery. We are using a LC filter. Since the following equation is verified:

$$V_0 = \frac{1}{T_s} \int_0^{t_{on}} V_d dt = \frac{t_{on}}{T_s} V_d = D V_d \quad (4.12)$$

if we subtract the mean value of  $v_o$  from its actual waveform we will notice the harmonics. The first harmonic is at the frequency  $f_s$ . In order to mitigate the amplitude of this harmonic, the LC filter must have a cut-off frequency that has to be at least two order of magnitude lower, so that the amplitude allowed from the filter will be small at the switching frequency.

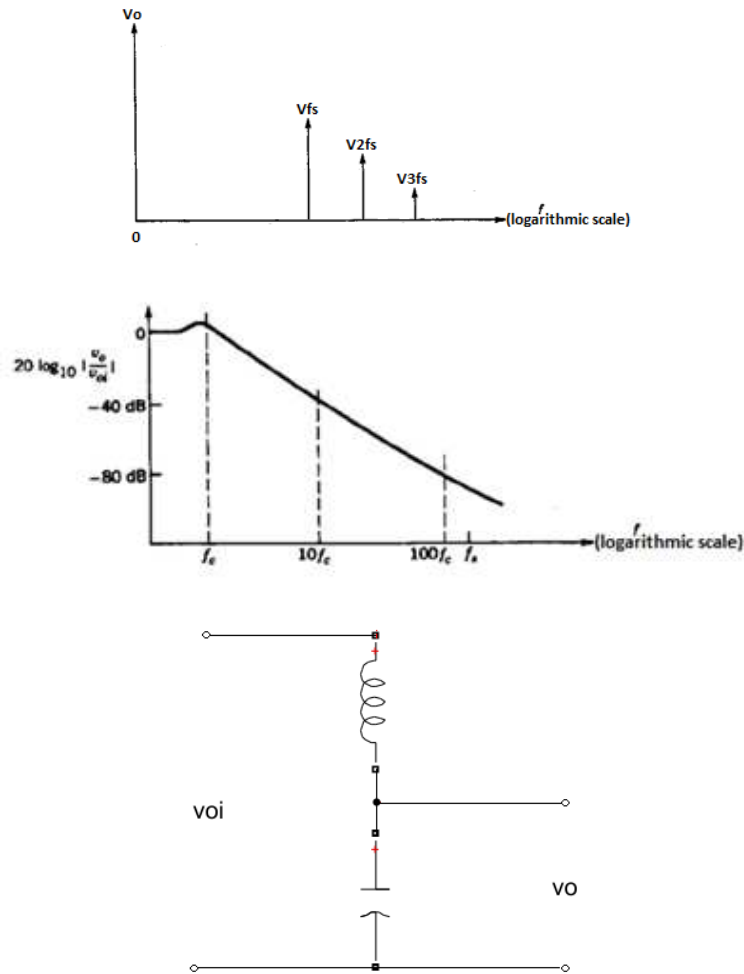


Figure 4.15 (a) Harmonic content of the DC voltage without filter; (b) Harmonic content of the DC voltage with filter [4]; (c) The voltages that are involved in the filter

By considering this simple circuit let's find the relation between  $v_o$  and  $v_{oi}$ :

$$\frac{v_o}{v_{oi}} = \frac{\frac{1}{j\omega C}}{j\omega L + \frac{1}{j\omega C}} = \frac{1}{1 - \omega^2 LC} = \frac{1}{1 - (\frac{\omega}{\omega_{LC}})^2} \quad (4.13)$$

where  $\omega_{LC}$  is the **Cut-off frequency**

$$\omega_{LC} = \frac{1}{\sqrt{LC}} \quad (4.14)$$

If  $\omega_A = \omega_{LC}$ , then there is resonance, and the overall impedance seen from the harmonic is nil, so its amplitude is big. But if  $\omega_s \gg \omega_{LC}$  for instance  $\frac{\omega_s}{\omega_{LC}} = 10$  then  $\frac{v_o}{v_{oi}} \approx \frac{1}{99}$  so the harmonic is highly mitigated. We have a dejection of -40dB/decade. If  $\omega_s = 2\pi f_s$  then  $LC = \frac{1}{f_s^2 4\pi^2}$  (4.15) so if  $f_s$  is small, LC is big in order to have a proper mitigation and hence the components will be expensive specifically the inductor. So in order to use cheap components, the switching frequency has to be really high.

## 5 Control approach and Regulator

Once we have chosen the converters and the interfacing components, such as inductor and capacitors we have to control the system properly. This means that the system has to reach the status we want in a short time. For instance, the user will choose to charge the vehicle for a given amount of kilometres, and according to the grid's, batter's and user's necessities a charging program will be defined in order to satisfy everyone. So if the grid is asking for power the system will discharge the battery rather than charging. It will charge the battery when there is no hurdle from the grid, and in such a time that the user will be satisfied. So in this case the system will compute the value of the power needed by the grid and that will be the reference value for the discharge. The controller has to condition the charger in such a way, that it will start discharging the battery of that amount and quickly. Another step has to be done.

### 5.1 Active and reactive power control

From now we'll consider an inductive connection between the grid and the load. We can represent the grid as a tern of alternating voltages with a phase-shift of  $120^\circ$  between each other. Then, as said above the connection between grid and load is inductive, and it includes the internal impedance of the Thevenin transformation representing the grid, and the line impedance. Values of the grid impedance are obtained from previous research and they are:

- $R_s=6.5547286 \cdot 10^{-4} \Omega$ ;
- $X_s=9.17662 \cdot 10^{-3} \Omega$ .

These values depend on the Short-circuit level of the grid, which means that when there is a fault, the system has the ability to bear a certain value of current, and in this case we have  $I_{sc}=25\text{kA}$ . For the connections, Standard Cables are considered and the kilometric resistance and reactance are:

- $r=0.524 \Omega/\text{km}$ ;                      for  $35 \text{ mm}^2$
- $x=0.0745 \Omega/\text{km}$ ;
  
- $r=0.268 \Omega/\text{km}$ ;                      for  $70 \text{ mm}^2$
- $x=0.0710 \Omega/\text{km}$ .

The choice between  $70$  or  $35 \text{ mm}^2$  has to be done by considering the flowing current in these cables.

In the high voltage grid and even in the medium voltage grid the connection between grid and load is mainly inductive, whereas in low voltage nets the connection is more resistive. However, the other part is always present but doesn't influence the outcome so much. Since both the inverter and rectifier operating modes are kept in consideration with a semi-active switch converter, to explain the operations we'll consider the inverter mode. In this mode the inverter generates a tern of alternating voltages so it will be represented in this way.

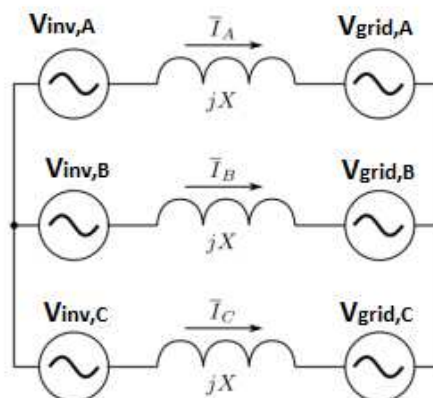


Figure 5.1 Three phase model of the grid and the voltage generated by the inverter [5]

By considering the phasor of the grid voltage as reference we are going to draw the phasor diagram with all the involved dimensions:

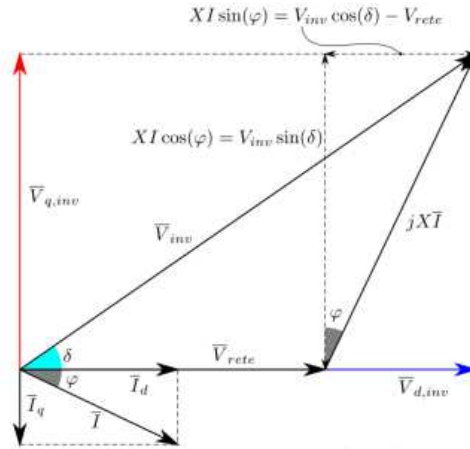


Figure 5.2 Phasor Diagram of the involved dimensions in  $d,q$  orientation [5]

$$XI \cos \varphi = V_{inv} \sin \delta = V_{qinv} \quad (5.1)$$

$$I \cos \varphi = I_d = \frac{V_{qinv}}{X} \quad (5.2)$$

$$P = 3V_{grid} I \cos \varphi = 3V_{grid} I_d = 3 \frac{V_{grid} V_{qinv}}{X} \quad (5.3)$$

So the active power exchange is controlled by varying  $V_{qinv}$ .

$$XI \sin \varphi = V_{inv} \cos \delta - V_{grid} = V_{dinv} - V_{grid} \quad (5.4)$$

$$I \sin \varphi = I_q = \frac{V_{dinv} - V_{grid}}{X} \quad (5.5)$$

$$Q = 3V_{grid} I \sin \varphi = 3V_{grid} I_q = 3V_{grid} \frac{(V_{dinv} - V_{grid})}{X} \quad (5.6)$$

The reactive power exchange is controlled by varying  $V_{dinv}$  or better the voltage drop in the inductor. In this case we would have to measure the voltage supplied by the converter, do the  $d-q$  transformation and control the two components of the voltage separately according to the active and reactive power exchange. The important thing to remember is that, here a highly inductive grid has been considered and therefore in the impedance the resistive component has been neglected.

### 5.1.1 Drop Control

Another possible approach is the Drop control; specifically, if the controlled system is single-phase and there is no possibility to implement the direct-quadrature conversion and therefore the active/reactive power has to be linked to something else. This is actually a simpler control method because it doesn't involve the  $d-q$  transformation hence, the Park transformation and therefore the knowledge of the grid voltage's angle is not necessary. Besides, these methods need only a proportional controller without any integral part. With this approach there is always a small error that is because it's inherent of the method and the major drawback is that, this method is inefficient for highly resistive lines that are a common characteristic of the low voltage grid. However, it's possible to implement this method anyway by changing some variables. Let's retrace the previous steps we did in order to determine the relation between  $P/Q$  and other parameters, but in a general line.



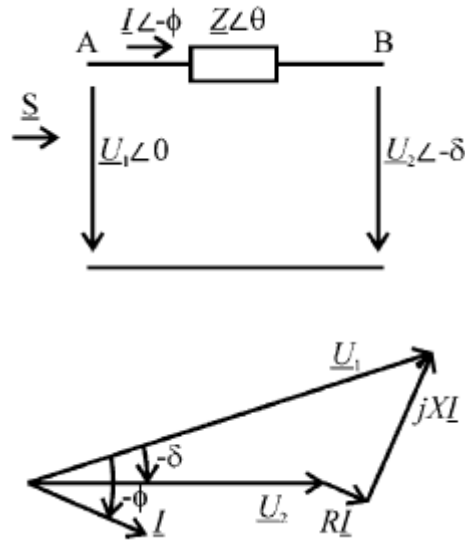


Figure 5.3 (a) Voltages in a generic impedance; (b) Phasors of the involved dimensions [12]

The power flowing in a line can be represented in the following way:

$$P + jQ = \bar{S} = \bar{U}_1 \bar{I}^* = \bar{U}_1 \left( \frac{\bar{U}_1 - \bar{U}_2}{Z} \right) = U_1 \left( \frac{U_1 - U_2 e^{j\delta}}{Z e^{-j\theta}} \right) = \frac{U_1^2}{Z} e^{j\theta} - \frac{U_1 U_2}{Z} e^{j(\delta + \theta)}. \quad (5.7)$$

Therefore, active and reactive powers are:

$$P = \frac{U_1^2}{Z} \cos \theta - \frac{U_1 U_2}{Z} \cos(\delta + \theta); \quad (5.8)$$

$$Q = \frac{U_1^2}{Z} \sin \theta - \frac{U_1 U_2}{Z} \sin(\delta + \theta). \quad (5.9)$$

Because  $Z e^{j\theta} = R + jX$  (4.25) we can rewrite the above mentioned equations in this way:

$$P = \frac{U_1}{R^2 + X^2} [R(U_1 - U_2 \cos \delta) + XU_2 \sin \delta]; \quad (5.10)$$

$$Q = \frac{U_1}{R^2 + X^2} [-RU_2 \sin \delta + X(U_1 - U_2 \cos \delta)]. \quad (5.11)$$

From which the following relations can be obtained:

$$U_2 \sin \delta = \frac{XP - RQ}{U_1}; \quad (5.12)$$

$$(U_1 - U_2 \cos \delta) = \frac{RP + XQ}{U_1}; \quad (5.13)$$

For  $X \gg R$ , the latter can be neglected and whether the power angle  $\delta$  is small then these approximations are valid:  $\sin(\delta) = \delta$  and  $\cos(\delta) = 1$ , hence;

$$\delta \cong \frac{XP}{U_1 U_2} \quad (5.14)$$

$$U_1 - U_2 \cong \frac{XQ}{U_1} \quad (5.15)$$

Again, the previous relations are verified in case of  $X \gg R$  and small power angles: the active power exchange between grid and converter depends on the power angle and the reactive power exchange depends on the voltage amplitude.

Since the power angle control is obtained by the dynamic frequency control, we can consider the latter as variable related to the active power. The frequency and voltage drop control are therefore:

$$f - f_0 = -k_p(P - P_0); \quad (5.16)$$

$$U_1 - U_0 = -k_q(Q - Q_0); \quad (5.17)$$

where  $f_0$  and  $U_0$  are the rated value respectively for the frequency and the voltage and  $P_0$  and  $Q_0$  are the references for the inverter. As can be seen the biggest advantage of this method is the simplicity given by the fact that we are using a proportional controller.

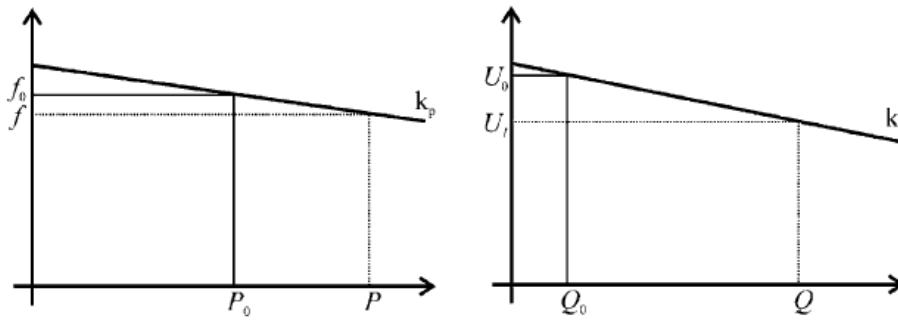


Figure 5.4 Frequency and Voltage drop control with P and Q [12]

Now, the low voltage grid is characterized by a high resistive factor, thus it's not negligible, on the other hand the reactive factor is low and therefore negligible. This makes the drop control method ineffective.

However, there is a way to continue working with the drop method that involves active and reactive power control by considering a transformation matrix. This tool transforms the actual  $(P, Q)$  couple in the  $(P', Q')$  modified couple.

$$\begin{bmatrix} P' \\ Q' \end{bmatrix} = \mathbf{T} \begin{bmatrix} P \\ Q \end{bmatrix} = \begin{bmatrix} \sin \theta & -\cos \theta \\ \cos \theta & \sin \theta \end{bmatrix} \begin{bmatrix} P \\ Q \end{bmatrix} = \begin{bmatrix} \frac{X}{Z} & -\frac{R}{Z} \\ \frac{R}{Z} & \frac{X}{Z} \end{bmatrix} \begin{bmatrix} P \\ Q \end{bmatrix}. \quad (5.18)$$

Once the new couple of powers are obtained, it's possible to apply them to the previously seen relations and consequently the results are:

$$\sin \delta \cong \frac{ZP'}{U_1 U_2} \quad (5.19)$$

$$U_1 - U_2 \cos \delta \cong \frac{ZQ'}{U_1} \quad (5.20)$$

Again, for small power angles, the modified active power depends on the power angle and the modified reactive power depends on the voltage amplitude. According to the R/X ratio  $P'$  and  $Q'$  can have different values in respect to  $P$  and  $Q$ . In fact, for mainly inductive lines  $P' \cong P$  and  $Q' \cong Q$  whereas for mainly resistive lines  $P' \cong -Q$  and  $Q' \cong P$ .

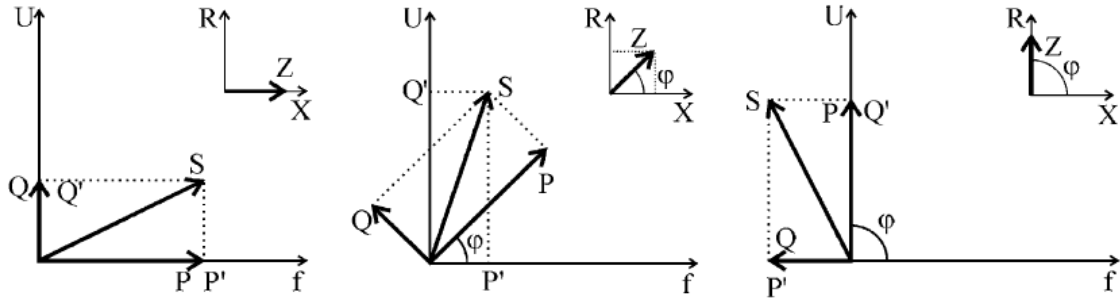


Figure 5.5 Phasor alignment according to the impedance [12]

Therefore, the modified drop control becomes:

$$f - f_0 = -k_p(P' - P'_0) = -k_p \frac{X}{Z}(P - P_0) + k_p \frac{R}{Z}(Q - Q_0) \quad (5.21)$$

$$U_1 - U_0 = -k_q(Q' - Q'_0) = -k_q \frac{R}{Z}(P - P_0) + k_q \frac{X}{Z}(Q - Q_0) \quad (5.22)$$

## 5.2 DC/DC Control

The AC/DC controller is committed to the regulation of both the active and reactive power by changing the amplitude and the angle of its output voltage. We have already studied how the different control methods of the AC/DC converter are, but in order to ensure the balance between the input power and the output power, the control of the DC/DC converter is essential. Since we are approaching DC control, this means that only active power is considered and only this will influence the control of the DC/DC converter. The aim of this control approach is to ensure the equivalency between the power supplied by the AC/DC converter, that is the power absorbed from the grid, and the power supplied to the battery by taking care about the correct ratio between the battery's voltage and the DC bus voltage, that is what determines a good interaction between grid and battery. In fact, as said before, if the voltage of the DC bus changes during either charging or discharging, this influences the power exchange in the sense that it doesn't satisfy the requirements.

Since we have to generate a PWM signal by comparing a constant signal with a triangular wave carrier, and because the constant signal represents the duty cycle, we are going to vary this input according to our reference. Again, a mechanism like the drop control is adopted: the reference for this converter is the active power that is the same of the one provided to the AC/DC converter because the two powers have to match. We are going to measure the actual power supplied to the battery and the difference between the power reference and the actual power, that will represent the power error, will go inside the controller. The output of the controller will be the required duty cycle, that will be compared with the carrier in order to provide the switching signals for the IGBTs. If the actual power is lower than the reference, that means, the error is positive and consequently the duty cycle will be increased whereas if the actual power is greater than the reference, the error will be negative and the duty cycle will be decreased. From this and the previous control approach, it's clear that an oscillation around the correct value is expected, hence a DC filter is used in order to cut the harmonics and provide a clean waveform.

One of the main issues of the V2G is the battery degradation due to the high number of charging/discharging cycles, that makes this solution ineffective for a practical implementation. However, nowadays caring charging patterns have been developed in order to minimize the damage afflicted to the battery. One of these consists on initially charging the battery with a **Constant Current (CC)**; the voltage of the battery cells will increase and when this will have reached the nominal value, corresponding to when the battery is at its maximum capacity, a **Constant voltage (CV)** will be provided. The current will decrease and the battery will keep charging with a small current. When the battery will be

at its maximum capacity then the supplied current will be very small and just enough to keep the battery charged. Other charging patterns could be used like the **Constant Power (CP)** or the **Trickle Charging** which consists of giving high current pulses once in a while in order to keep the battery charged, when the main charging process has ended.

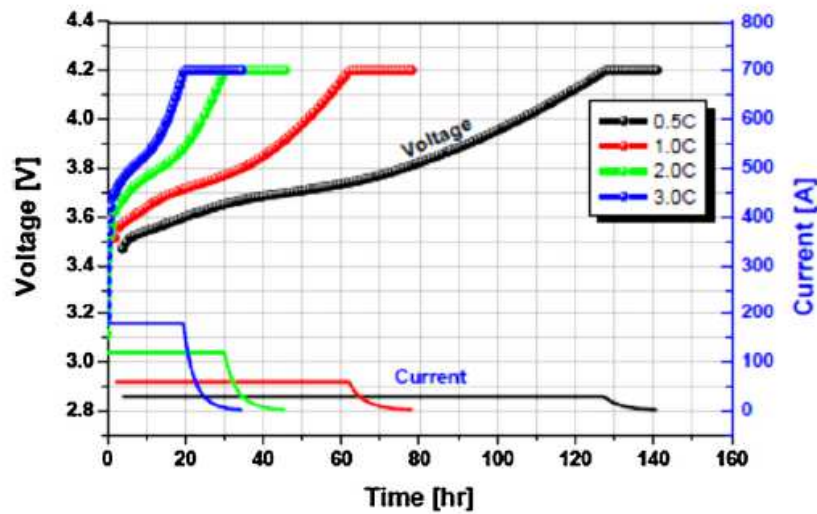


Figure 5.6 CC-CV charging at different C rates [11]

An example of CC-CV charging is presented. As can be seen, even though all these charging curves have the same target they reach it in different time spans. This is due to the intensity of charging that is different in each curve. In fact, with the black curve the battery is charged at 0.5C that means, in one hour only half of the capacity is charged, whereas with the red curve, that represents 1C, the whole capacity is charged in one hour; it's obvious that, in order to charge the battery faster the current needs to be higher. Higher is the intensity of charging, and faster it will be, but on the other hand, faster will be the battery deterioration. It's advised to keep the charging below 1C in order to have a reasonable life span of the battery.

### 5.3 The practical approach

In this project we are designing a **single-phase bridge** because they are widely diffused even nowadays in both on-board and off-board chargers hence, by putting smart regulation in them we could impact significantly on the grid. As said previously the considerations did in this work could be extended in three-phase DC charging by just considering a different scheme for the charger.

Since we are using a single phase controller, the d-q transformation is not feasible because it requires three dimensions that are shifted in phase by  $120^\circ$ . In the previous chapter the drop control has been described and here we are going to use something similar. We have to directly relate the active and the reactive power to some dimensions, that will be used to control the output voltage of the bridge. In this case we have related the active power exchange to the amplitude of the output voltage and the reactive power exchange to the phase shift of the output voltage or otherwise said the power angle.

The first thing that can be noticed is that, in our case, opposite dependencies have been used as of active/reactive power and power angle/voltage amplitude. This approach hasn't been explained yet but it's the consequence of the high resistance of the low voltage grid: since here  $X$  can be neglected over  $R$  then, for small power angles the active power can be controlled by changing the voltage amplitude whilst the reactive power is controlled varying the power angle.

One can immediately notice a problem in this approach and that is the proportionality relation between this two couple of dimensions: for instance, in order to change the reactive power exchange, we are going to change the phase of the output voltage, but these two variations don't have the same magnitude. In fact, the reactive power exchange

will vary between zero and a given value and consequently the phase will have to vary between zero and another value. For instance, if reactive power is varying between zero and the maximum value allowed then the power angle is changing between zero and ninety degrees because it corresponds to the maximum reactive power exchanged. The proportionality between this changes is given by the controller that we are going to use and specifically by the proportional part.

### 5.3.1 The system

We need a control system with feedback and a controller in order to reach the status we want in a given time. Basically, we are asking to the system to reach a given status in a reasonable time and we are measuring its output. Once it has been measured, we are comparing it with our reference value and considering a possible error to further control the system. If there is a positive error, it means that the output has to be increased whereas if the error is negative then the output has to be decreased. When the system reaches the desired status the error will be nil and therefore no further change will be imposed to the system. The system is represented in this way:

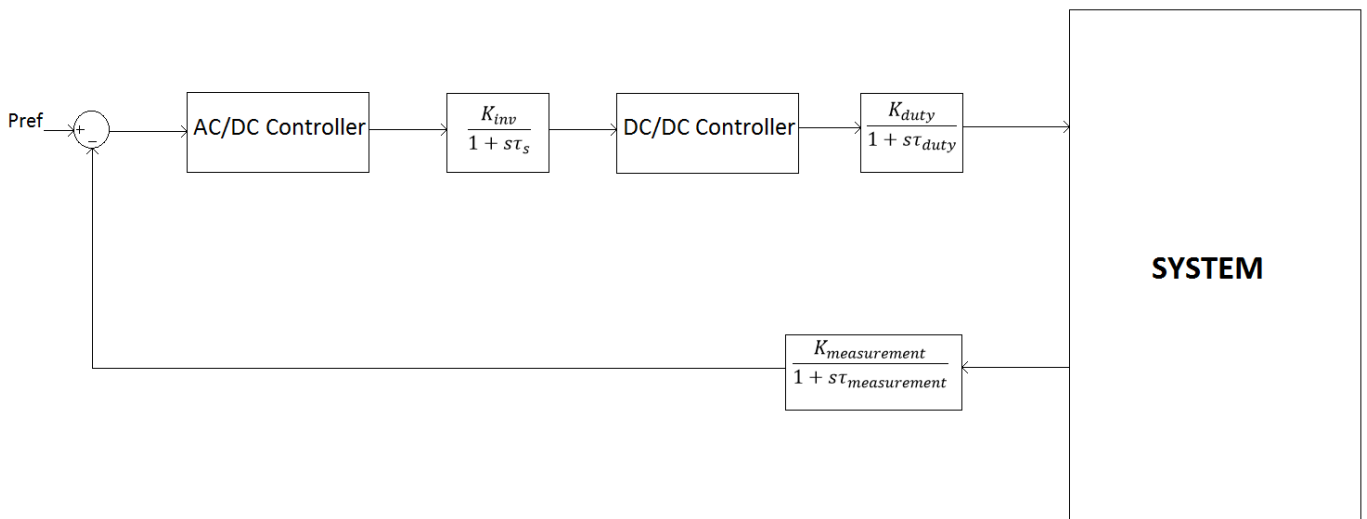


Figure 5.7 Block Diagram of the whole system

Here we are representing the system with a **transfer function** with the Laplace Transformation which means that the output is a function of the input. In order to do that, we have to model every part properly so we will be able to show their correct behaviour. These representations will always have a bit of error but in order to consider their average behaviour these are negligible.

Let's consider the charger first: what we do in order to control the power flow is to force a desired voltage phasor at the output of the AC-DC converter and it gives us what we have requested for but with a delay. In fact, the phasor we have requested for is obtained from the next switching step of the converter, because it's then that something changes. So we can represent the whole charger with a simple pole that considers this delay. The pole is located in the switching frequency  $f_s$  and the Laplace transformed representation considers a time constant,  $\tau_s$ , that is the reverse of the switching frequency:  $\frac{K_{inv}}{1 + s\tau_s}$  where the constant K considers all the proportionality between the desired output and the input. In order to control the output, we have to measure it, so we are using measuring instruments. These instruments show a bigger output if the input dimension is bigger and a smaller output if the input is smaller. This means that they are linear and they give the correct value after a time constant  $\tau_{measurement}$ . Hence the representation for these measurements is  $\frac{K_{measurement}}{1 + s\tau_{measurement}}$ .

### 5.3.2 System's parameters

Once the correct representation of the system is obtained a proper controller has to be designed in order to reach the status we want quickly. At first few dimensions from the Control theory have to be defined:

- **Rise time  $t_r$**  of the Step response of the system, is the time required from the system to reach the 90% of the steady state value  

$$t_r = \min\{t \geq 0: |w_1(t) - W(0)| \leq 0.1 |W(0)|\}; \quad (5.23)$$
- **Percentage Overshoot  $S$**  =  $(\sup_{t \geq 0} \frac{w_1(t) - W(0)}{W(0)})$  (5.24) is the possible overshoot counted in percentage points;
- **3dB Bandwidth** or just **Bandwidth**, the upper bound of the frequencies that implies an absolute value in dB of the frequency response of the system in that frequency that is greater or equal to the absolute value in dB of the frequency response of the system computed in zero minus 3dB; more simply, it's the range of frequency that has an attenuation less than 3dB;  

$$B_p = \sup\{\tilde{\omega} > 0: \forall \omega \in [0, \tilde{\omega}] |W(j\omega)|_{db} \geq |W(0)|_{db}\}; \quad (5.25)$$
- **Relative Resonance Peak  $M_{rel}$**  =  $|W(j\omega_r)|_{db} - |W(0)|_{db}$  (5.26) if there is a Resonance Pulsation  $\omega_r$ ;
- **Crossing pulsation  $\omega_c$**  the only not negative pulsation, if existing, for which  $|\check{G}(j\omega_c)| = 1$ , or otherwise it's the frequency for which the Bode diagram of the frequency response of the system crosses 0dB, and if it exists
- **Phase margin  $m_\psi = \arg(\check{G}(j\omega_c)) - (-180)$** ; (5.27) is how many degrees separate the phase of the frequency response of the system from  $180^\circ$ .

Smaller is the Rise time and faster is the system to reach the steady state because the Step response is faster. The Bandwidth shows which frequency are preferred, because at that frequency there is the maximum reduction of the absolute value of the frequency response. Bigger is the bandwidth and bigger is the range of frequency without reduction. The Crossing Pulsation and the Phase Margin are strictly related to the Feedback control theory: they are referred to the transfer function of the open loop system and its demonstrated that they are related to the previous dimensions. In fact, bigger is the Crossing pulsation and smaller is the Rise Time and bigger is the Bandwidth. Bigger is the Phase Margin and smaller is the Resonance Peak and smaller is the Overshoot and vice versa. In practical, a Phase Margin that is smaller than  $45^\circ$  is not accepted; is better to have a phase margin of  $90^\circ$ . If there were strict requirements on the Rise Time and the Maximum Overshoot, then we would have designed the controller properly: we are using a **PID controller**.

### 5.4 PID Controllers

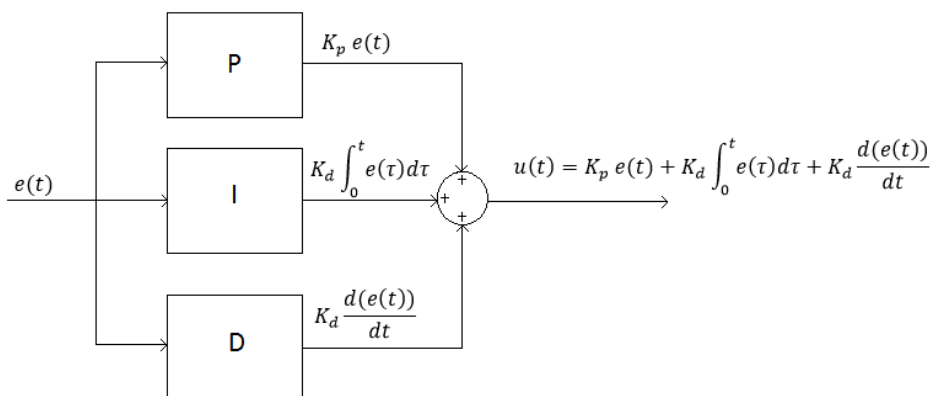


Figure 5.8 Components of a PID controller

If we represent a generic system in the way that is described above, as said before, we need a controller to reach the Steady State value. So if  $e(t)$  is the error in input to our system, the controller gives us an output  $u(t)$ . This output has three components:

- a component which is **Proportional** to  $e(t)$ ;
- a component which is proportional to the **Integral** of  $e(t)$ ;
- a component which is proportional to the **Derivative** of  $e(t)$ .

$$u(t) = K_p e(t) + K_d \int_0^t e(\tau) d\tau + K_d \frac{d(e(t))}{dt}; \quad (5.28)$$

Where  $K_p, K_i$  and  $K_d$  are constants that give different weights to each value. Let's analyse the different effects of each part:

- the proportional part has effect on the instantaneous value of the difference between  $r(t)$  and  $y(t)$ ; bigger is  $e(t)$ , bigger will be  $u(t)$ ;
- the integral part is responsible of cancelling a possible offset of the output if there is a non-nil average value of the error; bigger is this offset and bigger will be the output of the integral part;
- the derivative part gives an output whose amplitude depends on how fast the error is changing; if its changing quickly then the output will be big.

It's also possible to have special cases of these controllers where not all parts are used: this is the case of the P, PI, PD controllers.

#### 5.4.1 P Controller

$$C_p(s) = K_p; \quad (5.29)$$

The proportional controller gives an output that is proportional to the input with a proportionality constant. This means that, since we are feeding these controllers with an error given by the difference between the reference value of our dimension and the actual value that has been measured, if the error is changing, the output of the controller will change in the same way given that these controllers are linear. So if the error is decreasing, the output will go down faster or slower according to the proportionality constant.

There is a big problem with these controllers: there is always an error in the steady state which means that the system won't reach the desired value. This is due to the fact that these controllers are not proper: a rational function  $f(s) \in \mathbf{R}[s]$  is **proper** if  $\lim_{s \rightarrow \infty} |f(s)| < +\infty$ ; is **strictly proper** if  $\lim_{s \rightarrow \infty} |f(s)| = 0$ . That means, if the controller is proper then the steady state error is nil. This is not the case because in the transfer function there is no  $s$  parameter at the denominator.

#### 5.4.2 PI Controller

$$C_{PI}(s) = K_p + \frac{K_i}{s} = \frac{K_i}{s} \left( 1 + \frac{K_p}{K_i} s \right) \quad (5.30)$$

The proportional-integral controller gives an output that is composed by two components: one component is proportional to the input and the second component is proportional to the integral of the output. As said before, the proportional part compensates the error while the integral part compensates possible offsets. Since the transfer function of these controllers are proper the steady state error is nil and hence the system will reach the desired value.

### 5.4.3 PD Controller

$$C_{PD}(s) = K_p + K_D s = K_p \left( 1 + \frac{K_D}{K_p} s \right) \quad (5.31)$$

The proportional-derivative controller gives an output that is composed by two components: one component is proportional to the input and the second is proportional to the derivative of the output. Here, the derivative part compensates rapid variations of the error. Again, since the transfer function of this controller doesn't have any  $s$  parameter at the denominator it's not proper and therefore there will be steady state error and it won't reach the desired value.

For our purpose we can use either a PI or a PID controller.

In any case there is a substantial problem and that is the choice of the constants of these controllers. In fact, the constants weigh the different parts, changing a lot the behaviour of the controller and the system. Ideally, in order to choose the proper controller, the transfer function of the system has to be known and for this the entire system has to be modelled with mathematical and physics relation. For our studies such a deep analysis is not required because we are interested in average behaviours and steady state goals. Hence, these parameters will be assigned empirically by checking the effect of each change and correcting any possible wrong choice.



## 6 Simulink model

In order to study the behaviour of the smart charger at its low level, that means at the component level, we have to simulate its operation with some simulation program so we'll be able to estimate the ideal response. In fact, in these simulations the switches and the other components are supposed ideal and so they don't have losses. This assumption is done in order to simplify our study and concentrate in more important issues, such as the transient behaviour and the effect of possible filters. Because of this assumption the switching losses due to hard switching, which means switching with not-nil voltages and currents that cause power loss, diodes', capacitors' and inductor's losses won't be considered. When we will work with the physical device all these losses will be present but their magnitude won't affect significantly the outcome of the system. Moreover, because of this assumption we'll be able to study a big range of situations that the smart charger might face since we aren't investigating in detail that would require deep studies.

In the Matlab/Simulink environment we can build our system, impose reference values and study the behaviour of the device in order to understand where to act if we want to make it more efficient. Here, we will build a block diagram with all the components and connect them like we were linking them in the reality, and run the simulation for a fixed time. Since we are interested in the low level designing we'll focus on the switching of the components and change it according to our target and measurements.

We'll recreate the grid with its model and connect it through a RL impedance, that represent the actual source impedance and the line impedance. For this work we have considered a second level charger that can be put on-board or off-board and can be placed either in the streets or at home. We have considered a distance of 10 km of the charger from the nearest substation and therefore the values of R and XL are :

$$R=5.24 \Omega;$$

$$X_L=0.754 \Omega;$$

$$L=2.4\text{mH}.$$

### 6.1 The Complete System

At first we are presenting a scheme of the total system, then we will show how the Simulink model represents each part of this system, continuing with the detailed explanation of each part, how it works and its contribution to the final result.

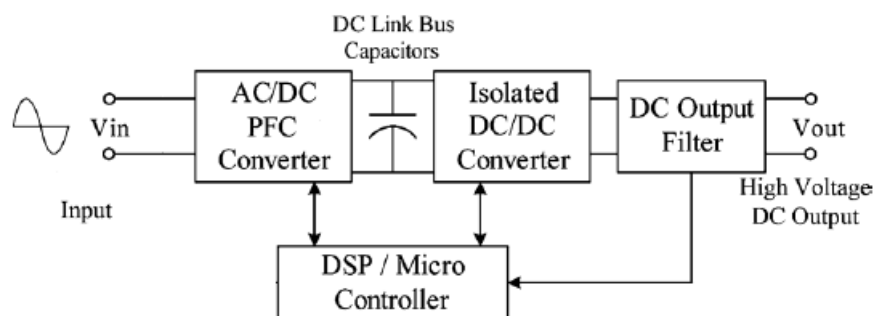


Figure 6.1 Complete scheme of a bidirectional low level charger [13]

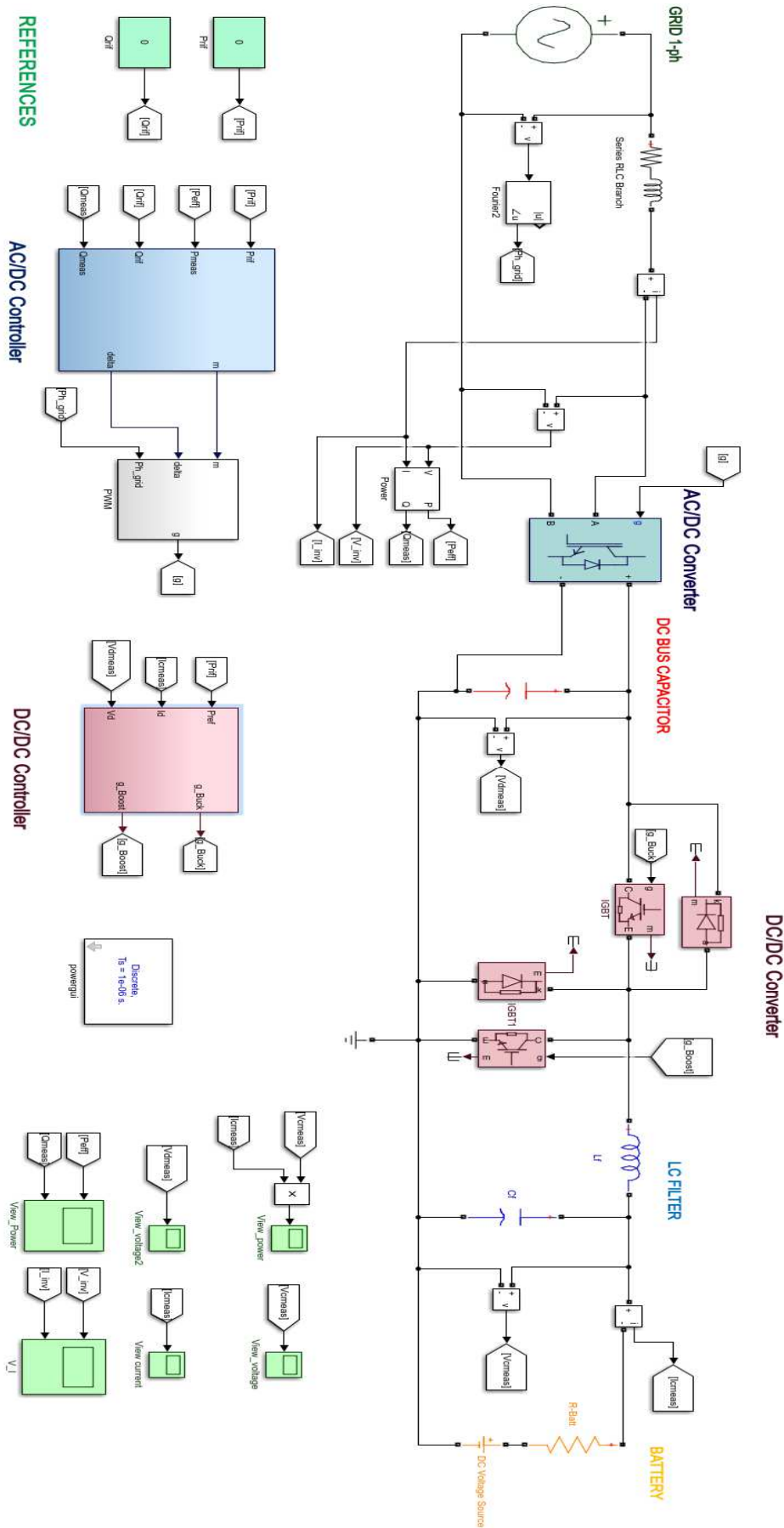


Figure 6.2 The complete Simulink model

The input is taken from the grid, and since the developed charger is single phase, this is meant to be connected to a phase of the grid, hence the grid is represented by a single phase AC generator. The Thevenin representation requires an impedance and the one that has been considered in this case is the grid impedance, as aforementioned. The high value for the resistive component confirms the earlier assumption of a highly resistive grid, that is the feature of the low voltage grid. Because of this characteristic the control approach adopted will be the opposite as of the active and reactive power. The grid supplies the initial stage of the charger that consists of a single phase full bridge which employs IGBTs and diodes polarized against. The switching of these IGBTs are decided by the AC/DC controller that requires the power references and the measurements of active/reactive power and the phase of the grid voltage, and provides the switching signals for the devices.

Let's focus for a moment on the AC/DC controller. In many studies, a model of the controller is considered. Essentially, these models represent either three or one AC voltage sources, that are the voltages supplied by the converter over the three or one phase. Sometimes, the control of the AC/DC controller is not even considered and it's asked to supply a fixed voltage with a fixed reference. This is because, as we previously said, the AC/DC controller is in charge of providing a voltage that is dictated by the reference whereas the DC/DC controller deals with the power provided to the battery. But since we have to reverse the power flow and make the converter work as a rectifier, by changing the power angle, a ready-made Simulink block has been used. This is also because we are building a low level controller, that deals with all the issues given by a high frequency PWM, which is mainly the high frequency ripple, and therefore a clean, average voltage can't be considered. With this block is possible to choose the switching devices, the number of phases, the presence of polarized-against diodes, and even the losses of the switches that are represented by a resistive factor; in these considerations however, we are considering ideal switches because we want to focus on the dynamics, thus, losses aren't what we are looking at.

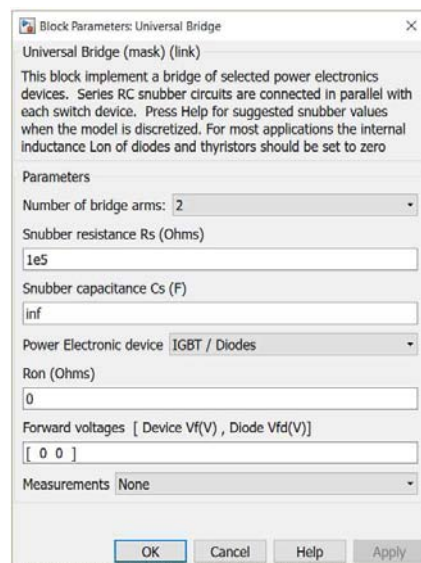


Figure 6.3 Parameter window of the universal bridge

In the G2V mode the output of this converter is DC while in the V2G mode the output is AC; in any case the DC side needs to be stabilized, thus, the DC Bus capacitor is used. The function of this capacitor is to make constant the DC output of the converter or to provide a constant supply to the converter when it's asked to supply AC. Hence, it has to be a big capacitor, so that even with high power flows, the DC Bus voltage is kept nearly constant. Since a PWM control is applied to both AC/DC and DC/DC converters, these will inject high frequency current ripple in the DC bus. The main purpose of the DC bus capacitor is to attenuate these ripples in order to provide a clean signal to the battery, otherwise it would increase the degradation. There aren't accurate and rigorous methods for the DC bus capacitor size design, but rather empirical or based on simulations. It's safe to say that most of the time experience dictates the right choice. Roughly, for small powers a size of hundreds of micro-farad is enough so no further theoretical considerations will be done on this topic. We will rather choose a reasonable value for the DC bus capacitor and change it later on, if it doesn't satisfy the simulation's requirements.

Following the DC bus there is the DC/DC converter, which is in this case a half bridge converter, working like a Buck converter during the charging or like a Boost converter during the discharging. So it's clear that only one switch operates at a time and it uses the diode of the other switch that is kept turned off. For the DC/DC controller measurements like the DC power, DC current and the DC bus voltage are required, and it will provide the switching signals for the converter.

After the DC/DC converter a DC filter has been used and the design of the size of the components is noted in the following lines: in this case a maximum relative ripple rate of 5% has been considered. The output of the converter during the charging phase is a Buck converter, hence, the DC filter has to be designed in order to minimize the voltage ripple supplied by this one.

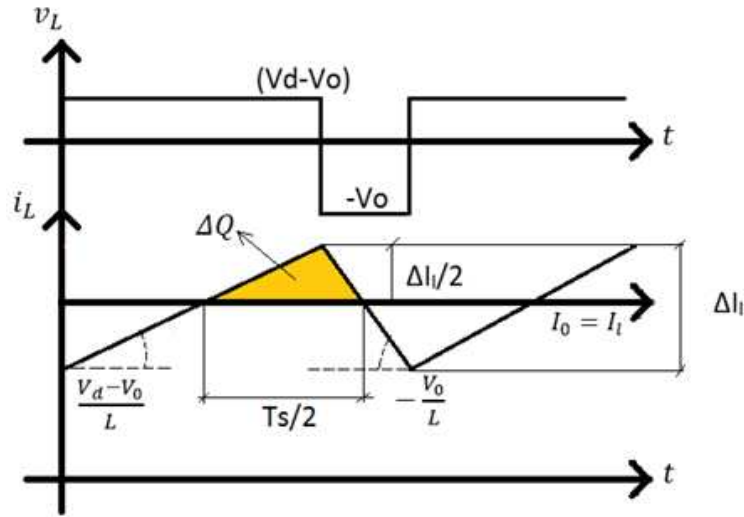


Figure 6.4 Voltage and current in the inductor of a LC filter

The voltage ripple  $\Delta V_0$  is therefore:

$$\Delta V_0 = \frac{\Delta Q}{C} = \frac{1}{2} \frac{\Delta I_L T_s}{2} \frac{1}{2} \frac{1}{C} = \frac{\Delta I_L T_s}{8C} \quad (6.1)$$

Since:

$$\Delta I_L = \frac{V_0}{L} (1 - D) T_s ; \quad (6.2)$$

$$V_0 = \frac{\Delta I_L L}{(1-D) T_s} ; \quad (6.3)$$

Hence

$$\frac{\Delta V_0}{V_0} = \frac{\Delta I_L T_s}{8C} \frac{(1-D) T_s}{\Delta I_L L} = \frac{(1-D) T_s^2}{8LC} = (1 - D) \frac{\pi^2}{2} \left( \frac{f_c}{f_s} \right)^2 ; \quad (6.4)$$

where

$$\frac{1}{8LC} = \frac{4\pi^2}{4\pi^2} \frac{1}{8LC} = \frac{\pi^2}{2} \frac{1}{4\pi^2 LC} = \frac{\pi^2}{2} f_c^2 . \quad (6.5)$$

Moreover, given that:

$$f_c = \frac{1}{2\pi\sqrt{LC}} \quad (6.6)$$

$$LC = \frac{1}{f_c^2 4\pi^2} . \quad (6.7)$$

For a desired value of the voltage ripple, which is represented by the  $\frac{\Delta V_0}{V_0}$  factor a certain value for  $f_c$  is obtained. By considering the worst case, that is for  $D=0$ , a certain value of the LC product is obtained. In our case  $\frac{\Delta V_0}{V_0} = 0.05$ ,  $f_s=20\text{kHz}$ , thus, the cut-off frequency for the DC filter is:  $f_c=2013.2\text{Hz}$  when the minimum duty cycle is considered. The value for the LC product is  $6.25 \cdot 10^{-9}$ .

At this point the individual values for the inductor and the capacitor can be chosen according to the available sizes. Because for the inductor only  $1\text{mH}$  is present and for the capacitor the closest size is  $7\mu\text{F}$ , these are the selected values. The consequent LC product will be different and imply a different percentage voltage ripple:  $f_c=1902.3\text{Hz}$  and  $\frac{\Delta V_0}{V_0} = 0.045$ . As theory wants, the cut-off frequency of the chosen filter is much smaller than the switching frequency so that, after  $f_s$  any harmonic is attenuated.

After the DC filter there is the battery pack that is represented in this case by a simplified model. As we have already discussed, the model that has been adopted considers a voltage source whose magnitude depends on the charge level. Plus, a resistive factor is introduced, whose size depends on the battery's SOC in a small extent. However, since this studies have a reasonable level of approximation, the information of the SOC won't be considered for this time. Hence, the dependency of the internal resistance on the SOC is neglected and a safe value, that is the biggest attainable, is considered. In the paragraph, "Batteries for Electric Vehicles", an equation for the value of the resistive component was given and even there the dependency on the SOC was small. Anyway, even by considering the highest SOC, that is 1, the obtained value is  $R=0.019803\ \Omega$ . In that occasion, there were other factors which determine the value of the resistance, like the temperature and the C-rate but their influence hadn't been considered. Even if, these dependencies occur, the value of the internal resistance will not exceed the  $R=0.1\ \Omega$ .

## 6.2 AC/DC Controller

The function of the AC/DC controller is to ensure the correct power flow between grid and the DC side of the charger. This is done by varying the supplied voltage in order to meet the references. Since we are still considering the AC side, it's exactly this the last spot where we can control the reactive power; after this stage, only DC control is applied, hence, solely active power is considered. As previously explained, since certain conditions have been imposed on the model, like a high resistive factor, due to a low voltage grid, here, we are going to reverse the usual power angle/voltage amplitude control. Because of this, by varying the power angle, which is the phase shift between the grid voltage and the voltage supplied by the converter, we are going to control the reactive power, whereas by changing the voltage amplitude, the active power will be regulated. The chosen configuration for this converter is the single phase full bridge which doesn't allow d-q transformation, because in that case a three phase system would be required. The drop control is rather considered and that means, fixed ranges of power variation are caused by fixed ranges of the parameter's variation. We are now presenting the full scheme of the controller; it will be deeply analysed hereafter.

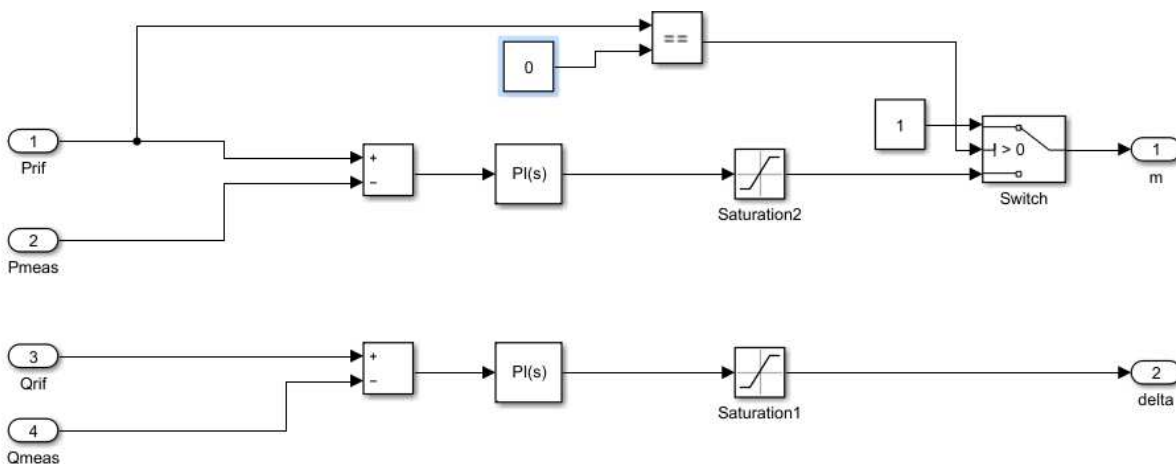


Figure 6.5 AC/DC controller

Here, we have two control lines: one for the active power and the other for the reactive power. A simple feedback loop has been applied: with the measurements of active and reactive power, we are comparing them with the references and this will provide an error at the input of the PI controller. The magnitude of this error will vary depending on the actual measured value and the reference that has been set, so the biggest errors are  $P_{refMAX}$  and  $Q_{refMAX}$  when there isn't power exchange yet, so the measured power will be nil. Therefore, the waveform representing the actual exchanged power will start from zero and reach the reference after a certain time. This means, that at the same time the initial error, which is the maximum, is decreasing and it will be zero when the actual power reaches the reference. As mentioned before, different controllers can be used but in order to have a nil error at the end we have to adopt at least a PI controller. The proportional controller, though can be easily used for the drop control, will have not nil steady state error, hence it won't reach the reference. So, in this case PI controllers have been used and the values of the constants have been assigned empirically.

In order to control the switches, measurements of active and reactive powers have been done; these measurements are provided by a dedicated block that calculates P and Q on the AC side. To do this, the voltage supplied by the converter in on the AC side and the line current are measured.

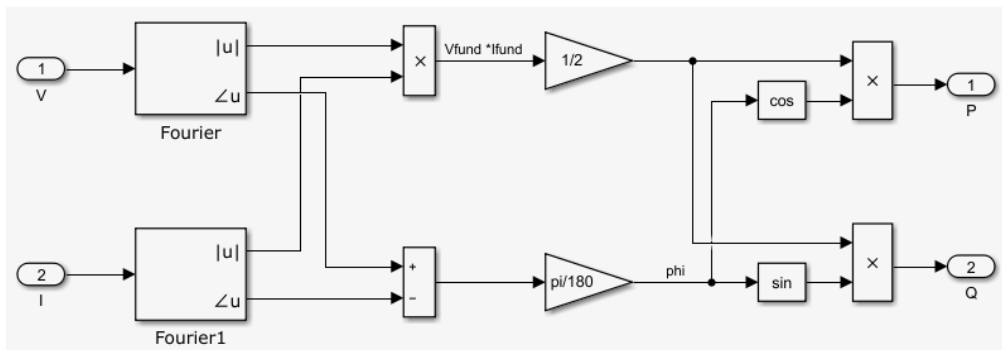


Figure 6.6 Inside the mask of the P,Q measurement block

Once the voltage and current are measured, their fundamental values and their phases are extracted through the Fourier box. Their amplitudes are multiplied and their phases are subtracted; then the phase shift is considered with its sine and cosine and multiplied by the VI product in order to have active and reactive power.

These values are compared with the respective references and the error feeds the PI controller. The analytical representation in the Laplace domain for this controller is the following:

$$C(s) = K_p + K_i \frac{1}{s} = \frac{1}{2350} + \frac{1}{50} \frac{1}{s}$$

where for  $K_p$  and  $K_i$ , the values that have been used are respectively 1/2350 and 1/50 for the active power controller.

So, the output of the PI controller will be a sum of two values: one is directly proportional to the error with the constant that has been set, the other is proportional to the integral of the error, hence, it makes nil any difference between the reference value and the steady state value; the weight of this quantity has been set according to empirical methods, that means, multiple simulations have been done and this value has come out as the best in terms of dynamic response. At the output of these PI controllers, a saturation block has been used, and the necessity of this block is explained hereby. In order to follow the reference value, whenever the error is positive, the contribution of the PI controller will make the output raise. If this variation make the output get over the reference, then the error becomes negative and the controller will decrease the output. Again, if the output goes below the reference the error will be positive and the output will be increased and so on. Step by step, the error will decrease in amplitude with a tendency to become nil, so we'll observe an attenuating oscillation. But in any case the output can't go over certain values cause otherwise the physical response of the converter won't be acceptable: for instance, if we consider the active power section, it controls the voltage amplitude, thus, the amplitude ratio between the sinusoid and the triangular carrier; the latter is fixed at 1V. We want to work in the linear region which means that the amplitude of the

sinusoid doesn't go over the amplitude of the carrier. Otherwise there would be parts of the fundamental period where the signal would be high. This would result in a "loss of information" in the sense that, there is no correspondence between the variations of the reference sinusoid and the variations of the fundamental that underlays in the output. Since the output of the PI controller, that deals with the active power error, is exactly the amplitude ratio, a saturation block that limits the output between  $[-1,1]$  has been used. For the reactive power, that is deciding the power angle, the values used for the constants are  $K_p=90/4000$  and  $K_i=1/10$  and a saturation block that limits the output of the controller has been adopted. This is because the maximum request of reactive power corresponds to the maximum power angle and when the highest reactive power is absorbed/provided there is limited active power exchange due their mutual relationship with the apparent power. In this particular case we have allowed a power factor correction (PFC) of up to 0.89 so the provided reactive power is 50% of the maximum active power. We are supplying/absorbing a maximum of 2kW for the active power and 1kVar for the reactive power.

### 6.2.1 PWM Generator

The outcome of the previous stage are the amplitude ratio  $m$  and the power angle that the voltage supplied by the inverter needs to have. But what is necessary for the control of the single phase full bridge are the four switching signals for the IGBTs. Given that, Unipolar PWM allows a limited harmonic content this is what is going to be implemented in the next stage. Having the two parameters in input, that are the amplitude ratio and the power angle, there is the necessity of a phase measurement in order to know what it the phase of the grid voltage. The power angle is the phase difference between the grid voltage and the inverter's voltage, therefore, the power angle has to be added to the grid voltage's phase. However, since the grid voltage is considered as a reference, usually it's phase is roughly nil, so the measurement of this parameter is done just to ensure a certain level of accuracy. Hereafter, we are presenting the strategy adopted for generating the switching signals.

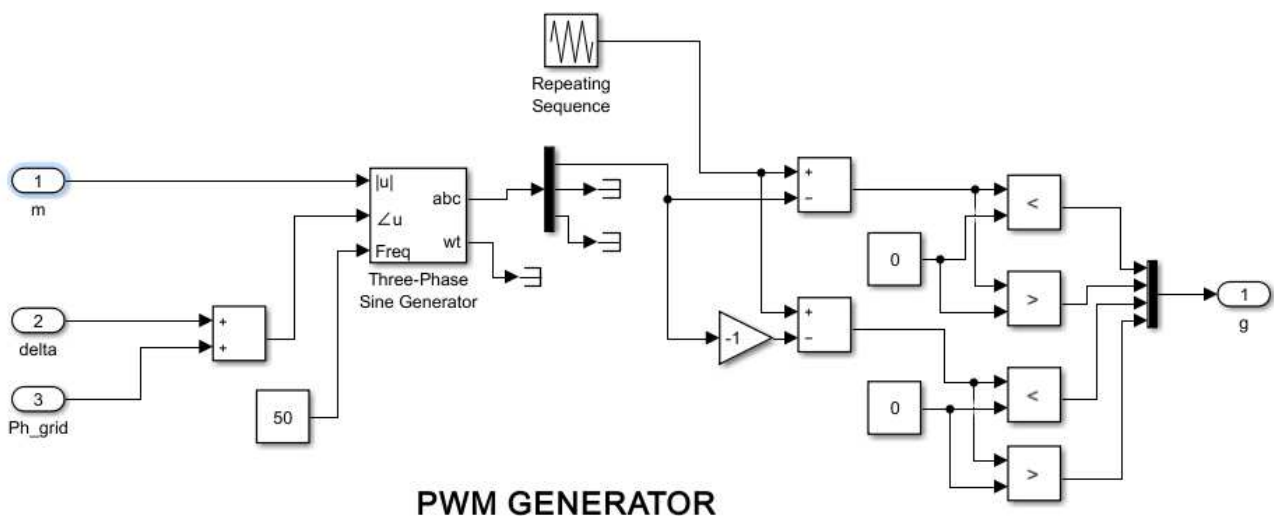


Figure 6.7 PWM Generator

Once the required variables and measurements have been collected, for the previous explanation, the phase of the grid and the power angle are summed together and the result along with the amplitude ratio feeds the Three-Phase Sine Generator. This block generates three sinewaves with a phase shift of  $120^\circ$  between each other, according to the provided parameters: the amplitude of the sinewaves will be dictated by the amplitude ratio  $m$  and the phase shift of the phase a is given by the phase parameter, hence, the other phases will have a phase shift of  $120^\circ$  and  $240^\circ$  starting from this initial value. A frequency of 50Hz has been set for this sine wave, which represents the modulating signal, so the fundamental component that will be contained in the alternating voltage of the AC/DC converter will have this frequency, or in other words, a period of 20ms. The output of this block is a vector containing the signals referring to the three phases so a de-multiplexer block has been used to separate each one from the others, and since we are controlling a single phase bridge, only the phase a is required and this is why terminators have been connected to the other phases.

In the Unipolar PWM the two legs of the bridge have opposite modulating signals, hence, the sinusoid obtained from the sine generator is inverted and fed into the row of the second leg. Once these two sinusoids are obtained, they are compared with the carrier signal that is the same for both the legs. This signal is a triangular wave that goes from -1 to +1 in a period given by the frequency that has been chosen. In this case the frequency is 20kHz, in accordance to the real situation where IGBTs are switched at this frequency at maximum. Thus, the period is 50µs. Since a Repetitive Sequence Block has been used we have to define the behaviour of the signal in a period and this is going to be repeated in the following periods.

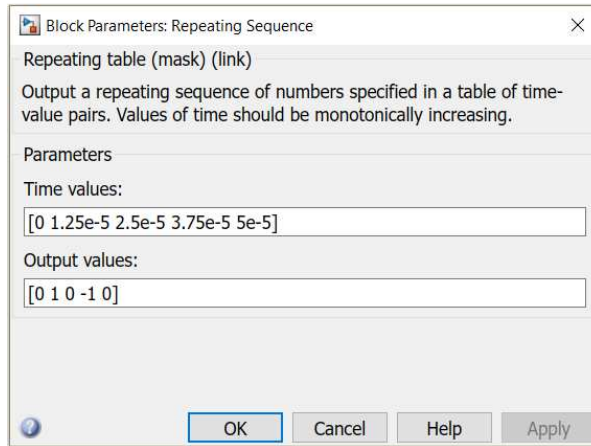


Figure 6.8 The Repetitive Sequence Block mask for SPWM

As can be seen, the period has been divided in four parts, that represent the variations of the carrier signals and for each part, the initial value and the final value have been defined. The outcome of this block is the following.

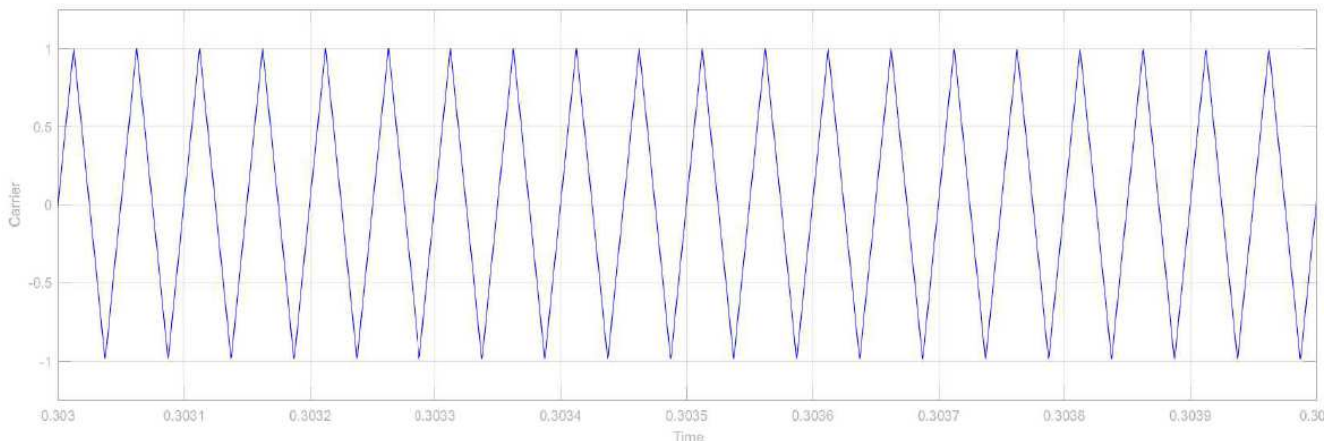


Figure 6.9 Carrier for the SPWM

Going from 0.303s to 0.3035 there are ten periods of the signal, that means a single period is made by:

$$T_c = \frac{0.3035 - 0.303}{10} = \frac{0.0005}{10} = 5 * 10^{-5} s. \quad (6.8)$$

This signal is compared with the two sinusoids: whenever the modulating signal is higher than the carrier, the output is high whereas whenever the carrier is higher than the sinusoid the output is low. So the sinusoid is subtracted from the carrier and the result is compared with zero: so when the result is lower than zero the output is high, otherwise is low. This is for the switches positioned above. For the switches positioned below the operation is opposite, hence, when the result is higher than zero the output is high. At the end, four Boolean signals are obtained where two of



them are the opposite of the others. These signals are put in a single vector signal with a multiplexer and then, used to feed the single phase bridge. The resulting switching signal from the Unipolar PWM is presented below.

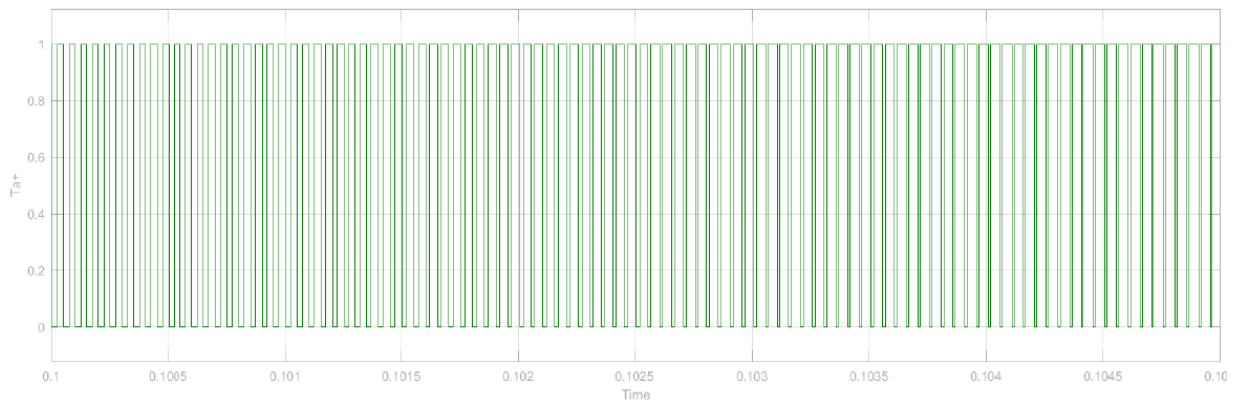


Figure 6.10 Firing signal of the switches with the SPWM

As can be seen the width of the pulses changes according to the amplitude of the sinewave; this is exactly what the Pulse Width Modulated signal should do. We are presenting what is the result of the Unipolar PWM control in regards of the alternating voltage of the AC/DC converter.

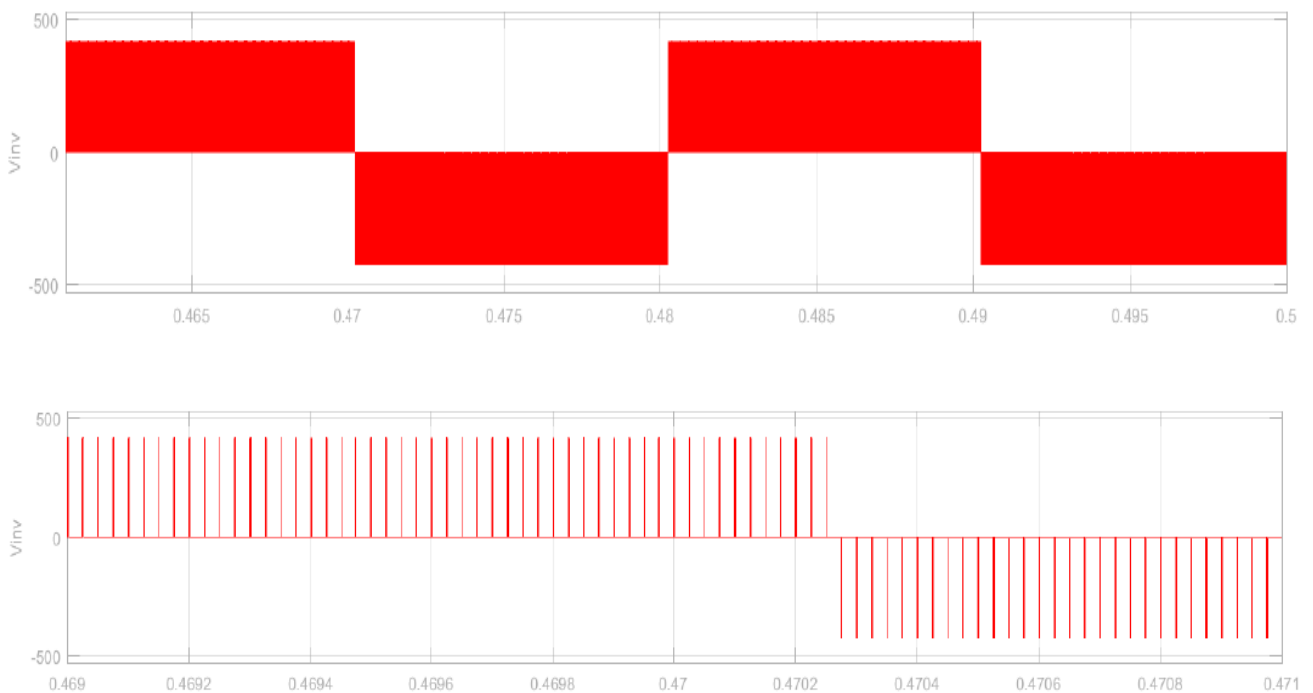


Figure 6.11 (a) Output voltage of the single phase bridge with SPWM; (b) Zoom of the output voltage

As expected the voltage is alternating and periodic and one period is 0.02s. The waveform consists of pulses that changes their width but this time they go also in the opposite semi-wave, because the voltage has to be alternating. The amplitude of these pulses will be adjusted according to the active power exchange that we want to be exchanged between grid and battery and the angle between the fundamental of this waveform and the grid voltage will be regulated according to the reactive power exchange. Specifically, we are charging a big capacitor which has been put in the DC bus and this keeps the magnitude of the voltage constant at the DC side. In the alternating side the magnitude of the pulses depends on the voltage that has been set at the DC bus. There is a ratio between the peak value of the AC voltage and the average value of the voltage at the DC side, that is  $\frac{v_{peak}}{v_{avg\_DC}} = \frac{2\sqrt{2}}{\pi} \cong 0.9$  (6.9) for this bridge.

Regarding the V2G mode, when we are reversing the power flow, which means that the battery is discharging in order to supply the grid, a negative value for the reference will be imposed. This is because the convention that has been adopted considers **positive** those **currents that goes from the grid to the battery**. So in the V2G mode the whole charger, which includes AC/DC and DC/DC converters, is set as generator.

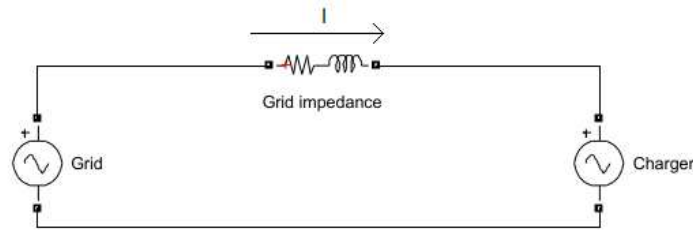


Figure 6.12 Grid and charger voltages in G2V

In this case the G2V mode is on, and the battery is set as load and its absorbing power. In the V2G mode, since an opposite power reference and consequently an opposite voltage reference is imposed, the whole charger is set as a generator and this time the battery has to supply power.

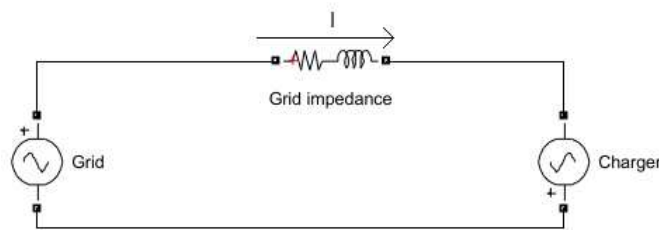


Figure 6.13 Grid and charger voltages in V2G

For the reactive power the power angle that will be provided to the sine generator will be negative, so that when it's added to the phase of the grid it will result in a negative phase. This means that the phasor which represents the converter's voltage is in advance in respect of the phasor representing the grid voltage.

## 6.2 DC/DC Contoller

After the DC bus a second converter is used in order to regulate the voltage ratio between the battery and the DC bus according to the power exchange, so the active power and the reactive power exchanges are independent from each other. The controller for the DC/DC converter is the following.

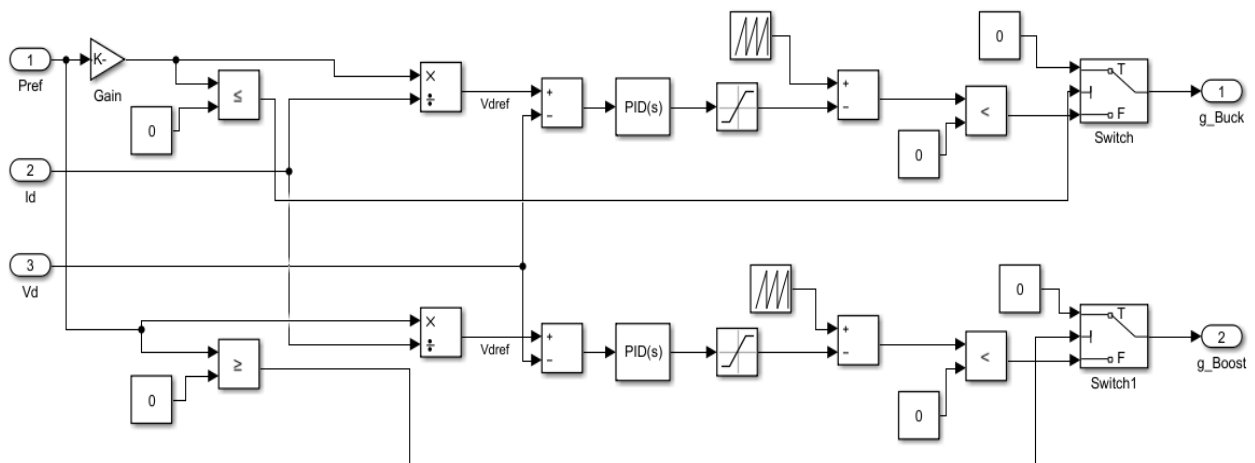


Figure 6.14 DC/DC controller

Also for this controller some measurements are required in order to supply the correct switching signals for the two switches. As previously said, this DC/DC controller consists of two independent parts: one is used to charge the battery with the power supplied from the grid; the Buck converter. The other is used to discharge the battery in order to provide power to the grid; the Boost converter. The configurations of these converters and how they increase or decrease the average value of the DC output voltage have been previously explained; now we are focusing on how to switch the two parts properly. The main duty of this converter is to allow the active power exchange between the DC side of the AC/DC converter and the battery ensuring a reasonable DC bus voltage. Moreover, it has to allow us to use batteries with different nominal voltages and have anyway the same operation. Besides, since the assumption of a highly resistive grid, with its consequences, is partially true, this implies that “cross-influences” are present: in a small part the active power exchange is influenced by the power angle and reactive power exchange is influenced by the voltage amplitude. Consequently, without the DC/DC converter, if we ask the charger to establish a certain power exchange, this will result in a certain voltage amplitude, but due to the minor dependency of the reactive power on this parameter also the reactive power exchange will be influenced. In order to avoid this mutual interference, the DC/DC converter is used, so the correct voltage ratio between DC bus and battery is calculated and maintained. In this way, the reactive power exchange is independent from the active power exchange.

Only one between the two configurations is used at a time, so the other must be switched off. This is the reason why, right from the initial stage the active power reference is compared with zero and whether it's positive the Buck mode is used and the respective switch, the IGBT1, is switched on and off while the other configuration, referring to IGBT, is constantly kept switched off. But if the active power reference is found negative, which means discharge of the battery, the Boost configuration is switched on and off whilst, IGBT1 is kept switched off. This is the duty of the selectors put at the end, which verify whether the power reference is positive or not and according to this give an output that is either controlled or nil.

Once the correct switch corresponding to the correct configuration has been selected, the active power reference is divided by the current absorbed by the battery, which is one of the information that this controller needs. The result of this operation is the reference value of the voltage, and it's compared with the actual value of the DC bus voltage, that has been measured at the terminals of the DC bus capacitor. The comparison gives a voltage error which feeds the PID controller. Like the previous ones, the duty of these controllers is to give an output that is proportional to the error, the integral of the error and the derivative of the error. Ultimately, the purpose of these controllers is to make nil the error, any possible offset and fast variations of the voltage. Here, there are three constants that weighs the three parts of the controller and also in this case they have been chosen empirically. Ideally the transfer function has to be known analytically so that a tailored controller can be designed. But this is often unachievable, due to the high complexity of the system, hence, empirical methods are used. The values that have been assigned for the constants are:

$$K_P = \frac{5}{325}; \quad K_I = 2; \quad K_D = \frac{1}{10000}.$$

Specifically, the reason why such value for the proportional part has been used, is because its function has been considered. This part provides an output that is proportional to the feeding error: the maximum error is when the system is still at its idle state and the full power exchange is requested. Whereas, the maximum value for the output dimension, has been set to 5.

So, as just said, the output of these controllers represent the duty cycle  $D$ , which is the fraction of the period where the signal has to stay high. An increase of the duty cycle, because of a positive error, means an increase of the time for which the signal is high, consequently the time for which the IGBT is switched on, hence an increase of the average value of the output voltage. Whereas, a decrease of the duty cycle, because of a negative error, corresponds to a decrease of the time for which the signal is kept high, thus, the time for which the IGBT is switched on and this results in a decrease of the average value of the output voltage.

The duty cycle is then compared with a repetitive signal, which is in this case a saw-tooth signal at high frequency. There is no restriction in the choice of the frequency, in the sense that, it doesn't have to match the one of the carrier of the AC/DC converter. Since there is this freedom we will try two different frequencies, one that matches the AC/DC

controller and the other is going to be the double: 20kHz and 40kHz. Also in this case the repetitive sequence block has been used and the following setting imposed.

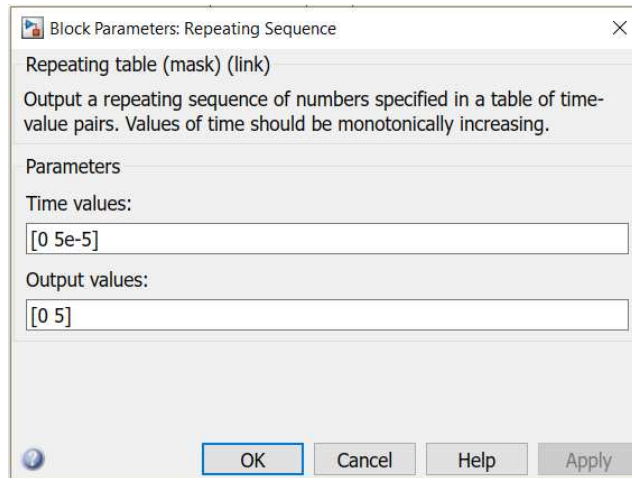


Figure 6.15 Parameter mask of the Repetitive Sequence block for PWM

As can be seen, the imposed period is  $500\mu\text{s}$  that corresponds to a 20kHz frequency. The outcome of this block is the one that is presented hereafter.

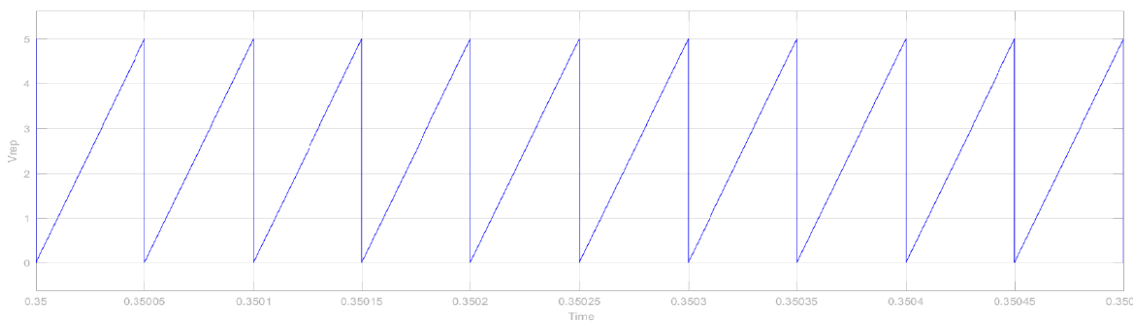


Figure 6.16 Carrier signal in PWM

Again the correspondence of the set period of  $50\mu\text{s}$  with the actual period of the signal is verified.

This signal is compared with the duty cycle: when the duty cycle is higher than the saw-tooth, the output signal is high, whereas, whenever the saw-tooth signal is higher than the duty cycle, the output signal is low.

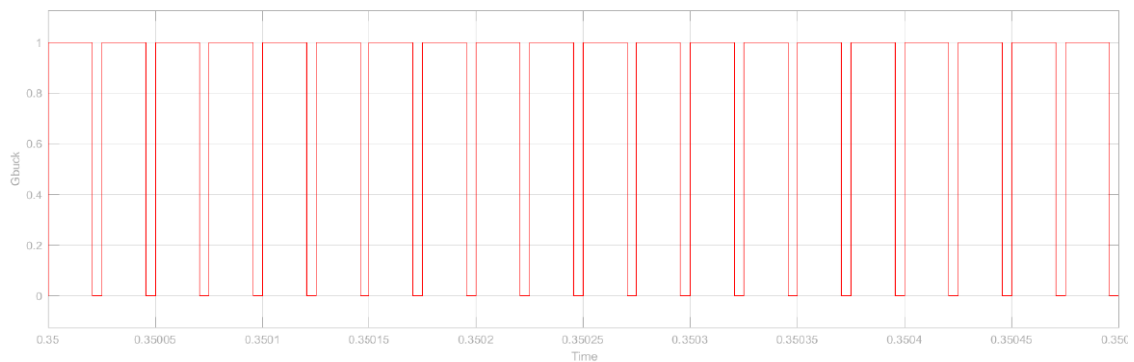


Figure 6.17 DC/DC converter's output voltage with PWM

The switching signals for the IGBTs vary between zero and one, with a frequency decided by the PWM

## 7 Simulations

### 7.1 G2V Simulations

We are going to simulate the behaviour of the designed charger against certain power references, in order to verify if it is able to follow them. In this case the grid is supplying the battery through the charger, and the convention that has been used considers positive the power exchanges that are involved. The grid is represented by an alternating voltage source whose RMS value is 230V, and it's followed by the grid impedance which has been previously quantified. The capacitor used for the DC bus has the size of 10mF. It's a huge capacitor, because normally for low voltage tests capacitors of maximum mF are used, and this is what we are going to do in the practical test, but in the simulations we can adopt even those not economically efficient choices just for the sake of the quality of the results. Here, we want to minimize the voltage and power ripples in order to interface properly with the battery. In fact, the battery can't bear high ripples which would procure damages, both in terms of reduction of the maximum available capacity and acceleration of aging. Initially, for the DC filter, the design values for the components will be used, but later, we will try to change those values in order to benefit its outcome in regards of voltage and current ripple, and we will study the consequent changes in the overall behaviour. In these simulations, positive active power exchanges will be asked to the charger, the level will be frequently changed and the charger will have to chase the requested value both in the grid side and in the battery side.

For an initial validation of the model, a fix active power reference and then a reactive power reference will be imposed to the charger and it will have to reach these values at the steady state. The first power references for the charger will be  $P_{ref}=2000W$  and  $Q_{ref}=0Var$  and the simulation time is 2s.

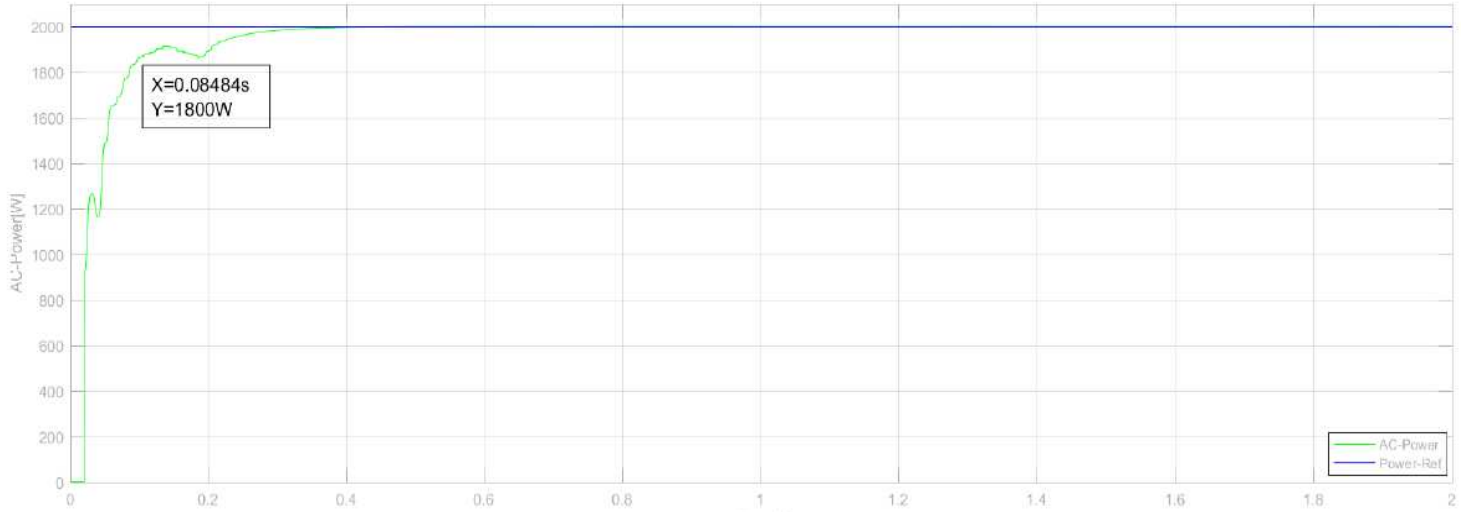


Figure 7.1 Active power exchanged with the grid against a reference of 2000W

As can be seen, the behaviour of the measured active power exchanged with the grid is monotone except just two spots. The measurements are taken at the AC/DC converter's terminals, where it's connected with the grid. In accordance to the definitions given earlier, the Rise time  $t_r$  is the time required to cross the 90% of the steady state value. Here, we are asking a steady state value of 2000W, hence, the 90% of this value is 1800W. As depicted in the figure we have a Rise time of  $t_r=0.08484s$ . This corresponds to the Settling time as well, that is the time required to enter in a region whose width is less than 10% of the steady state value, because in this case, once the power has overcome the 90% of the steady state value, it doesn't go under that anymore. This is a nice behaviour, considering also the relatively low Rise time; however, the two spots where the active power changes its trend affects the correct behaviour, because if we consider the matter from the battery's point of view, those are spots where the battery from being charged, is discharged and kept charging again. But since these events are only a few and their magnitude is

limited, they don't affect the overall operation in a significant way, so this trend is acceptable. Another thing to notice is the correct following of the reference: since PI controller have been used, the actual power follows perfectly the reference at the steady state, in fact the steady state error is nil.

In the next figure the reactive power is represented whose reference has been fixed to 0.

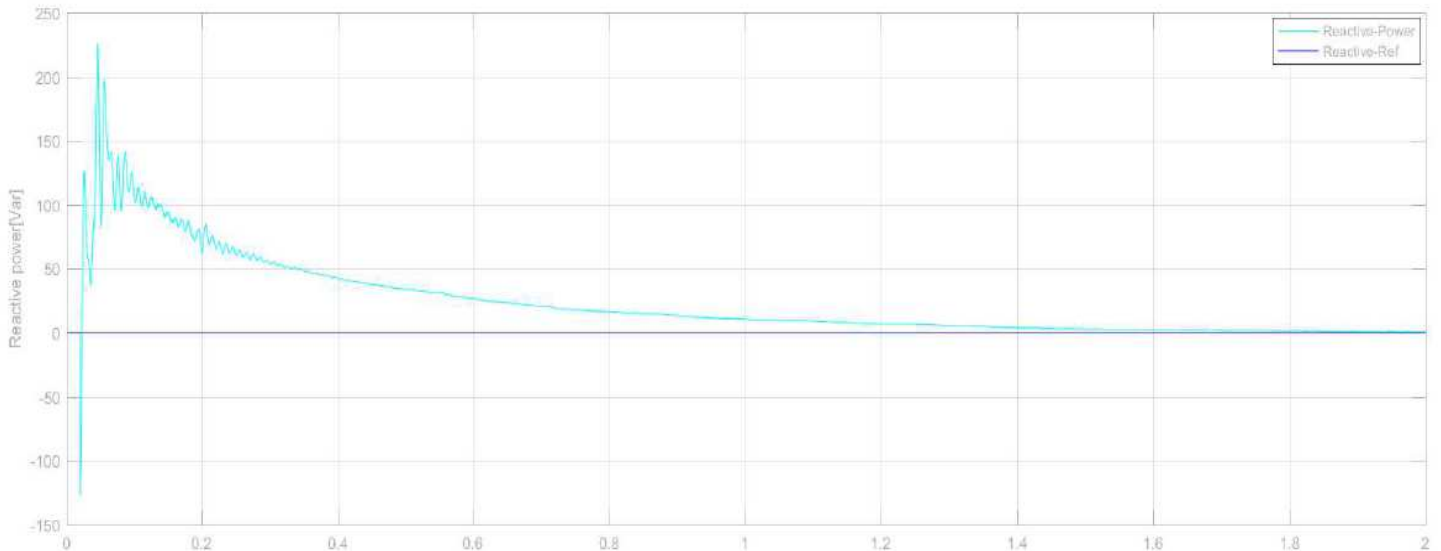


Figure 7.2 Reactive power exchanged with the grid against a reference of 0Var

As can be seen from the figure, the control system is able to effectively control the reactive power to zero in the steady state. However, there is an initial reactive power that is not nil, but the magnitude is really small considering that highest peak is lower than 250Var and for most of the time the reactive power is below 100Var. There is also a negative peak that reaches -130Var but due to its singularity, the small value and the negligible duration these fast variations won't be considered. After 0.6s the reactive power absorbed is below 25Var and this is acceptable.

This behaviour is due to mainly two factors: we have represented the grid impedance how it should be done; with a resistive component and an inductive component. As we already said we wanted to show the actual situation of the low voltage grid, which has high resistive component compared to the inductive component. So, the inductive component is already small but still present. This implies a request of reactive power from the inductive component, at least in the initial settling phase of the system that is when the system, starting from an idle condition tries to reach the imposed condition. In fact, the reactive power decreases significantly after roughly 0.2s which coincides with the settling time of the alternating current absorbed by the charger. In a pure inductance, the voltage at its terminals is completely dependent on the current's variation. If the current is constant, then there is no voltage at the terminals of the inductor, thus, it can be considered as a short circuit. But, if the current is changing then there is a not negligible  $\frac{di}{dt}$ , hence, there is a voltage at the inductor's terminals and there is a request of reactive power. Another factor that influences this behaviour is the DC bus capacitor. Since no initial voltage has been imposed on it, the capacitor will start the operation being charged at the battery's voltage value, because in the initial instant there is no current and no voltage; the only component that is active, is the battery. So the capacitor is under a voltage of 100V and starts charging; the voltage will increase. This is what happens to the DC bus voltage when the system has the so called black start: starting from an idle condition. But, soon the control system intervenes and settles the DC Bus voltage to an appropriate value, depending on the power reference. Also the DC bus voltage gets stabilized after 0.2s as can be seen from the following figure.

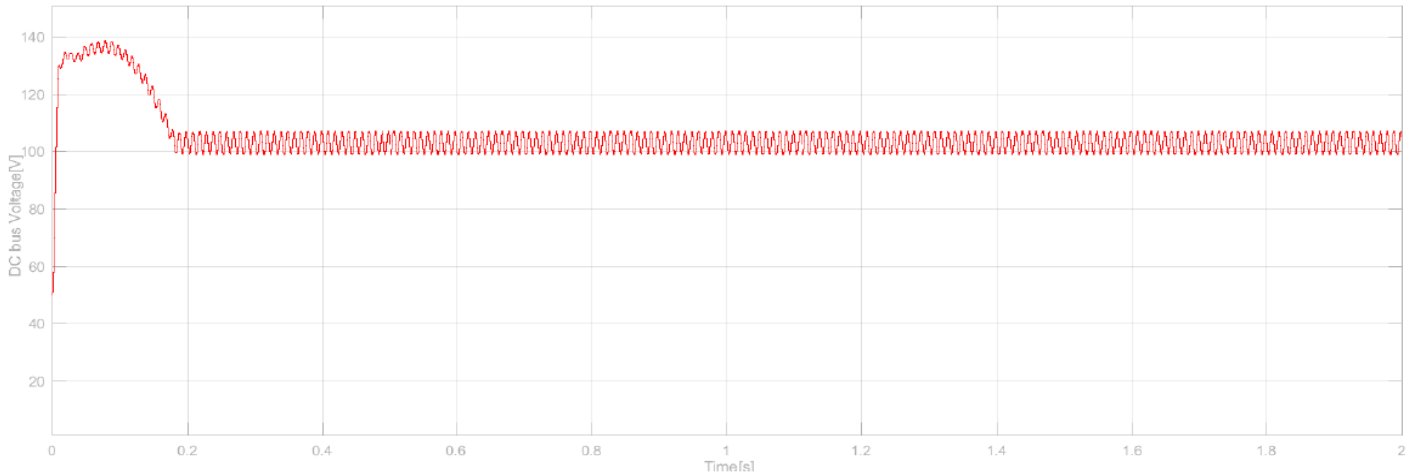


Figure 7.3 DC Bus voltage

Once settled, the voltage oscillates between 99V and 107V:  $V_{DCaverage} = \frac{99+107}{2} = 103V$ . The control system increases the voltage of the DC bus in order to allow active power exchange. The voltage ripple is therefore:

$$v_{ripple-pk-pk} = 107 - 99 = 8V$$

This value, compared with the steady state value is roughly 8% which might be acceptable in some electric systems, but since we are working with batteries, that are delicate devices, we need to reduce the ripple as much as possible. Therefore, an increase of the capacitor's size is suggested.

The following figures represent the voltage and the current of the AC/DC converter in the alternating side.

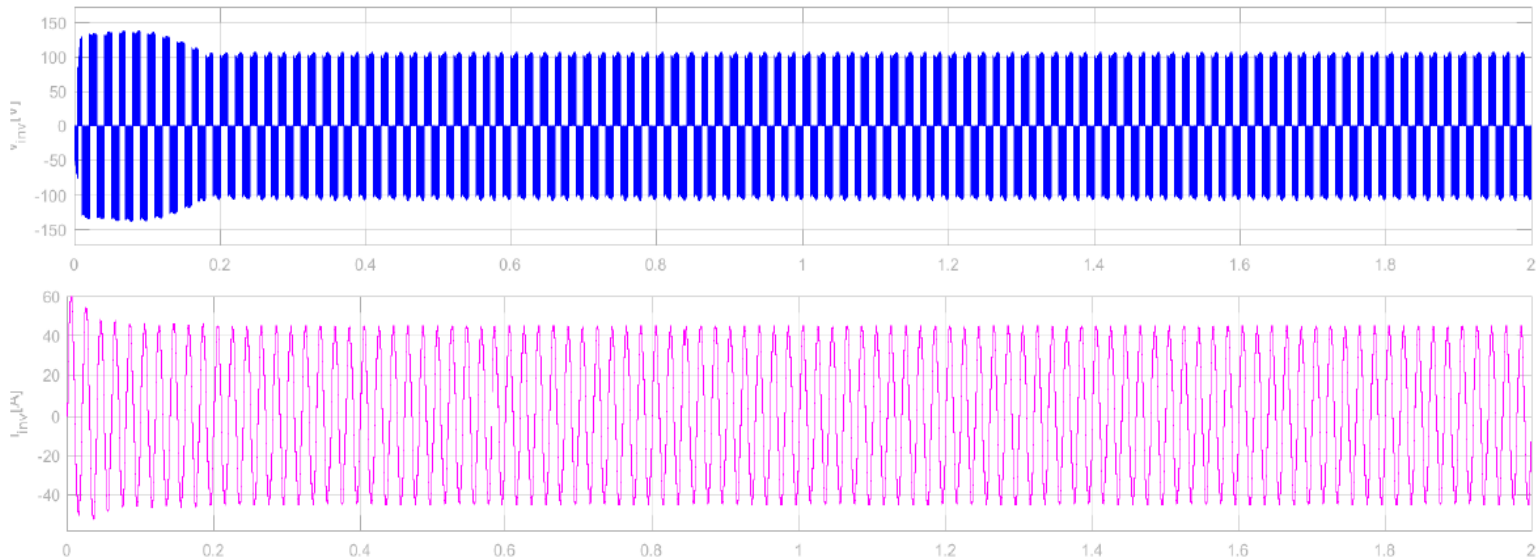


Figure 7.4 Converter's AC voltage and current

As previously said a settling time of 0.2s is required from the system in order to reach a stable condition. In order to have a reactive power exchange, there is a slight phase shift between the fundamental of the converter's voltage and the alternating current, that is given by the inductive component of the grid impedance. This is roughly  $\tan^{-1}\left(\frac{0.754}{5.24}\right) = 8.19^\circ$  and that's why there is the initial reactive power exchange. After the initial phase the control system is able to effectively regulate the reactive power exchange to zero by controlling the power angle.

Once the AC side has been declared complying to the requirements, results from the DC side need to be analysed. Here, we are measuring the DC power transferred to the battery by the DC/DC converter, hence the power measurements are taken at the terminals of the battery. The current through the battery, that is also the current through the filter inductor is measured and multiplied by the battery voltage. The power calculated in this way is the active power, because we are in the DC side of the charger, and it will have a ripple with double frequency compared to the current or the voltage. The following figure depicts the active power exchanged with the battery with a reference of 2000W.

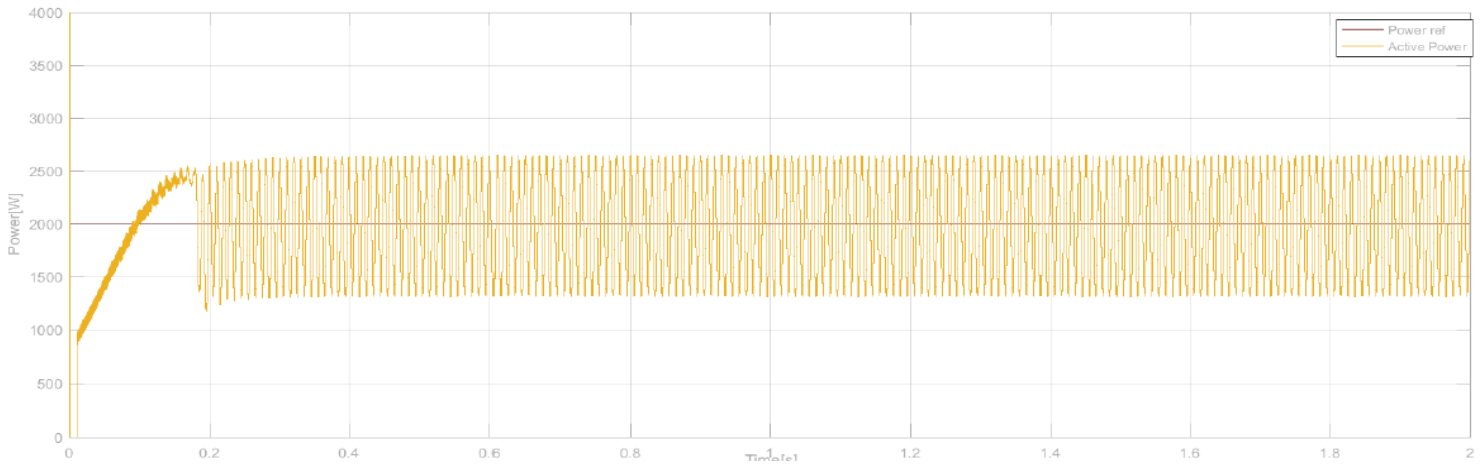


Figure 7.5 DC power supplied to the battery

As can be seen there is a huge ripple in the active power in terms of amplitude. This is totally unacceptable, considering that the peak-to-peak value of the ripple, once the behaviour has been stabilized, is:

$$p_{ripple} = 2646 - 1316 = 1330W;$$

It is the 66.5% of the steady state value. Supplying the battery with this kind of power waveform would damage it seriously. An excessive heating that might lead to burning, a significant reduction of the total capacity as well as a huge increasing of the internal resistance are the most optimistic consequences. It's likely to be worse than that.

The reason behind this wrong behaviour is the current supplied by the DC/DC converter. As we previously said, the current that goes in the battery, goes also through the filter inductor. The duty of this inductor is to smooth the shape of the current by eliminating the biggest part of the ripple; a residual ripple is expected at the output but the magnitude should be acceptable. This is because, inductors oppose to current variations by developing a voltage at their terminals. This undesired outcome leads to the conclusion that the size of the inductor was not enough. The DC current supplied to the battery is represented in the following figure and it clears any doubt.

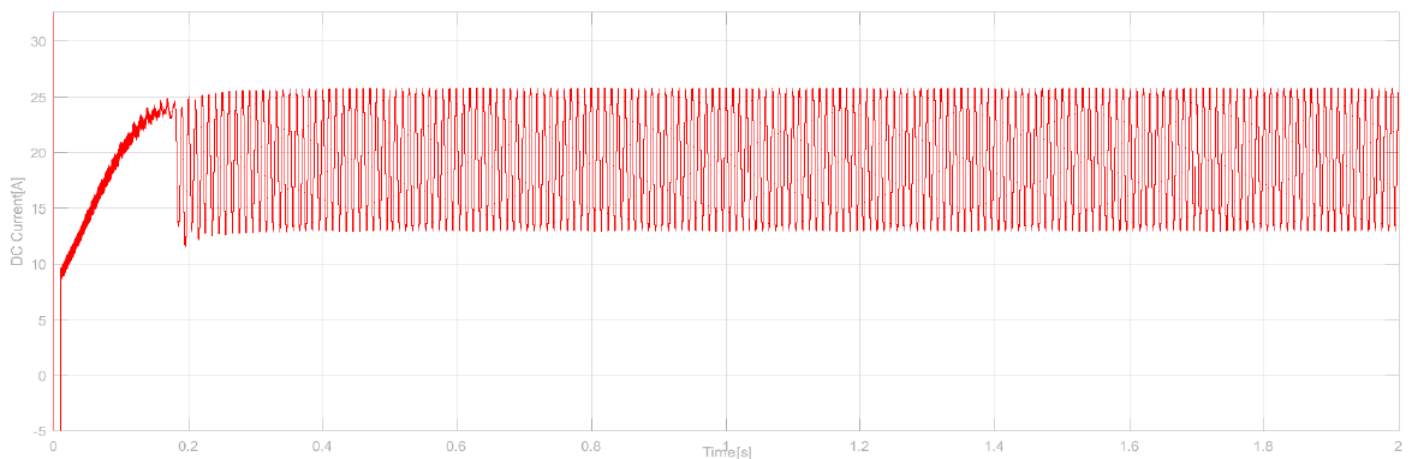


Figure 7.5 DC current feeding the battery



The initial transient can be neglected because of its small duration and the initial settling of the system from an idle condition to an active condition. The current ripple is excessive, and this is why the power ripple was way more than the expected. Here there is a peak-to-peak value for the current ripple of:  $i_{ripple} = 25.8 - 13 = 12.8A$ . This is the 65% of the steady-state value and it's inadmissible. In sight of these results it's clear that some changes have to be done to the system and the most immediate one is the inductor's size. We are increasing the size from 1mH to 10mH. The active and reactive power exchanged with the grid are represented hereby:

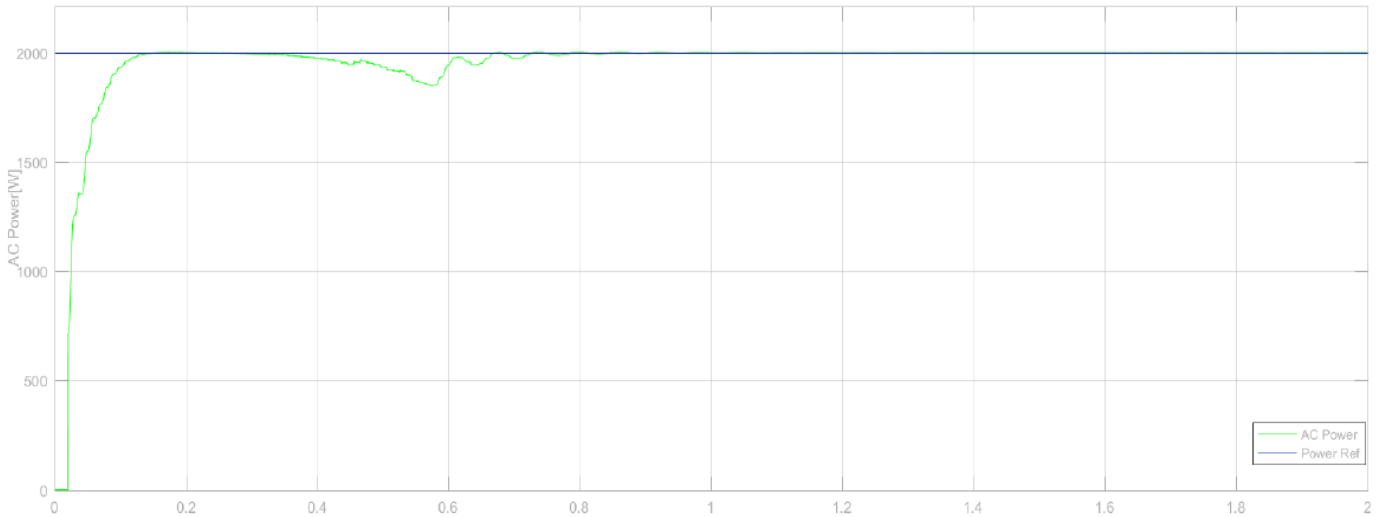


Figure 7.6 Active power exchanged with the grid against a reference of 2000W

Some changes have occurred: the initial phase is much cleaner than before but after reaching the steady-state value the actual power seems to go down. This abnormal behaviour continues till late 0.5s, then the control intervenes and pull the power up. Moreover, a small oscillation is observed that lasts till 1s degrading in the amplitude, but this is not a big deal. The main issue here is the decreasing of the power exchange after reaching the steady-state value and this is due to the increased inductor's size. In fact, the size of the inductor has been increased by a 10 factor and this affects significantly the transient behaviour. After roughly 0.2s the DC Bus capacitor has been charged and the voltage starts to stabilize. While getting close to the 0.5s, the effect of the inductor becomes more relevant compared to the capacitor. There is an oscillation factor that intervenes in this time and this is carried in the AC side too.

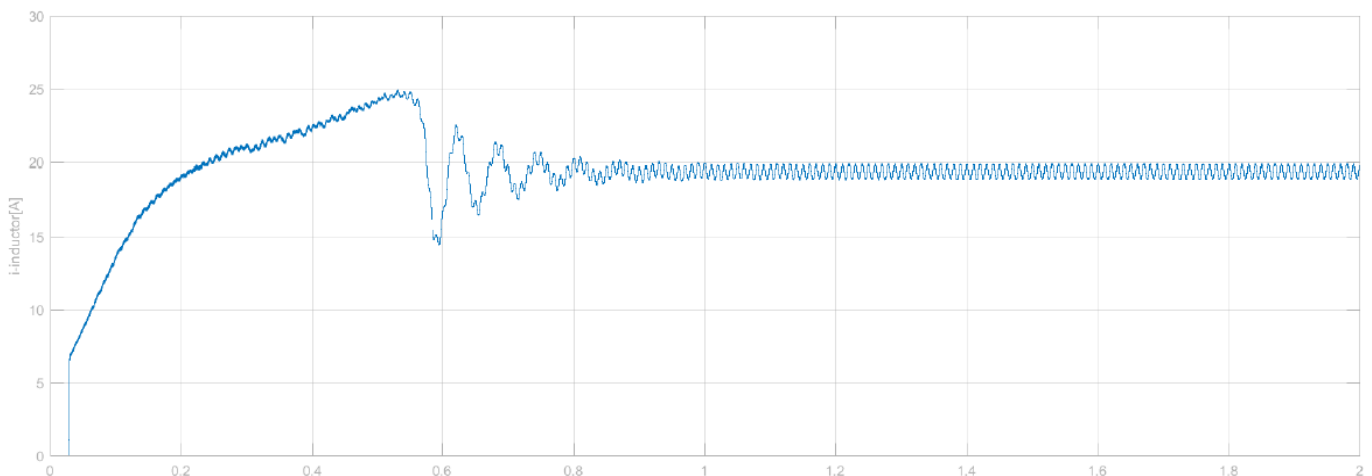


Figure 7.7 DC current feeding the inductor

As can be seen, both the oscillations terminate after 1s; this means the AC side is also affected by events that happen in the DC side.

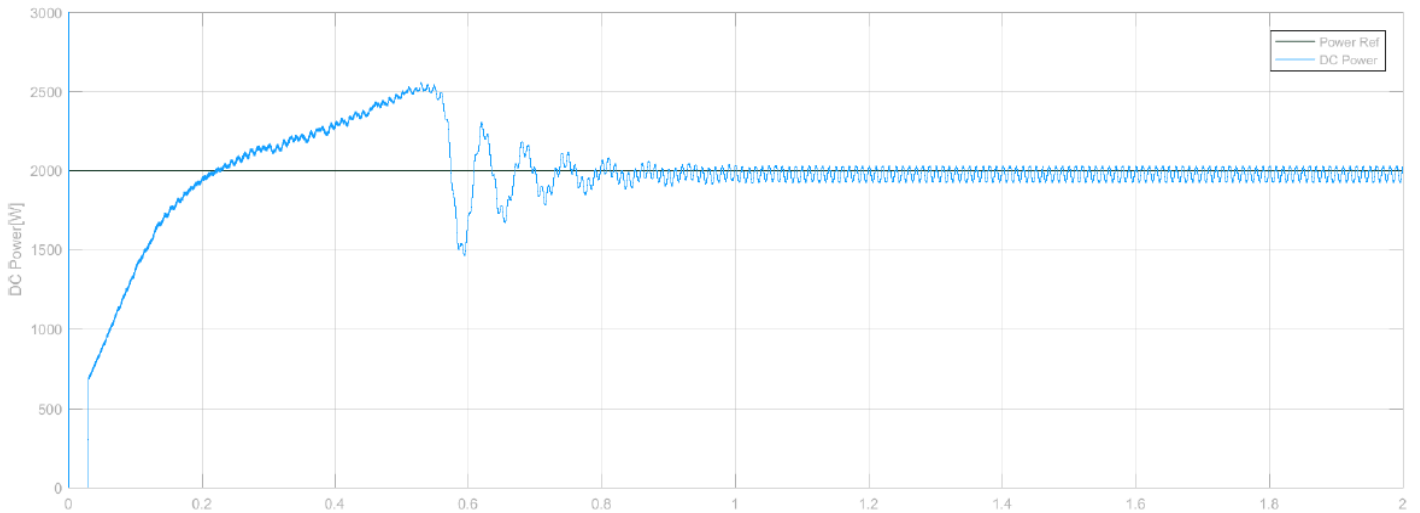


Figure 7.8 DC power supplied to the battery

The figure above represents the DC power exchanged with the battery. Compared to the previous situation this behaviour is definitely better but there are some differences. A significant overshoot in respect to the steady state value is present and the relative entity is about 25% of the steady state value. This is a huge value but expected because of the large inductor that has been used. On the other hand, the ripple has enormously decreased and currently there is a peak-to-peak value of:  $p_{ripple} = 2030 - 1926 = 104W$  that is approximately 5% of the steady – state value, which is acceptable. Furthermore, oscillations are observed and these are due to the high LC product of the filter circuit. There are two ways to clean the shape of this waveform further: a better control, that considers the current that goes through the inductor, the power absorbed by the inductor, the current of the capacitor, has to be implemented. But because our aim is to design a control focused on the steady state condition we won't continue further in this direction. The other option is to keep increasing the size of the components and these will shape the waveform better. By increasing the size of the inductor the current will be smoother and this will reflect on the power ripple, whereas, by increasing the size of the capacitor the voltage will have less ripple. But at the same time the LC product will increase and consequently the time constant of the system, which means that it will take longer to reach a stable behaviour because oscillations will occur. Moreover, other undesired events like undershoots and overshoots will be much more significant. The most efficient trick would be, to increase the switching frequency of the IGBTs so that the filter is more effective on the harmonics. This is the right thing to do, considering that we are simulating a model, but in practical tests, this frequency is limited from some constraints such as the switch's limits and the sampling accuracy.

The control approach is again able to control the reactive power to zero and no substantial changes are spotted in the new waveform that is presented hereafter.

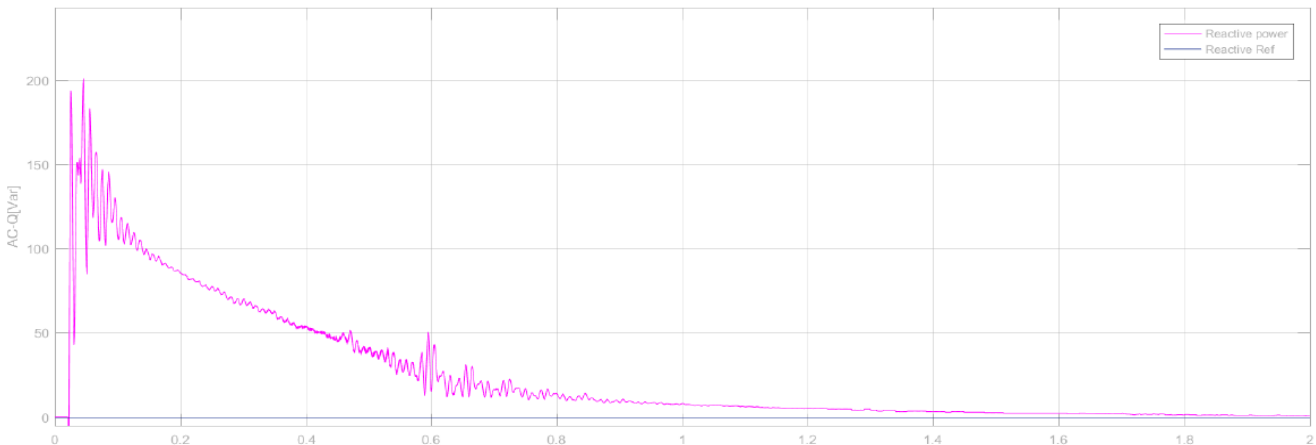


Figure 7.9 Reactive power exchanged with the grid against a reference of 0Vvar

Again there is a slight oscillation in correspondence of 0.6s and as explained before, this might be due to the energization of the inductor; this wasn't present before because the size of the inductor was ten time smaller.

We want to prove that the control system that has been designed, is able to control active power and reactive power independently. So, if until now we have been imposing not nil references for the active power and nil references for the reactive power, from now we will try the opposite approach. The active power will be asked to stay nil whereas the reactive power will be controlled to a predefined value.

So let's start asking a  $Q_{ref}=1000\text{Var}$  and a  $P_{ref}=0\text{W}$ ; the simulation time is again 2s.

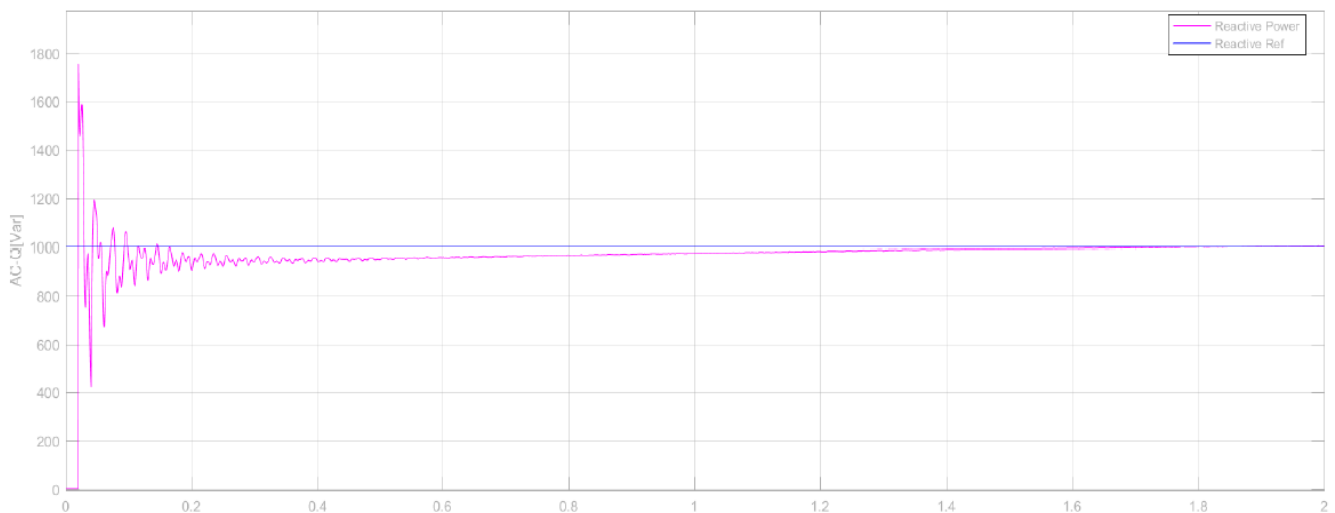


Figure 7.10 Reactive power exchanged with the grid against a reference of 1000Var

As can be seen some oscillations occur but their magnitude degrades quickly; a major peak is observed in correspondence of the very beginning and the magnitude is about 1750 Var; this oscillatory behaviour is mainly due to the control approach. In the reactive power chain, only PI controllers have been used, where the derivative part is missing. This part shapes the waveform correctly by opposing to rapid variations of behaviour, and consequently the behaviour is much smoother and only monotone. However, since the steady state behaviour is correct we won't investigate further in this direction. We said that this control approach allows us to control active and reactive power independently, thus, since a reactive power reference has been imposed, in order to prove such operation, the active power has to be taken in account. Therefore, we are presenting the active power below.



Figure 7.11 Active power exchanged with the grid against a reference of 0W

It's true that a strange behaviour, like the huge peak of active power, is present but by investigating carefully about the possible reason, it will be clear that, this is reasonable. Again, the blame has to be given to the black start, that is the settling of the system from an idle condition to an active condition. Specifically, the component that is involved in this case, is the DC Bus capacitor. Initially it's empty, with no charge, thus, once the system is powered there is a sort of power funnel, between the AC/DC and the DC/DC converters. Both, grid and battery provide charge to the capacitor and due to its large size, the transient involves nearly 2.3kW. This is because, in order to charge such a huge capacitor, a significant current is drained from the grid just to increase the voltage of the capacitor to level that doesn't allow active power exchange anymore.

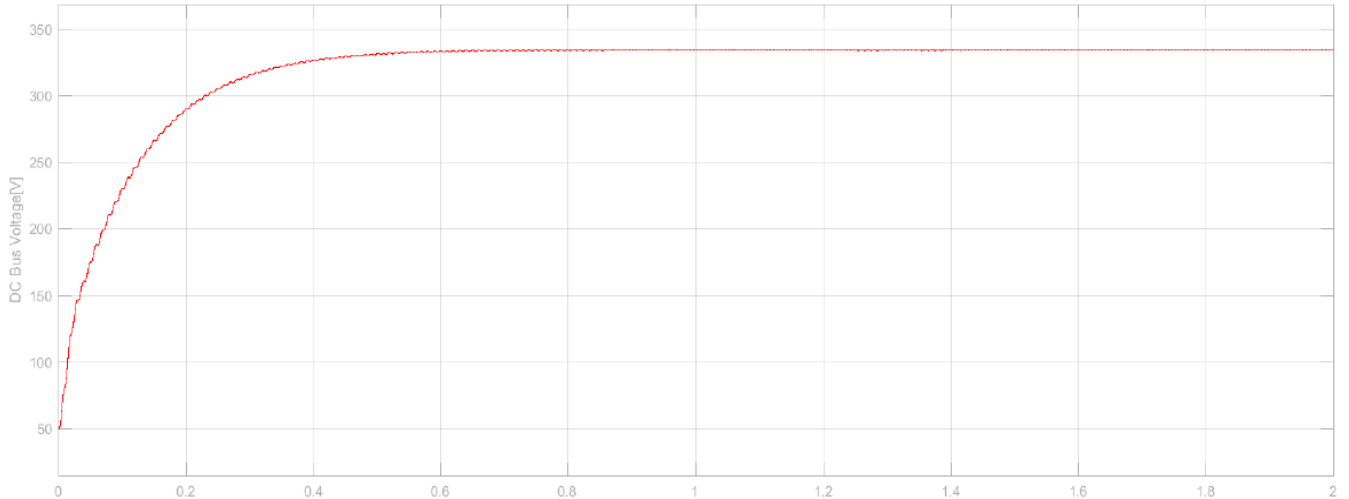


Figure 7.12 DC Bus voltage

In fact, if we have a look at the RMS values of the two voltages that are involved here, which are the grid voltage and the voltage supplied by the converter, we'll see a reasonable difference initially, but more the DC bus voltage rises the less current flows in the AC link.

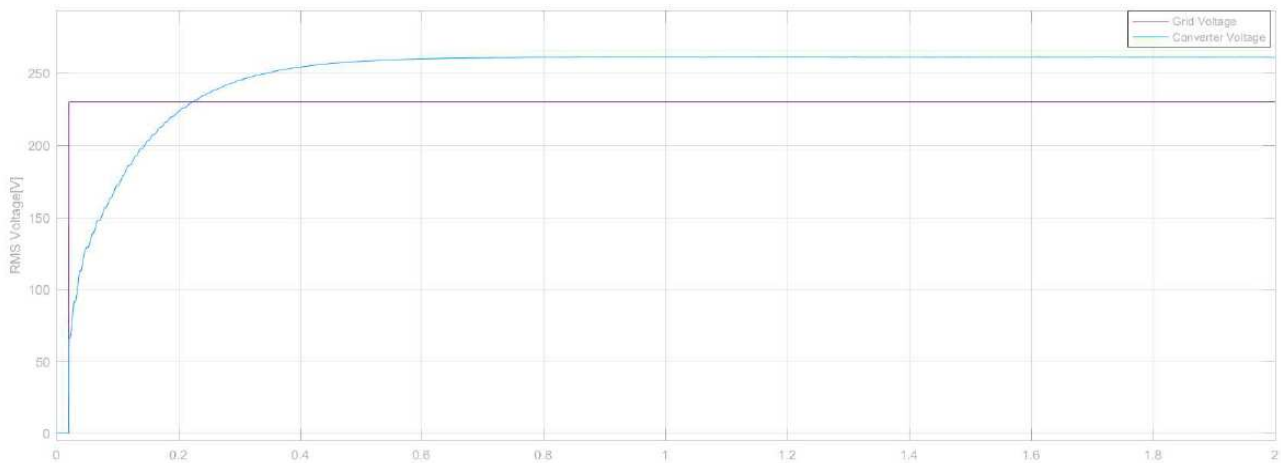


Figure 7.13 rms values of grid and converter's voltages

The value reached by the converter's voltage is 262V. The steady state value for the DC Bus voltage is 335V.

$$V_{AC-peak} = \frac{335}{\frac{2\sqrt{2}}{\pi}} = 372.09V;$$

$$V_{AC-rms} = \frac{372.09}{\sqrt{2}} = 263.1V.$$

These are reasonable values considering that there is a voltage drop in the grid impedance. To complete this analysis, we'll show the current that flows in the AC link.

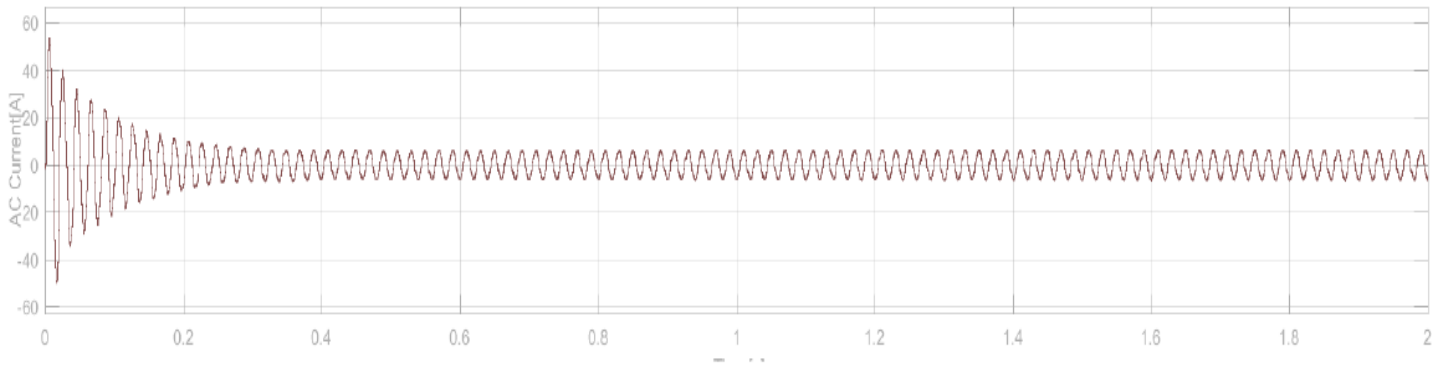


Figure 7.14 AC current of the converter

As can be seen the AC current increases in the first instance, when the difference between grid voltage and converter’s voltage is still significant, but then decreases and sets on a stable behaviour. In fact, the RMS value of this current initially increases then decreases, as can be observed in the following figure.

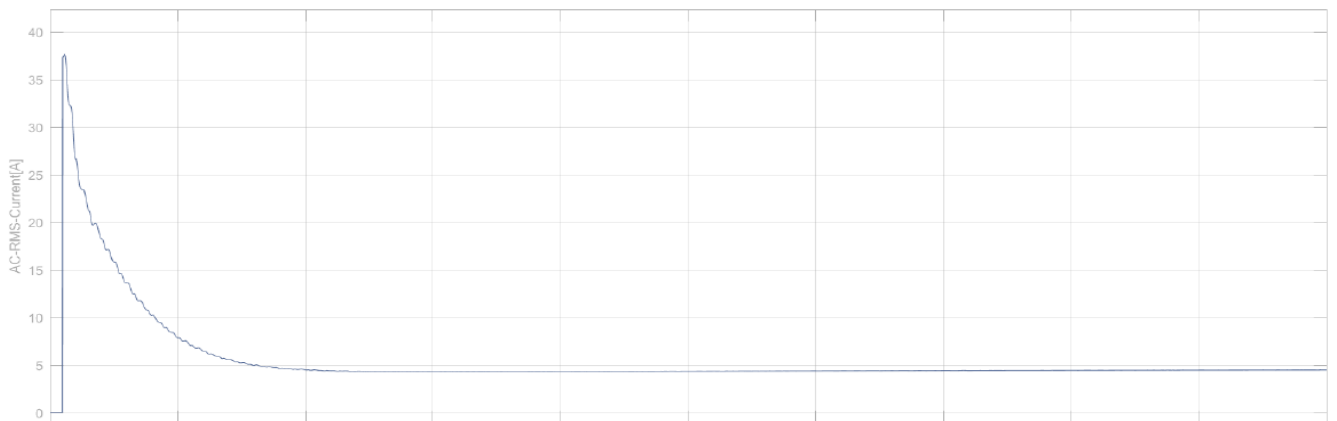


Figure 7.15 rms value of the AC current

What we can eventually say is that, in the normal operation the DC Bus capacitor will be already charged, hence such dynamics won’t be required. Until now we have always taken into account the two sides of the bidirectional charger: the AC side and the DC side. We have just ensured the correct operation of the AC side, so the DC side has to be considered. The correct operation will imply a nil active power exchange between the DC side of the charger and the battery, and this is what we expect from the next figure which represents the power delivered in the DC side.



Figure 7.16 DC power supplied to the battery

The power exchanged with the battery is successfully controlled to zero except of the initial peak that was predicted earlier, because of the settling of the system: this includes the aforementioned charging of the DC Bus capacitor as

well as the components of the DC filter like the huge inductor and the relatively small capacitor. Moreover, no ripple is observed.

The next goal to be set for our studies is the chasing of a variable reference. Here, we will impose a reference that changes from a high value to a low value of power exchange, and a successful control will chase the predefined value without any steady-state error. A plus point will be considered if the following is quick and without significant oscillations. This time the simulation time is extended to 4s because of the variations and the reference will start from 2000W going down to 500W. Since the batteries of commercial electric vehicles have voltages around 300V, for the next tests this will be the voltage considered for the DC voltage generator, which represents the battery. This shows how the charger is able to deal with different voltages; the DC/DC converter adjusts the voltage ratio of the DC bus in order to interact with the new voltage. But because the voltage has become bigger, and also for future prevention, in order to increase the stability of the DC Bus a larger capacitor has been used:  $C_{DC-Bus}=100\text{mF}$ ; and a larger inductance is necessary in order to reduce the DC current ripple; hence, an inductor of  $L_f=100\text{mH}$  has been used. Obviously, these increases will affect the dynamics of the charger: transients like the one for the initial charging of the DC bus capacitor will last longer and because the inductance of the filter has been increased, this will result in a more oscillatory behaviour. The following figure represents the active power exchanged with the grid during G2V operations.

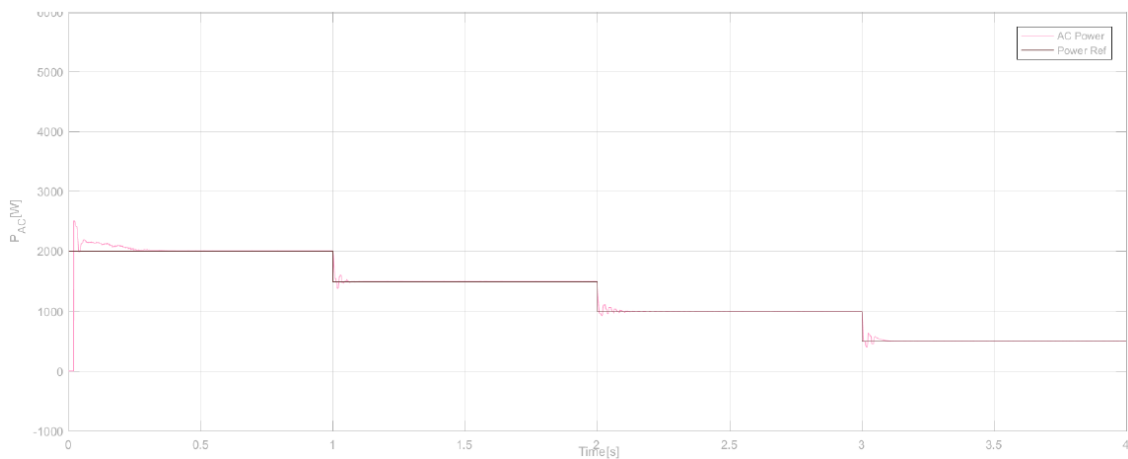


Figure 7.17 Active power exchanged with the grid against a variable reference

As can be seen, except an initial overshoot and a small overpower compared to the reference, that runs out by 0.25s anyway, no further significant errors are observed. There are small oscillations when the reference is changed but these last very little and their magnitude is little. In these tests, the reference for the reactive power is kept to zero because we want to prove that the charger is able to control active and reactive power independently. So, in the next figure the reactive power exchanged with the grid is depicted.

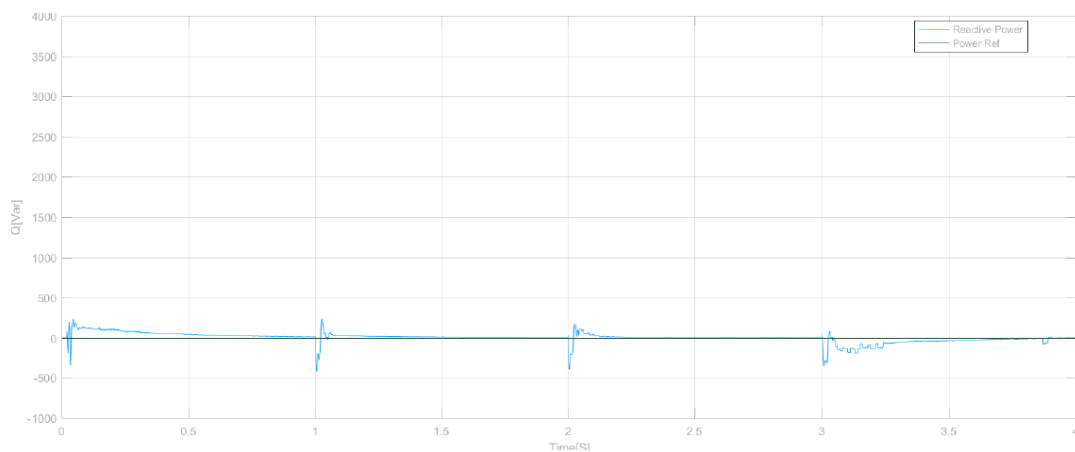


Figure 7.18 Reactive power exchanged with the grid against a reference of 0Var

The reactive power is effectively controlled to zero, though there are some oscillations. Initially the whole system needs to be energized: the DC Bus capacitor has to be charged and so are the filter inductor and capacitor. This requires a not nil reactive power that has to be provided to the system by the grid. This is why the system starts the operation with a positive reactive power exchange. In fact, afterwards, no such reactive power is asked as the dynamics are only limited to quick and not long lasting oscillations.

As explained before, in order to ensure the correct operation of the charger, the active power provided from the DC side has to be monitored and this has to match the power absorbed by the charger. This power is calculated by multiplying the current flowing in the filter inductor, which is the current that feeds the battery, and the voltage of the battery. The following figure shows therefore the DC power.

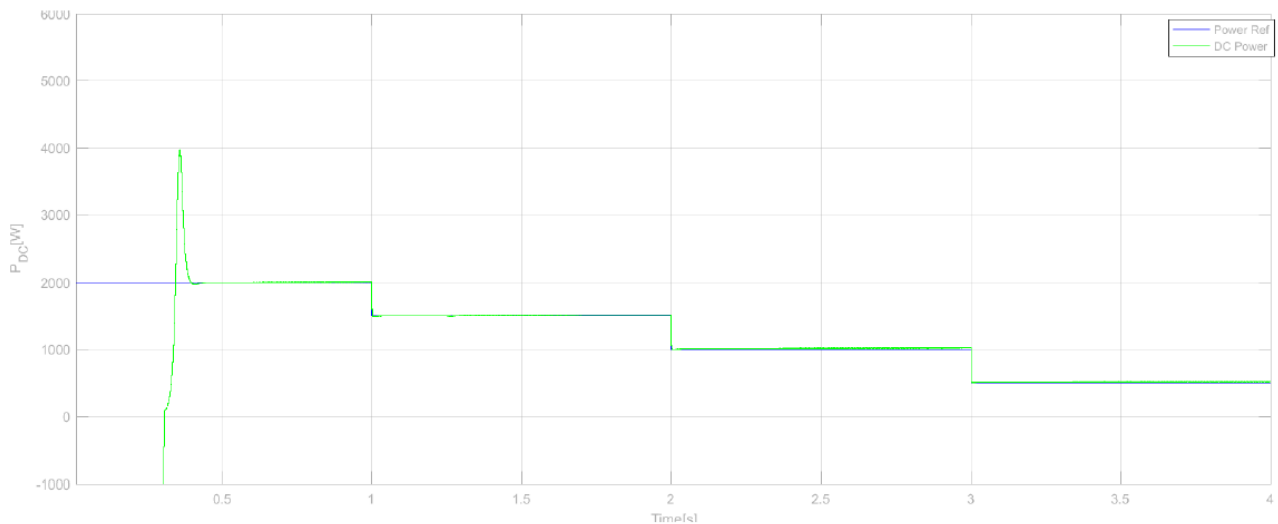


Figure 7.19 DC power supplied to the battery

The transient caused for the energisation of the system is evident, but since the charger is expected to work in steady state, this aspect will be ignored. The charging transient ends by 0.3s and after, an overshoot of nearly 100% is observed while reaching the reference value. This is completely expected considering the high value of the inductor, and can be prevented by applying a better control that considers the transients as well. By 0.4s the charger is working perfectly and the reference is accurately followed. There is a power ripple of 6.5W which is completely fair because it's the 0.33% of the steady state value. The DC current is presented in the figure hereafter.

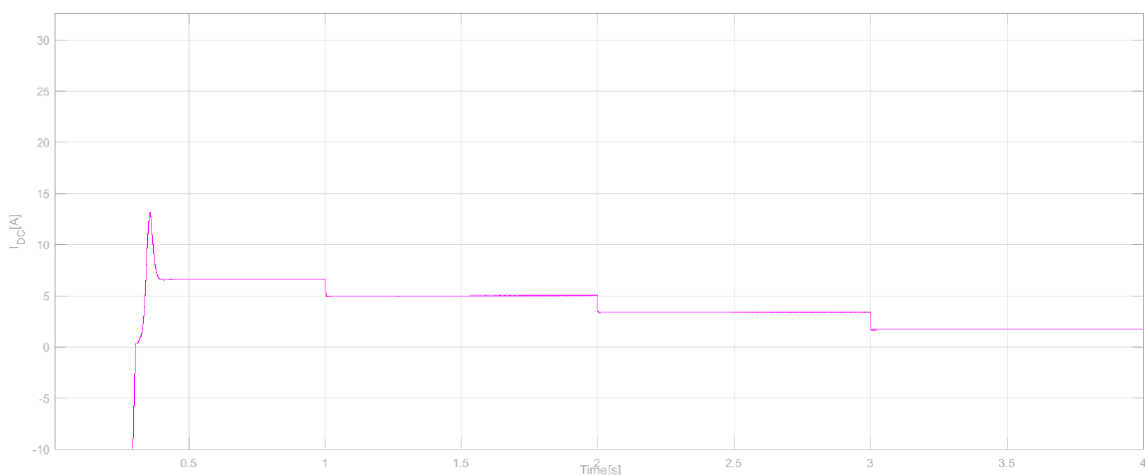


Figure 7.20 DC current feeding the battery

The shape of the current perfectly retraces the one of the power; this makes us finalize that such behaviour of the power is highly influenced by the current; in fact, the current flowing in the inductor is the same as the one flowing in the battery. The overshoot is caused by the large inductor. In the next figure the DC Bus voltage is reported.

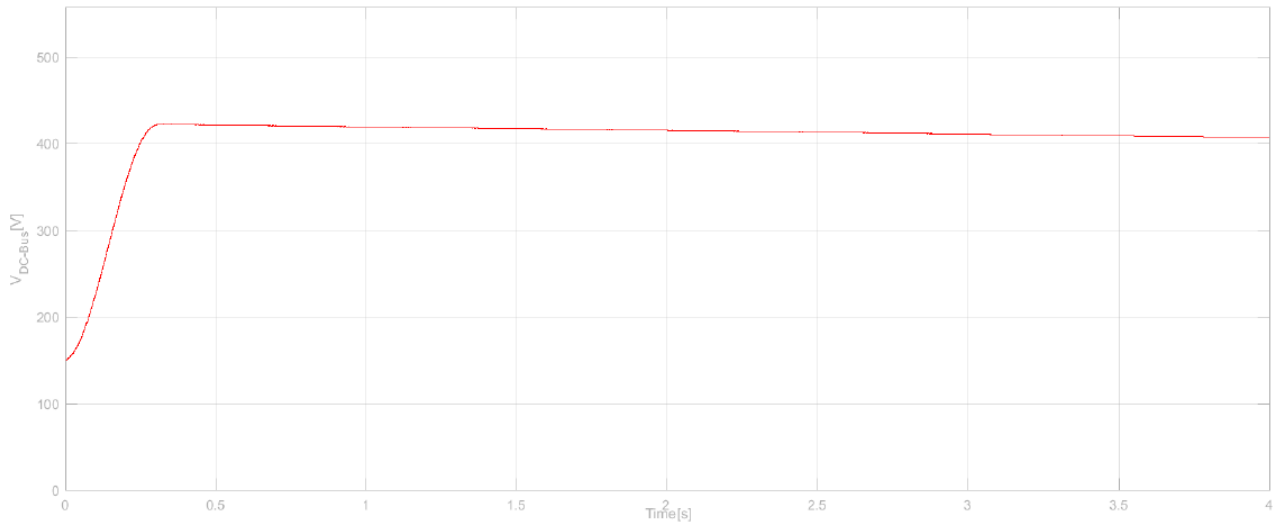


Figure 7.21 DC bus voltage

This representation confirms what we said earlier. The large capacitor that has been adopted needs 0.3s to be charged and in fact, the discrepancies from the ideal behaviour last till 0.3s. In this figure a small discharge of the DC Bus capacitor is observed: it's charged at 425V and ends up being at 410V. A voltage drop of 15V is acceptable considering the huge power exchange established; we can say that the control system is able to keep the power train stable. In the next figure the alternating voltage supplied on the AC side of the converter and the alternating current are depicted.

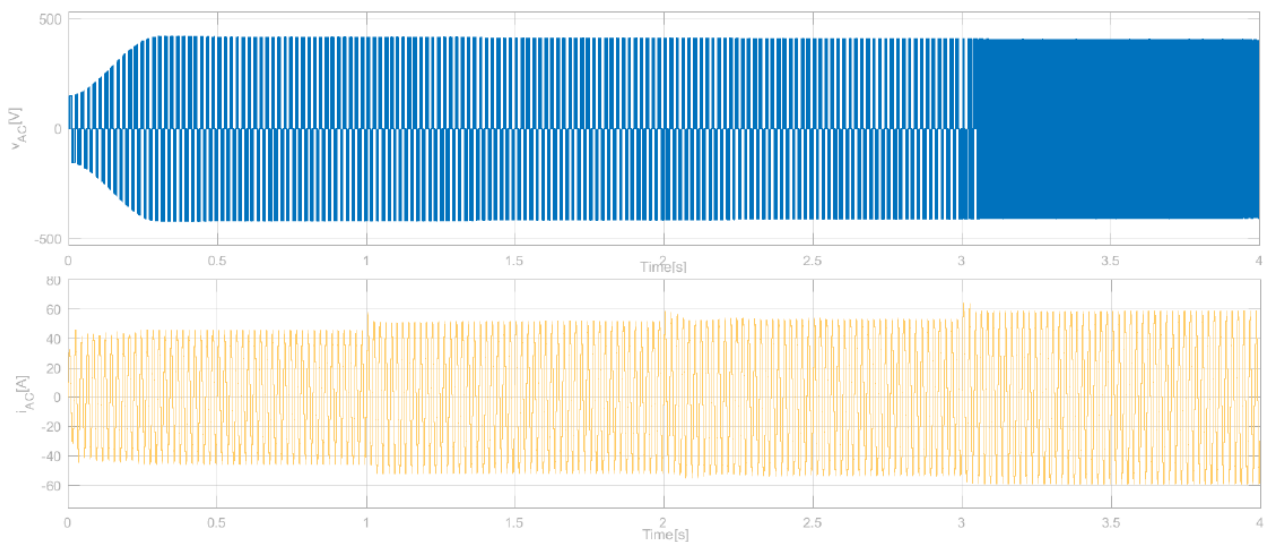


Figure 7.22 AC voltage and current of the charger

The alternating voltage needs 0.3s to stabilize to the steady state value and remains pretty constant. On the other hand, the alternating current is regulated according to the power exchange. It goes up to nearly 60A for the peak value. At every change of the power reference corresponds a change of the current.



## 7.2 V2G Simulations

In this section, V2G simulations are conducted which means, this time is the battery that supplies the grid. This causes the discharge of the battery, so in a real situation the SOC of the battery goes down. Here, the battery is represented by a simple DC voltage generator with a series resistor, hence such phenomenon is not considered. This is the innovative part of the electric vehicles charging technology because it allows to support the grid when necessary. In our case this is done reversing the sign of the voltage for the AC/DC converter and using the Boost converter instead of the Buck converter. So for the AC/DC converter the following figure explains what happens:

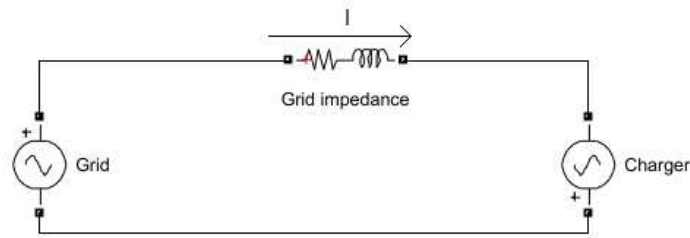


Figure 7.23 Grid and converter's voltages in V2G operations

the reference of the converter's voltage is reversed, hence, now it's set as a generator. As of the DC/DC converter, only IGBT<sub>1</sub> is working along with the diode. For the V2G operation we will look at the reference following straight away. A negative reference for the active power will be imposed, starting from -2000W and increasing to -500W. The changes will occur every 1s and the steps will be of 500W. The total duration of the simulation is therefore of 4s. Meanwhile the reactive power is kept to zero. The following figure represents the active power exchanged with the grid.

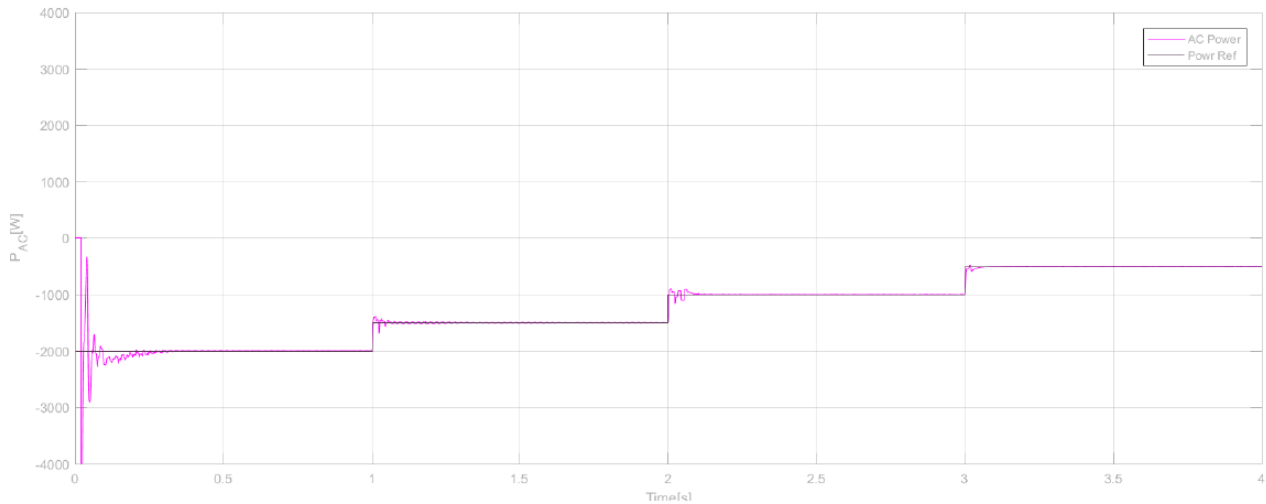


Figure 5.24 Active power exchanged with the grid against a variable reference

As can be seen the power is negative which means the current is flowing from the battery towards the grid and the battery is discharging. Again the first energisation influences the dynamics because it creates some oscillations. However, these disturbances are overcome after 0.3s: the oscillations are no more significant after 0.1s but the slight discrepancy of the actual active power from the reference lasts till 0.3s. As we previously noticed this corresponds to the time needed by the DC Bus capacitor to be fully charged, in fact after these events no more disturbances are observed except of minor oscillations but not long lasting and of minor entity: the power follows the reference adequately. Since it's very important to control the reactive power to zero while the active power is changing let's have a look at it in the next figure.

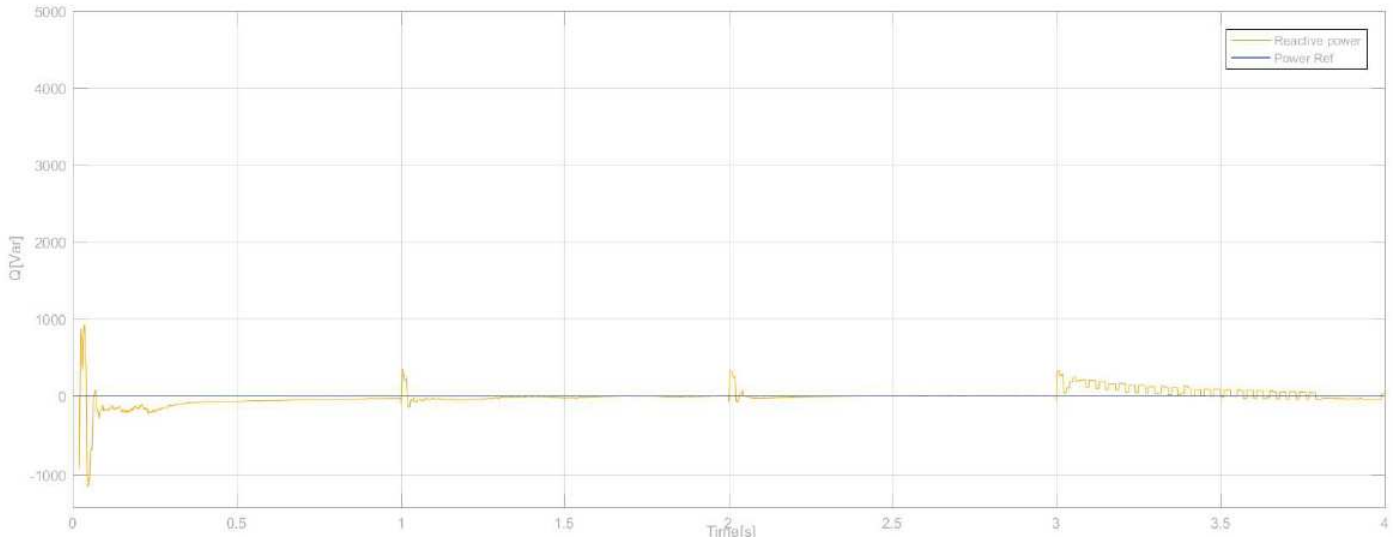


Figure 7.25 Reactive power exchanged with the grid against a reference of 0Var

As can be seen the control system is able to effectively keep the reactive power controlled to zero. The initial oscillations are however present: in fact, for the energisation some reactive power is required, and after these oscillations no more significant disturbances are observed except the ones in correspondence of the changes of the power reference but in any case of negligible entities. Something that can be observed is that, the initial oscillations are more significant in the V2G operation compared to the G2V operation. It's important to control the DC power exchanged with the battery, hence it's depicted hereafter.

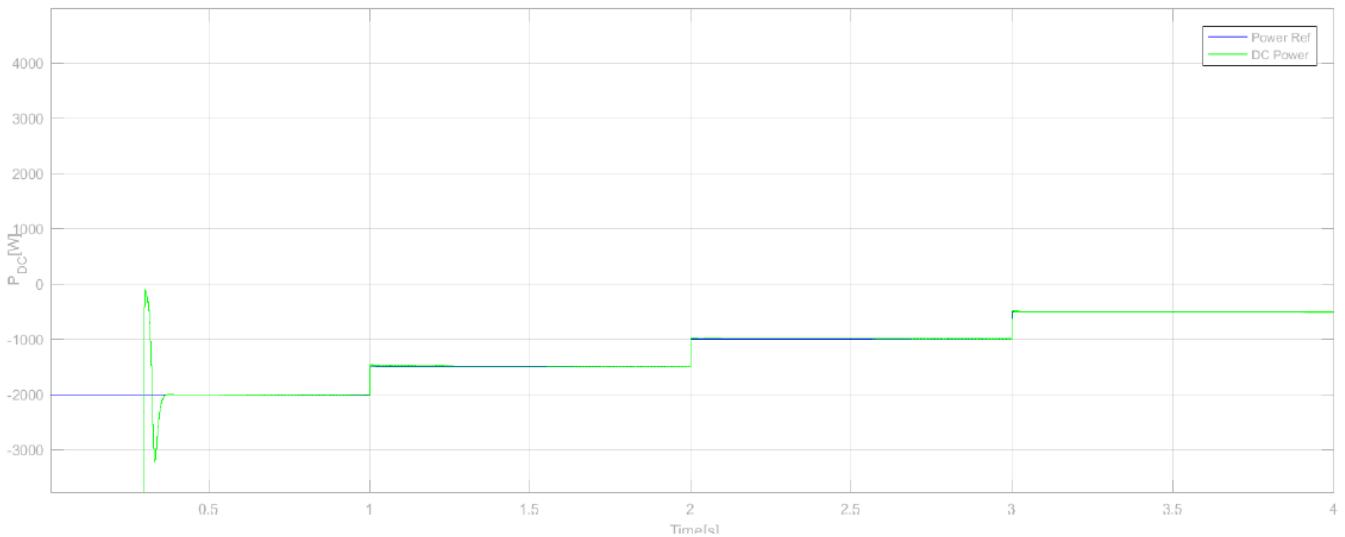


Figure 7.26 DC power supplied to the battery

The initial settling is yet present but this was expected, like the overshoot of nearly 100% of the steady state value; as explained earlier in these tests, this is due to the large size of the filter inductor. Something new is the undershoot that follows the overshoot; this is again due to the inductor and specifically the current that flows in it that is yet incapable to settle. There is nothing serious to worry about because the oscillations terminate within 0.4s and this demonstrates that the system is stable; after these events the system is able to perfectly follow the reference. In the next figure the DC current that flows in the inductor is depicted, and also here the initial oscillations are present, because the current is the cause.

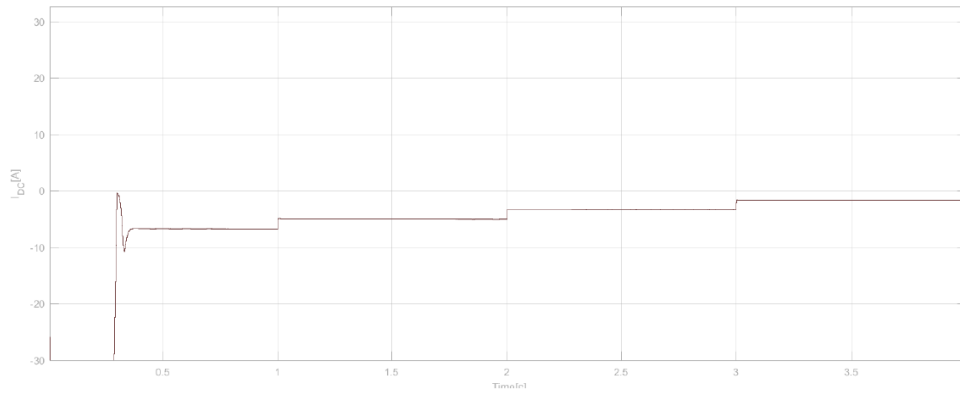


Figure 7.27 DC current feeding the battery

The current is regulated according to the power exchange and after few rapid oscillations, a stable condition is reached in 0.4s. However, something commendable about this control system is the absence of a significant ripple in the DC side unlike the previous configuration. Something interesting is the DC bus voltage, that yet again explains some dynamics, and is represented hereafter.

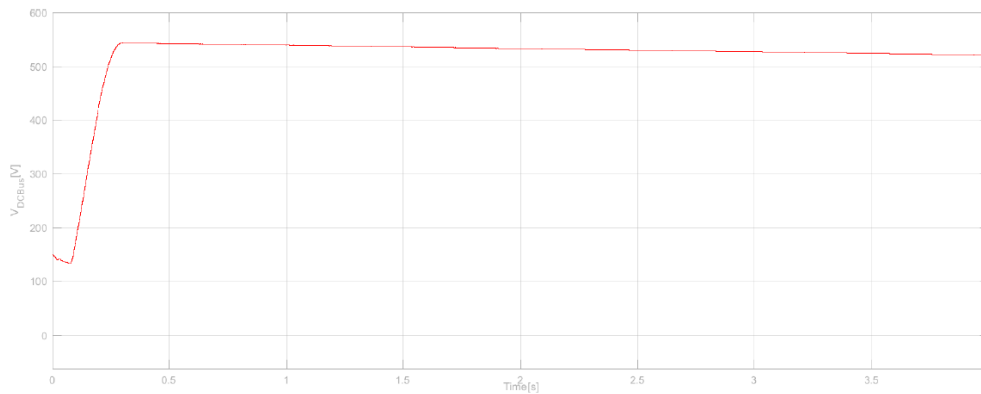


Figure 7.28 DC Bus voltage

The DC bus capacitor is charged up to 540V which is higher than the G2V operation. This is because the converter is increasing the voltage on its DC side, so that the voltage on the AC side will be consequently increased in order to allow a power flow towards the grid. The charging of such capacitor requires again 0.3s when the system is initially energized and this is the reason of the initial oscillations observed so far. Like in the G2V operation, the power flow causes a voltage drop in the DC bus capacitor, which falls to 425V; this is again a voltage drop of 15V and it's reasonable. To conclude the simulations, let's represent again the alternating voltage and current on the AC side of the converter in the following figure. The alternating current is regulated according to the variable power exchange and the voltage is stabilized after 0.3s.

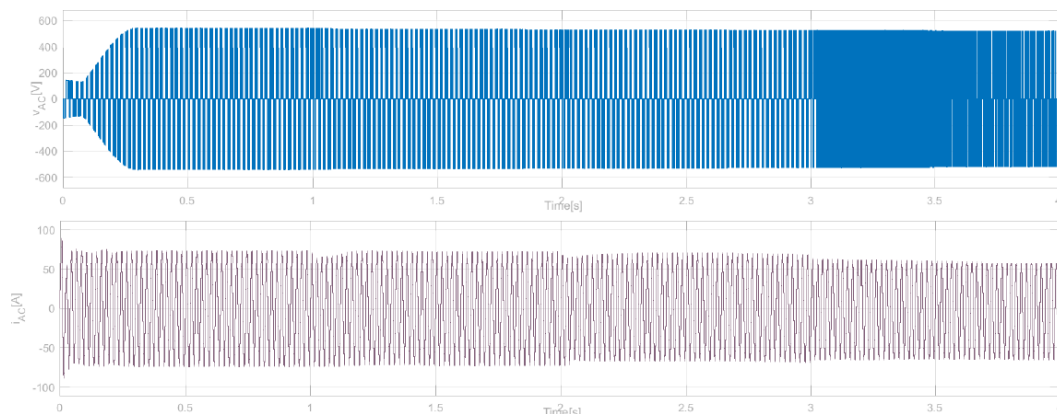


Figure 5.29 AC voltage and current of the charger

## 8 Physical Bidirectional Charger

As last task, a physical bidirectional charger has been built and tested. It was interfaced with the grid through a single phase transformer which provided a single phase sinusoid with approximately 50Vrms. The nominal value was 50Vrms, however, each device had different values, so, because it was used as a reference, and the dSPACE board can't accept voltages greater than 10V, initially a voltage divider was used. This voltage supplied the circuit and it's represented in the following figure:

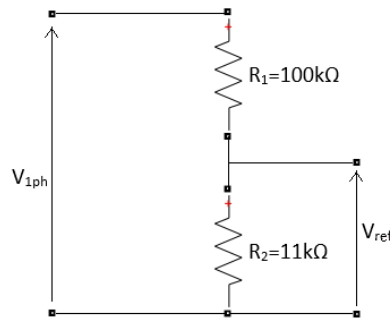


Figure 8.1 Schematic of a voltage divider

High valued resistors were used because the power transferred to the board was at signal level, thus few mWs were exchanged. The ratio  $R_2/R_1$  is roughly 1/9, therefore at the terminals of  $R_1$  there are 45Vrms whilst at the terminals of  $R_2$  there are 5Vrms. These values were just indicative considering that in the Simulink model a proper voltage ratio was applied in order to recreate the exact waveform. The only important thing here was to capture the shape of the waveform provided by the grid. Because there were small powers involved not much voltage distortion was expected from this circuit. However, because these were small signals, the board was highly sensible to possible disturbances and because of the wiring, the measuring instruments, power resistors etc. there were many sources of disturbance. Thus, it wasn't an effective method for having a reference, so afterwards, a simple voltage probe had been used which limited the output between  $\pm 10\text{V}$ ; it had an output voltage ratio of  $0.2\text{V/V}$  so considering this a multiplying factor of 20 has been used in the Simulink model.

### 8.1 The dSPACE platform

One of the most important devices of the entire experiment was the dSPACE board and the related software. The dSPACE can be used along with the Simulink program and it allows us to implement a virtual block diagram by receiving analogic signals in input and by supplying analogic signals in output. Obviously Simulink operates in digital and because dSPACE is coordinated by this one, the internal part of it, works in digital as well. But since we are controlling analogic devices conversions from digital to analogic (DAC) and from analogic to digital (ADC) are required. In fact, the dSPACE interface board has several channels assigned to ADC, to acquire measurements and other channels that are dedicated to DAC, to supply control signals.



Figure 8.2 dSPACE board

Some of the ADC channels are Master and other are Slave. This means that the Slave channels are controlled by the Master one, hence in order to receive useful measurements we have to use the Master channels. Every ADC channel has a maximum range of  $\pm 10V$ , therefore, the ideal way to interact with the dSPACE board is to use probes that reduce the measured values with known ratios and to consider internally reverse multiplying factors. In our case the Master ADC channels were only four, hence only four measurements have been considered to design the control system and these are: AC voltage reference, AC exchanged current, DC battery voltage and the DC exchanged current. There were eight DAC channels that could had been used but only four of them were required in order to control the single phase full bridge converter. As can be perceived, in this practical experiment, only an AC/DC converter has been used both because of the lack of time and because the driver board was inadequate. This means, active power and reactive power exchange were dependent on each other but it won't represent a big issue because anyway, no reactive power exchange has been recorded; the reason will be explained later.

The dSPACE board that has been used is the RT1103 and there was also the related library in Simulink. In this library, there were blocks that allowed to control either Master or Slave channels both from ADC or DAC. Given that, the board had a sampling with the maximum frequency of 100kHz, the switching frequency was limited to 10kHz. In fact, if the devices are switching at 10kHz which means that, variations happen in less than 100ms, in order to obtain information with acceptable accuracy the sampling clock has to be at least two time faster: 20kHz. By operating in this way only two samples will be recorded each period and yet it doesn't give us enough accuracy; a faster clock is required. In any case the maximum frequency of 100kHz can't be exceeded and staying low improves the speed and the quality of sampling.

### 8.2 The Simulink model

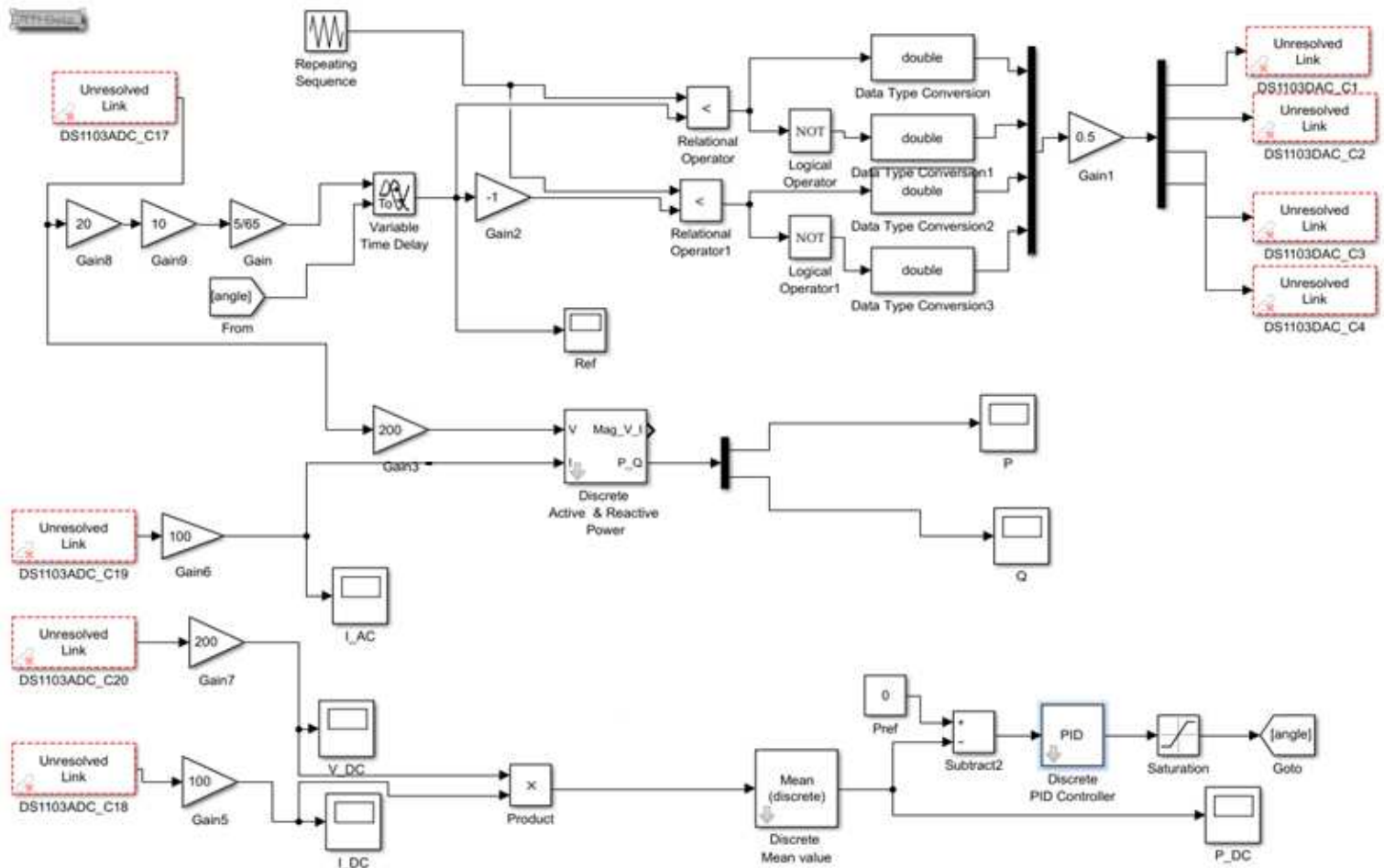


Figure 8.3 Simulink model of the tested charger

The ADC channel 17 receives the measurement of the grid voltage from the voltage probe, and this is used as reference. Basically, every variation in amplitude or phase, which depends respectively on reactive and active power, is applied relatively to the voltage grid. The amplitude is increased or decreased in respect to the amplitude of the reference and the phase is modified in regards of the phase of the reference. We need to clarify something: in the simulations a realistic situation of a highly resistive grid as the low voltage grid has been considered. This means that the dependencies of active and reactive power on power angle and voltage drop are opposite: the active power exchange is regulated according to the voltage amplitude whereas the reactive power is controlled depending on the power angle. In this practical case a huge reactor has been considered: this allows a range that goes from nearly nil value of mH to 700mH. Ideally, such a huge value wouldn't be necessary, but during the experiment the necessity of a large inductor surged in response to a huge current; this will be explained later.

As we said earlier in this paper, the probes that have been used, have some step down voltage ratio in order to represent the measured signal with small powers. In order to retrieve the correct value of the dimension, we need to know these ratios and reverse them in the signal processing. That's exactly what has been done here: the voltage probe divides the original signal by a factor 20:  $v_{probe} = \frac{1}{20} v_{original}$ ; (8.1). So in order to be able to use the actual value, the output of the channel 17 has to be multiplied by 20.

Furthermore, the same channels have their own gain: ADC channels divide the original signal by a factor 10 whilst DAC channels multiplies the internal signal by a factor 10. As a result of this, input signals have to be multiplied by 10 and output signals have to be divided by 10 before supplying. This is why a second gain of 10 is applied to the output of ADC channel 17.

The third and last gain is applied because what has been captured from the probe is the entire signal, which means the peak-to-peak signal; the peak value of the "grid voltage" was 65V. But in order to apply the PWM control we have to compare the reference with a repetitive signal, and the output of this procedure has to be the firing signals for the switches. Usually the level for these signals are set to 0-5V. Therefore, the measured voltage is scaled down in a waveform whose peak value is 5V.

In order to modify the power angle, we need to control the time shift: this is because the waveform evolves in time, hence shifting in time means shifting in angle. If an entire period of the waveform is about:

$$T_{fundamental} = \frac{1}{50[Hz]} = 20[ms] \quad (8.2)$$

because the reference is a sinusoidal one, the period engages  $2\pi$  rad or  $360^\circ$ ; it needs 20ms to complete a period of  $2\pi$  or  $360^\circ$ . If we want to increase the power angle we have to increase the angle between the grid voltage, that is represented by the reference signal, and the supplied voltage, that has to be created by the converter. This means, the supplied waveform is delayed in respect of the reference voltage. Whether for instance, the signal has to be delayed of  $45^\circ$ , it will be translated in radians and then in seconds.

$$360: 2\pi = 45: x \quad (8.3)$$

$$x = \frac{2\sqrt{2}}{\pi} rad \quad (8.4)$$

$$360: 20 * 10^{-3} = 45: x \quad (8.5)$$

$$x = 2.5ms. \quad (8.6)$$

How much the waveform has to be shifted depends on the power exchange, thus, it's imposed by the active power control chain. The time shift is implemented by the dedicated block Variable Time Delay.

After this stage, the Unipolar PWM is applied: a repetitive signal is compared with the reference and its opposite. These two comparisons provide the firing signal for the two legs of the bridge; by reversing this signals, with a not port, those required for the switches positioned below are obtained.

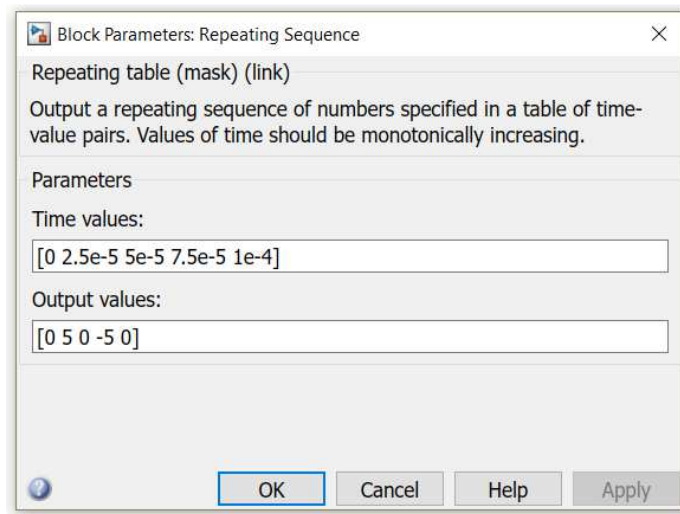


Figure 8.4 Parameter mask of the Repetitive Sequence block

Because the outputs of the logical comparison blocks are Boolean and the DAC channels can be controlled only by Double signals, four Data Type Conversion blocks have been used. Moreover, the outputs of the logical comparison blocks have a high value of 1V, so in order to be able to turn on the gates of the IGBTs a multiplication by 5 is required, which supplies a firing signal of 0-5V. As mentioned before, the output of the Simulink model has to be scaled down by a 10 factor because of the dSPACE board's gain in the DAC channels.

A difference between the simulations and this real experiment can be noticed: while before the simulations are done in continuous time, here there is a **discretization** of the process, because dSPACE works with discrete steps. Because of this feature, every block that has been used, from the P&Q calculation, to the RMS value calculation and also all the gains have a discrete sample time. In fact, inside all the gains, a fixed sample time has been specified.

The second input that has been considered in the model is the AC current. Given the gain of the current probe, that was 1/10, the output of channel 18 has been multiplied by 10 in order to have the actual value but that's not all. In fact, as mentioned before, the gain of ADC channels needs to be considered, hence, a further multiplication by 10 has been used. At this point, the active and the reactive power can be calculated with the dedicated Discrete Active & Reactive Power block.

The other two ADC channels were assigned to DC dimensions, such DC voltage and DC current. Also these dimensions have been measured with probes, hence their gains along with the gain of ADC channels have been considered. By multiplying these two dimensions, the active power exchanged with the battery was obtained and observed with a dedicated scope. Since a slight ripple is expected from the DC power, given by the small oscillations of both the DC voltage and DC current, a Discrete Mean Value block has been used in order to consider only the mean values for the computations. The measured value of the DC power is compared with a reference that is going to be set by the user; for now, it's a constant whose value can be changed from the dSPACE layout. The error given by this comparison feeds a PID controller, which has to provide the control signal that is in this case the power angle variation. Starting from the assumption that, the active power is varying between its maximum and minimum value, and consequently the power angle, the proportional gain  $K_p$  has been decided. The maximum power exchange that was measured without any control was about 35W and for this experiment the maximum variation for the power angle is one fourth of the period, which is  $45^\circ$  or 5ms; let's not forget that the assumption of small angles is fundamental in order to apply the approximations and have a correct operation. The other constants have been decided empirically. After this, a saturation block that limits the output between [-0.005,0.005] has been used, because in any case we don't want to force a value of the power angle bigger then the aforementioned range. The value that has been decided is eventually applied to the Variable Time Delay block through a Go to tool.

### 8.3 The dSPACE layout

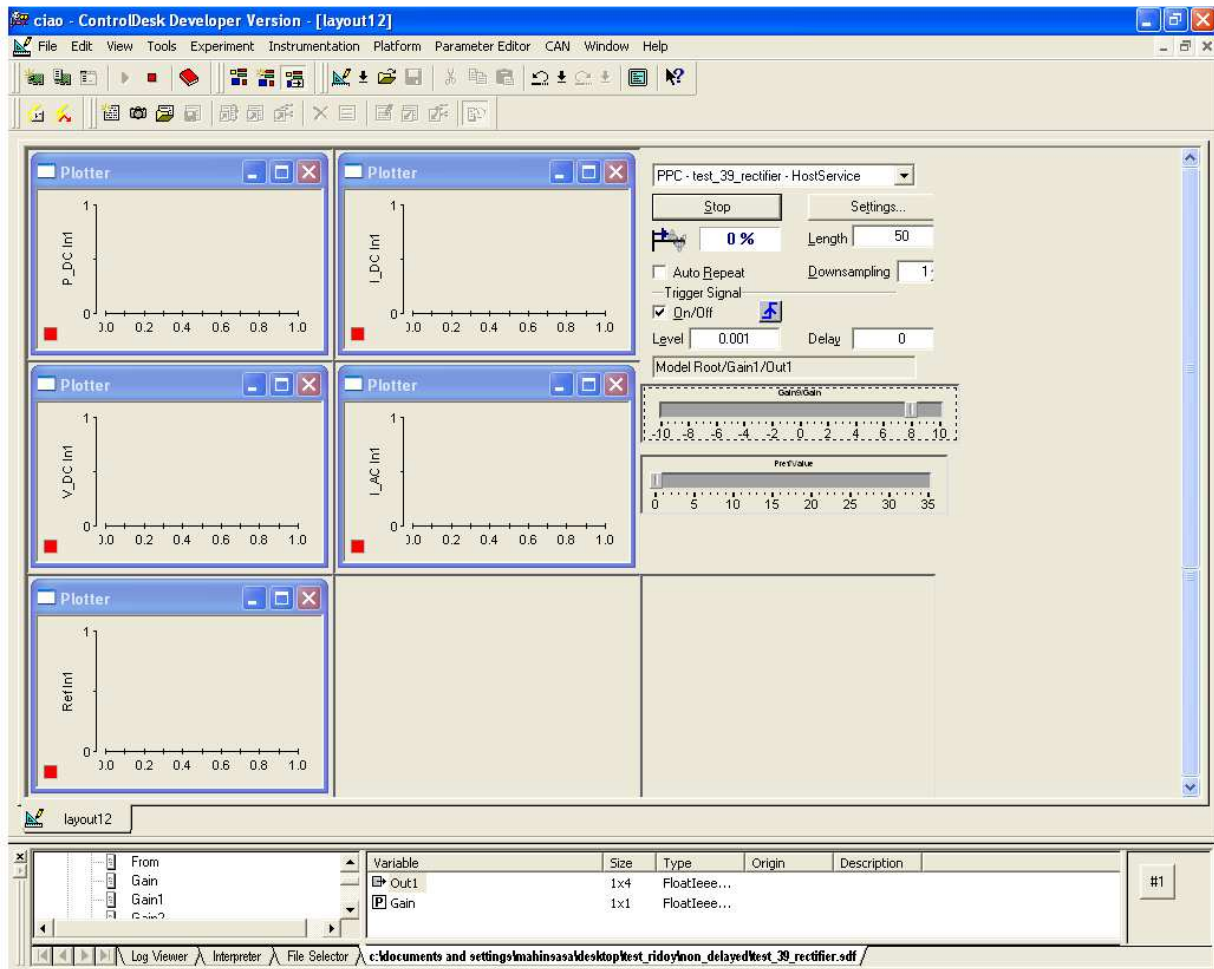


Figure 8.5 The dSPACE layout

After the Simulink model has been designed, once the main parameters like the sample time that was in this case  $40\mu\text{s}$  corresponding to a sampling frequency of 25kHz, it has to be built on the dSPACE board. In this instance the model is debugged in order to avoid any kind of error. If the result of this process is positive, then the board is successfully assigned to this and only this Simulink model. In order to work in real time, few more steps are required like the building of a layout. Above, the layout that was used has been presented and something immediately noticeable are the instruments like plotters and sliders. These are instruments included in the dSPACE library and allow us to work in real time by changing constants, gains or visualizing variations of certain dimensions. All the plotters have been assigned to different dimensions such as active power, DC current, DC voltage, AC current and the voltage reference. The first slider has been assigned to the variation of Gain9: by doing this we are going to change the amplitude of the voltage reference; for this one also negative values are allowed because we want to reverse the power flow. The second slider has to change the constant that represents the power reference. By increasing this we are increasing the power exchange.

Another essential tool is the Capture setting. It allows us to record the operation of the experiment for some time and to store all the data regarding the different plotters in a file. This file can be used in Matlab to print graphs that represents the variations of the involved dimensions. Furthermore, the trigger has to be set properly: once a predefined variable has exceeded the set value, the capturing starts. This variable was in this case the output of the Gain1, so as soon as the firing of the switches starts, the capturing begins.

In the section below there are all the tools that have been used in the Simulink model. By clicking on them a new window is opened where two things are related to the selected tool: its output and the tool itself. The output can be used to trigger the capturing whereas the tool itself can be assigned to any slider in order to modify its value.



## 8.4 The physical system

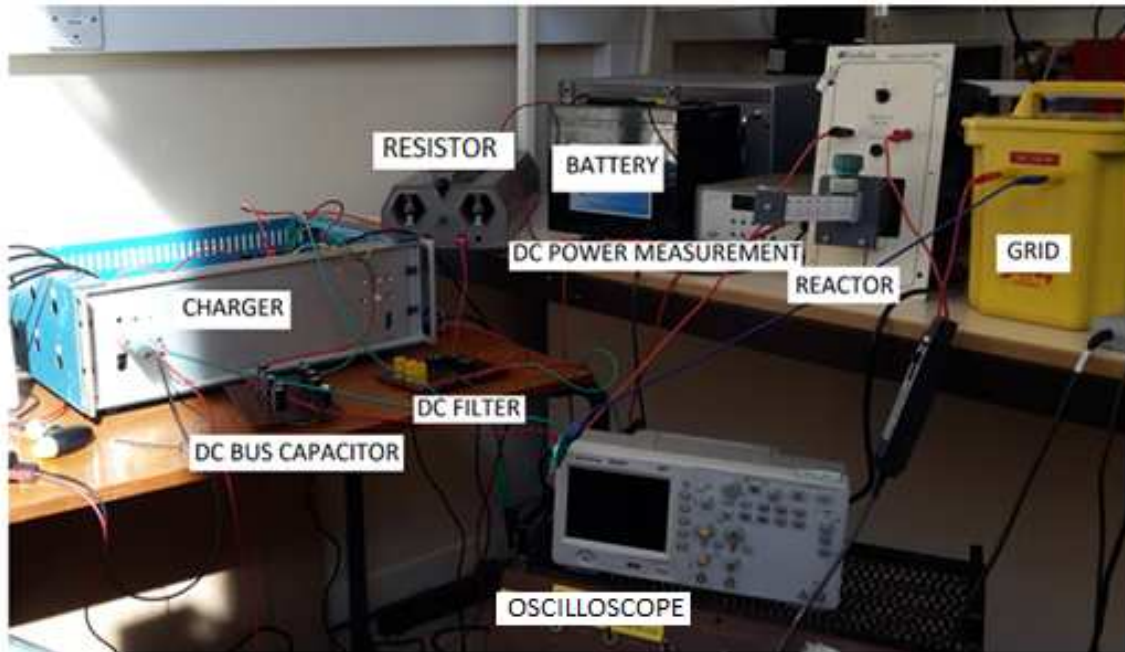


Figure 8.6 The whole physical system

In the figure shown above the complete system for the experiments is represented. The grid is represented by the single phase step-down transformer that supplies a waveform in phase with the grid and with a RMS value of 50V. In this particular case the device had a RMS value of 47V, as measured with a multi-meter; this fact has been considered in the Simulink model with a peak value of 65V. After this, for the interaction with the grid a reactor has been used: the device had a maximum value for the inductance of 700mH and the internal resistive factor was about 9 $\Omega$ . However, in the tests, the maximum value has been used only for initial evaluations in order to start with the safest configuration of the system, that implies high impedance and low current. After the safety was ensured, lower value for the inductor have been used to improve the quality of operation. The output of the reactor is connected to one phase of the AC/DC converter with a simple cable. The converter's box contains the board with the IGBTs, the input board with the BNC connectors and the driver circuit for the control of the IGBTs. Going out from the DC terminals of the converter's box there is immediately the DC Bus capacitor represented by ten capacitors in parallel of 100 $\mu$ F each. After the DC Bus capacitor there is the LC filter which consists of three inductors connected in series of 2.2mH each and three capacitors in parallel of 100 $\mu$ F each. Ultimately the values for the inductor and the capacitor were 6.6mH and 300 $\mu$ F respectively.

After this stage, everything should have been brought in DC, therefore DC measurements are taken through a DC power measurement. This device has two terminals for the current, which were connected in series with the load, and two terminals for the voltage, which were connected in parallel with the battery. Through these two measurements the device is able to calculate the DC power exchange with the battery. However, because there are harmonics in the output of the LC filter, we can't completely trust the watt-meter, at least in regards of the exact value of the power exchange. We can anyway monitor the sign of the power exchange and any variation caused by the control. The series resistance has been increased with a power resistor in order to ensure safety by limiting the current. This had a maximum value of 100 $\Omega$  and an amperage of 5A. Initially the full resistance has been used and the operation registered; more tests have been done afterwards once the resistance was taken down. Finally, after the power resistor there is the battery that is the same as those used in cars. It has a nominal voltage of 12V. The measurements that have been taken were located in proximity of the AC single phase transformer and the battery for both voltage and current. The complete schematic of the whole system is represented hereafter.

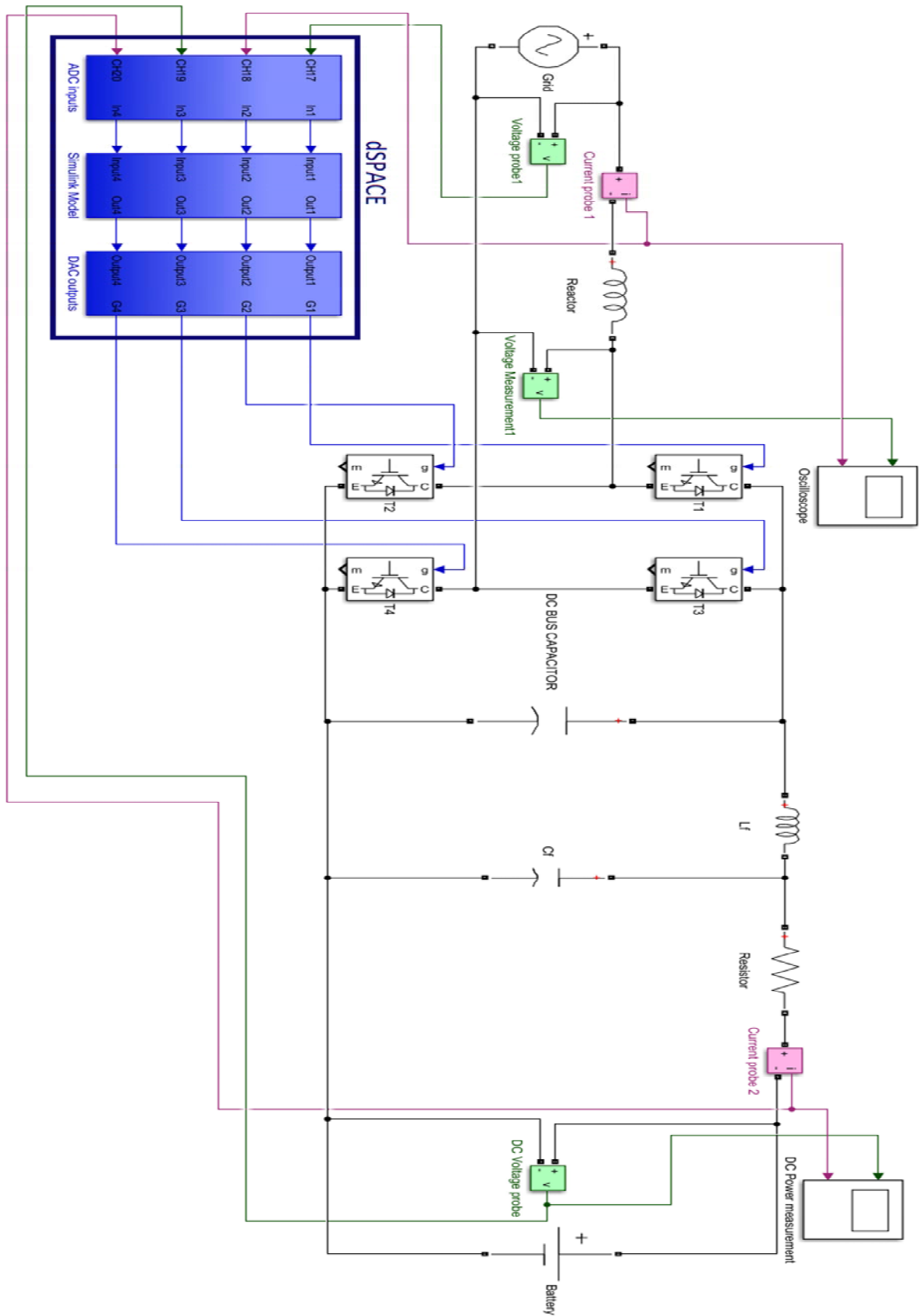


Figure 8.7 Schematic of the physical system

### 8.4.1 The Converter

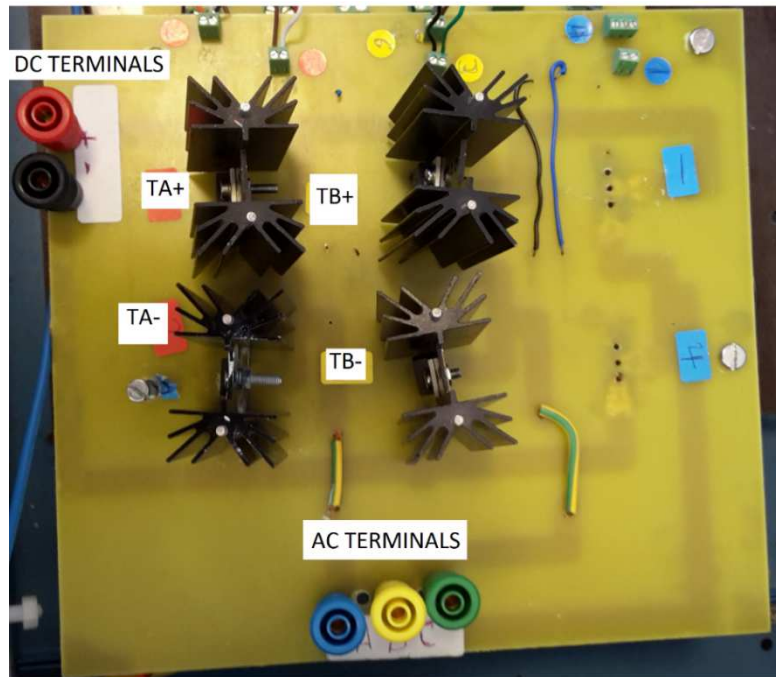


Figure 8.8 The physical AC/DC charger

The main part of the entire system is the AC/DC converter that is assessed to the power conversion from alternating to direct current. Like in the simulations, also here it consists of a single phase full bridge that is the classic solution for single phase systems. These converters deal with relatively small powers, thus, they are usually employed for inboard charging equipment. Specifically, in this case IGBTs have been used because of the simple control method: they are Insulated Gate Bipolar Transistor and in order to switch on one of them, sufficient voltage has to be provided between gate and emitter; a minimum threshold represented by the  $V_{GE-on}$  voltage has to be exceeded in order to allow current conduction between collector and emitter. The ones that have been used, are rated at 600V and 30A.

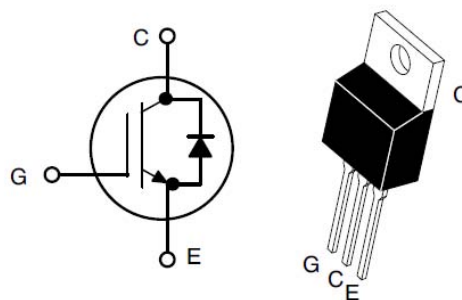


Figure 8.9 Schematic and real representation of an IGBT

In the following figure the back of the board containing the IGBTs is represented: the DC positive terminal is connected with all the collectors of the upper IGBTs and the emitters of the upper IGBTs are connected with the collectors of the lower IGBTs. The emitters of the lower IGBTs are connected with the DC negative terminal. The gates of each IGBT, represented by the upper pin, are connected with the upper side of the board along with another path that is connected to the negative DC terminal. This is used to provide the gate signals to the IGBTs, which are referred to the ground. The junction between the emitters of the upper IGBTs and the collectors of lower IGBTs are connected to the terminals of the phases a, b and c. Originally the device was meant to be a three phase bridge but because of the design requirements only two legs have been used. The remaining IGBTs have been taken off from the board because if they were damaged there would have been a short circuit between their collectors and emitters and hence, the positive DC terminal and the negative DC terminal would have been short circuited. A decent number of bridges

can be observed in the figure; this was due to the continuous welding and desoldering of the components that cause erosion of the paths and sometimes their detachment. The pins of the components have been welded with welding tin.

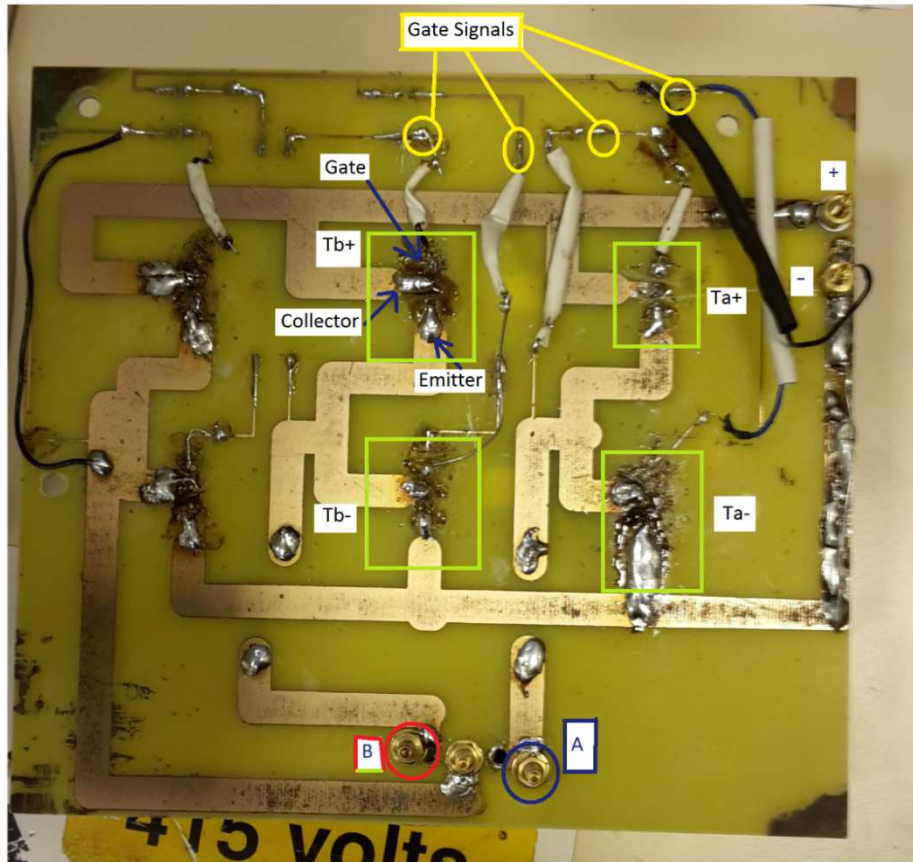


Figure 8.10 PCB of the charger's board

#### 8.4.2 The driver circuit

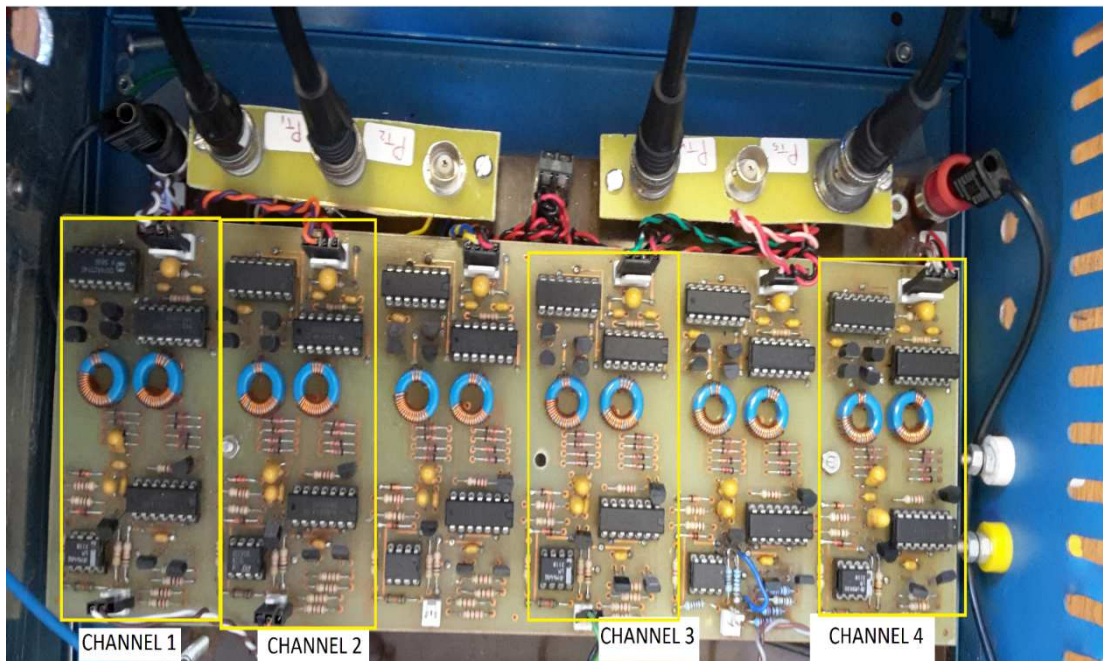


Figure 8.11 Driver board

In order to provide the firing signals to the IGBTs properly there has to be another board between the dSPACE outputs and the switches. The duty of this circuit is to receive the firing signals from the input terminals, to process it in order to provide a stable signal and to scale it properly. The board that has been represented in the previous page has been made available right from the beginning of the practical work. Not very much is known about this board except that, it has six channels, one for each component, that it provides a firing signal ranged between 0-15V and it needs to be powered by an external DC power supplier. The required voltage, was about  $\pm 5V$ .

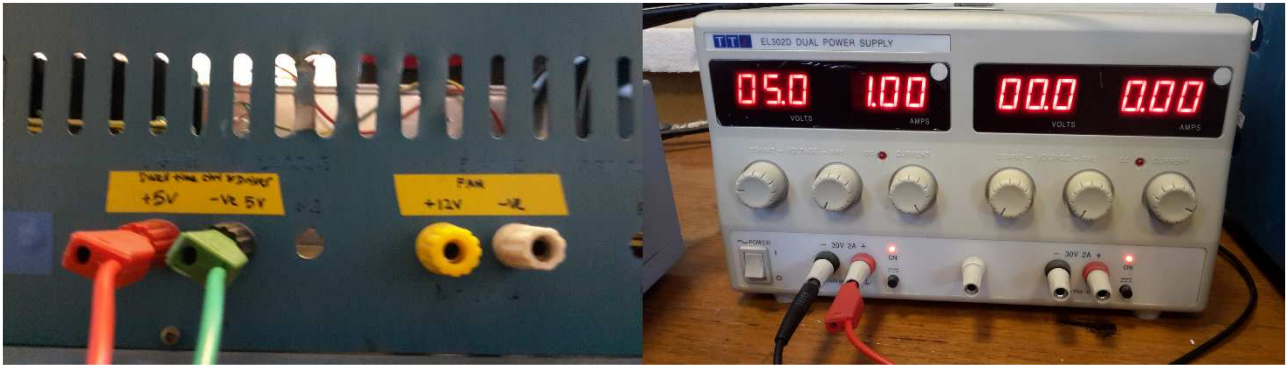


Figure 8.12 Supply of the driver board and the relative DC generator

Since, only a single phase bridge had been realized, only four of the six channels were used and these are highlighted in *Figure 8.11*. There is no distinction between channels assigned to upper IGBTs and those assigned to lower IGBTs, therefore they can be used without any restriction. An alternative of this board can be realized thanks to the following circuit.

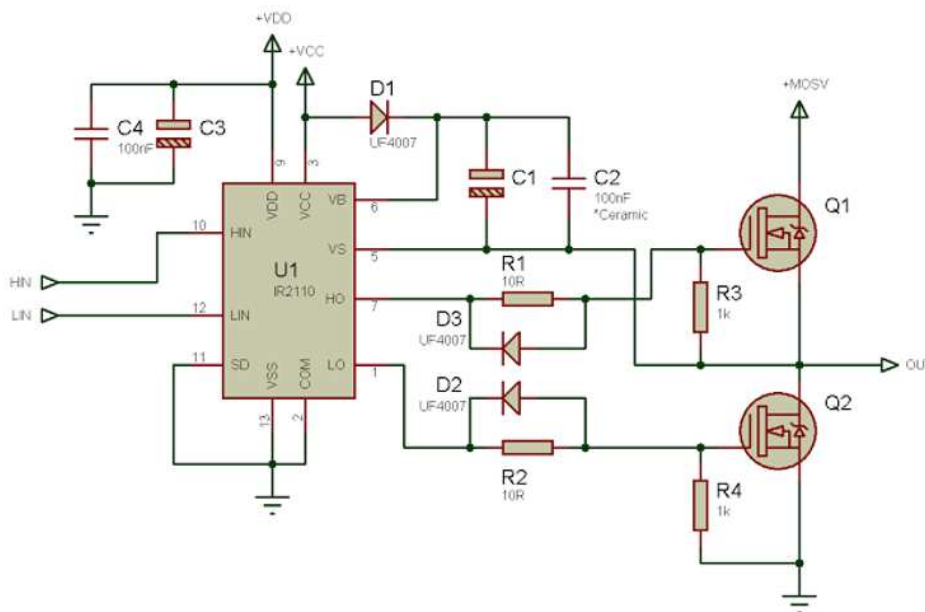


Figure 8.13 Application of the IC IR2110 as a IGBTs driver

The IC used in this circuit is the IR2110 and it's a High and Low Side Driver: it's designed to work with voltages up to +500V or +600V and provides gate drive from 10 to 20V. The inputs are taken, through the pins 10 and 12, from the DAC channels of the dSPACE, and the output is supplied through the pins 7 and 1. Every IR2110 can drive two IGBTs so unlike the existing board, only three of these ICs are needed. The VCC and VDD pins are the supply of the IC whereas VSS is the ground. VS and VD represent a floating channel that can drive an N-channel IGBT. The external circuitry has a different scope: it's used to create a delay in the firing signal, because if this is supplied exactly how the PWM generator provides it, then short circuit between the switches of one leg might occur, because of the dead time required by an IGBT to switch off. This method will be used in one of the experiments, hence it will be explained later.

### 8.4.3 DC Bus capacitor and DC Filter

As in the simulations, in every system that employs static converters, a way of stabilize the DC output has to be provided. This is represented by the DC Bus capacitor which is usually a huge one, thus, the possible ripple can't harm the stability of the DC output even if the disturbance is high. In the simulations capacitors of 10mF or 100mF have been used but the powers involved were much higher. In fact, a regular single phase domestic outlet was considered for the power supply and powers up to 2kW were exchanged. Here, for a safer operation, a lower power level has been used and because of this, the transformer supplied only 50Vrms so we are dealing with a very low voltage system. Moreover, for a part of the experiment a large resistor has been connected between the output of the LC filter and the battery in order to further limit the current. As we said earlier in this paper, there isn't an analytical method to choose the size of the DC Bus capacitor, though several studies have been conducted on this. Let's say that it's safe to adopt a capacitor of some mF for this power level.

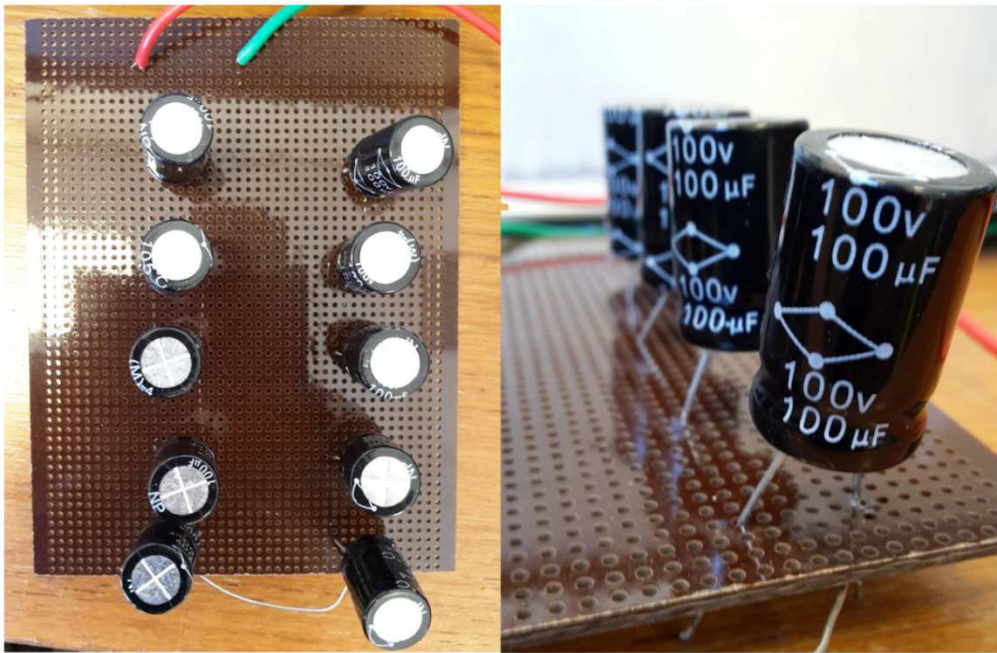


Figure 8.14 DC bus capacitor

In this board ten capacitors of 100 $\mu$ F have been connected in parallel in order to build a total capacitance of 1mF. The capacitors that have been used are electrolytic, but unlike the well-known capacitors these doesn't show any white band, that usually indicates the negative pole or the otherwise called cathode. This is because these capacitors don't have any polarization, hence, there is no preference in powering them. Such a choice has been made in order to avoid any kind of issue whether the sign of the voltage reverses. Because we are in the DC side of the charger this is unlikely to happen, but if this was the case, and polarized capacitors were used, a voltage reversal could have seriously damaged the electrolyte. In this way the system is bulletproof and even if any voltage reversal happens, because of any possible fault, this won't affect the DC Bus capacitor. As can be seen from the picture, the capacitors have a maximum voltage of 100V; a higher voltage isn't required because the supply is done at 50Vrms, therefore,  $V_{pk} = \sqrt{2} * 50 = 70.71V$ . This is the AC voltage, and once it's rectified the average value of the output voltage becomes:

$$V_{DC} = \frac{2\sqrt{2}}{\pi} 70.71 = 63.66V; \quad (8.7)$$

This is why a higher voltage isn't required. There is another matter that needs to be cleared: a higher DC Bus capacitor means a higher current absorbed by the capacitor when it's charging, along with a longer transitory that leads to the complete charging. However, these issues aren't investigated, because in the first instance the experiment is conducted when the system is completely active, that means the capacitors are fully charged.

In order to eliminate or at least partially reduce the ripple, an LC filter has to be adopted at the output of the DC Bus. This component has to be designed according to the switching frequency; in fact, recalling from previous steps, in the simulations, such filter was used in order to reduce the ripple generated by the DC/DC converter. Here, there isn't a DC/DC converter, but the need of the DC filter remains essential in order to reduce the ripple. The design of the size components doesn't change because, since there isn't any DC/DC converter a nil duty cycle will be considered:

$$\frac{\Delta V_0}{V_0} = \frac{\Delta I_L T_s}{8C} \frac{(1-D) T_s}{\Delta I_L L} = \frac{(1-D) T_s^2}{8LC} = (1-D) \frac{\pi^2}{2} \left( \frac{f_c}{f_s} \right)^2; \quad (8.8)$$

where:

$$\frac{1}{8LC} = \frac{4\pi^2}{4\pi^2} \frac{1}{8LC} = \frac{\pi^2}{2} \frac{1}{4\pi^2 LC} = \frac{\pi^2}{2} f_c^2. \quad (8.9)$$

Because the following expression is true:

$$f_c = \frac{1}{2\pi\sqrt{LC}}; \quad (8.10)$$

finally, the LC product is

$$LC = \frac{1}{f_c^2 4\pi^2}; \quad (8.11)$$

Because in this case the switching frequency is 10kHz we expect an LC product that is much bigger, because of the power two of the frequency ratio. If we want a percentage relative voltage ripple of 5%, with a switching frequency of 10kHz, the cut-off frequency of the filter has to be:  $f_c = 1007\text{Hz}$ . Hence, the LC product has to be:  $LC = 2.49 * 10^{-8}$ .

In order to have a smaller current ripple, we have used a high inductance, at the point that three inductors of 2.2mH each have been connected in series. With our actual sizes for the components the LC product results:

$$LC = 6.6 * 10^{-3} * 1 * 10^{-3} = 6.6 * 10^{-6}; \quad (8.12)$$

This is much bigger then the design value, thus, the ripple should be sensitively smaller: the actual cut-off frequency is  $f_c = 61.95\text{Hz}$ .

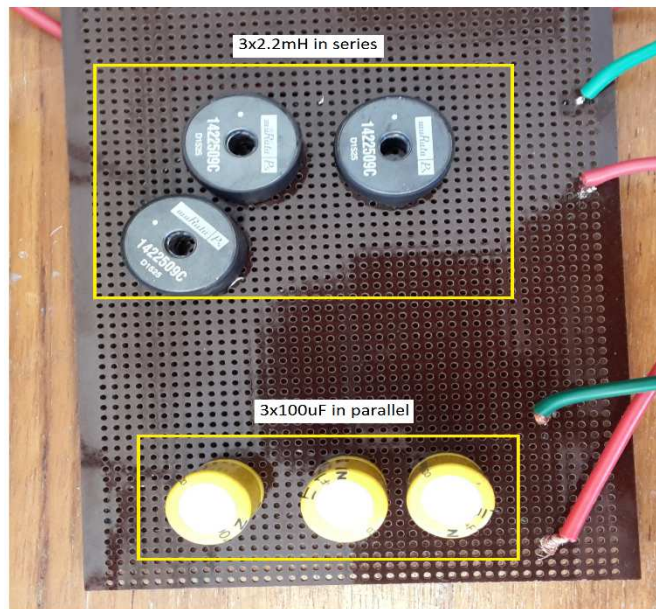


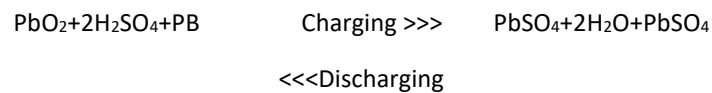
Figure 8.15 LC filter

#### 8.4.4 Other components



Figure 8.16 The battery

The battery that has been used is the Haze VRLA AGM one: this is a type of Lead-acid battery, and uses AGM (Absorbed glass mat) which is fiberglass, that is put between the battery plates in order to contain the electrolyte. The principle remains the same despite of the material: there are two plates of lead suspended in diluted sulphuric acid, but in the AGM case, this solution remains immobilized. The main reaction is:



This battery had a nominal voltage of 12V.



Figure 8.17 Single-phase transformer

The AC supply was provided by a step-down single phase transformer 240V-50V. Different fuses could have been set in order to allow different currents. Fuses with 600V and 10-12A have been used. Though the voltage of 600V wasn't strictly necessary for this experiment, because the voltages reached in the circuit were much lower than that, the



fuses were frequently burned because of the high current caused by short circuits. This matter will be explained in the next pages.

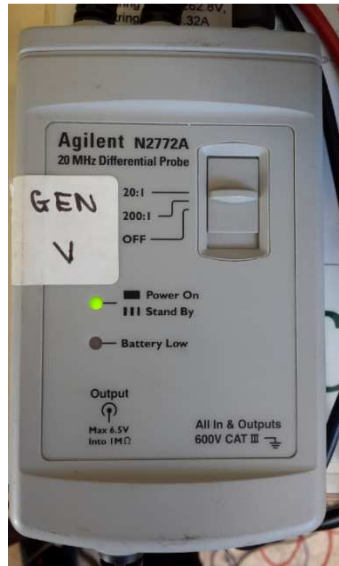


Figure 8.18 Voltage probe

The instruments that have been used to measure the dimensions such as AC voltage, DC voltage, AC current and DC current were voltage or current probes. These devices allow the measurement of high dimensions, by reducing their output according to a known voltage ratio. The output of these probes is always a voltage that follows all the variations of the actual dimension. For the voltage probe the Agilent N2772A has been used: it wasn't a self-supplied probe, hence it needed an external supply because it doesn't take power from the measured circuit. It allowed a maximum voltage ratio of 200:1, and since the maximum output was 6.5V, this device could have represented a voltage dimension up to  $6.5 \times 200 = 1300V$



Figure 8.19 Current probe

The current probe that has been used was the Agilent N2774A, and also this needed an external power supply. The probe had a rate of 0.1 V/A, which means that every A is represented with an output voltage of 0.1V. As can be seen the device can measure a current up to 15A and can follow variations up to 50MHz. There was an arrow sign in order to decide the positive direction of the current: both for the AC and the DC side, the directions that has been considered positive, was the one that allowed the charging of the battery, hence from AC to DC.

## 9 Relevant tests

### 9.1 Tests without a delay circuit and high resistance

In this section some tests are conducted in order to verify the correct operation of the charger. An initial explanation of the entire procedure is necessary: AC voltage with 50Vrms is supplied from the single-phase step down transformer, and this voltage is taken as reference for the PWM, once it has been scaled down. A reactor, whose value is nearly 280mH, follows the AC supply and connects the phase a of the converter while the phase b of the converter is directly connected to the second terminal of the transformer. On the DC side, going out from the positive terminal there is the DC Bus capacitor and then the inductor of the filter. After the inductor, there is the capacitor of the filter in parallel with the load. Here, after the LC filter, there should be the battery immediately but in this case a power resistor was used. The reason for this choice is explained hereby.

Ideally, with the PWM we have the firing signal for the switches: the comparison between the reference and the carrier, that is usually a periodic triangular signal, provides pulses that turn on and off the gates of the IGBTs. As long as only simulations are done this approach is enough, because every component is considered ideal and hence it doesn't have losses. However, in the reality, components aren't ideal and they are made of physical materials, which have inertia. If the IGBT receives a command to switch off, then the passage between collector and emitter starts closing. This means that the current conduction starts decreasing and the voltage between collector and emitter starts increasing:  $i_C(t)$  goes down and  $v_{CE}(t)$  goes up. But this process requires time and it doesn't happen immediately. The switch can't be considered off if  $v_{CE}$  hasn't reached its nominal value yet, and if meanwhile the other switch of the same leg is switched on there is short circuit in the leg.

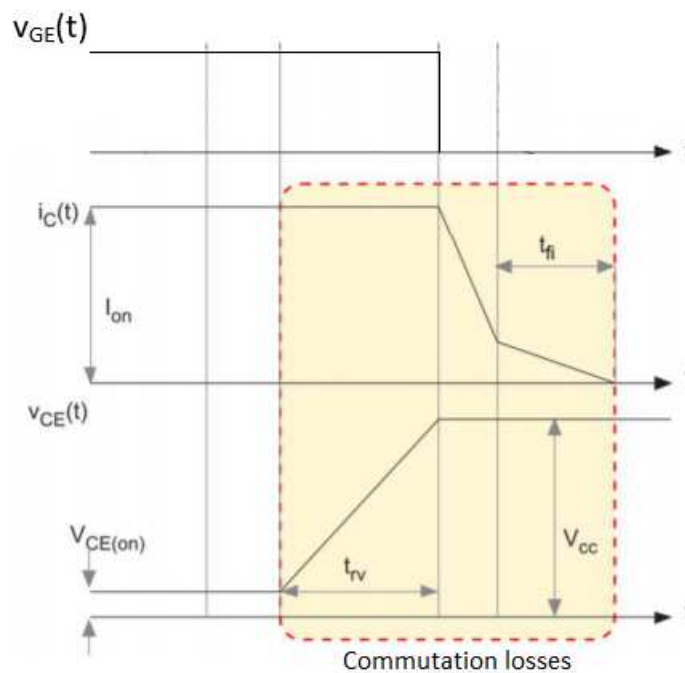


Figure 9.1 Switching off of an IGBT [19]

This is called commutation of the IGBT and as can be seen it implies losses in the component due to the common presence of both the current and the voltage. In order to avoid the issue of continuous partial short circuits, a delay circuit should be employed but for the initial testes this hadn't been considered, given that the wires that connects the outputs of the driver circuit's channels to the gates of the IGBTs, have a minimal resistance, and the combination of these resistances with the internal capacitance of the IGBTs should provide a delay time constant. Therefore, the firing signal for the switches, the ones that were provided to their gates, are represented in the following figure.

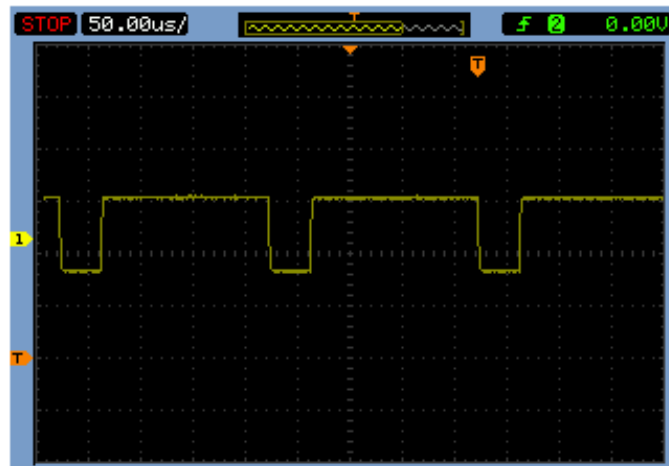


Figure 9.2 Firing signal of the IGBTs without delay

In this test a high current was observed when the power resistor hadn't been used. Initially the resistor was set to its maximum value, that is 100Ω, in order to ensure the safety of operation by verifying a reasonable current. Later the resistance has been set to roughly 8Ω in order to increase the current and consequently the power exchange. Another safety measure that has been adopted in this experiment was the reactor itself. The large value of the reactance limits the current by increasing the impedance. Since the reactance stays in the denominator of the following expressions, if it is high, it limits the power exchange.

$$P \cong 3 \frac{V_{grid} V_{qinv}}{X}; \quad (9.1)$$

$$Q \cong 3 V_{grid} \frac{(V_{dinv} - V_{grid})}{X}. \quad (9.2)$$

Moreover, since any DC/DC converter hasn't been used there isn't any possibility to have an independent reactive power exchange.

In this test we are going to control the active power exchange, between the charger and the battery starting from a negative value and increasing until the maximum positive value. After this, we are going to control down the power exchange to a negative value again. A test time of 50s is employed. A quick response and a stable power exchange are what we want.

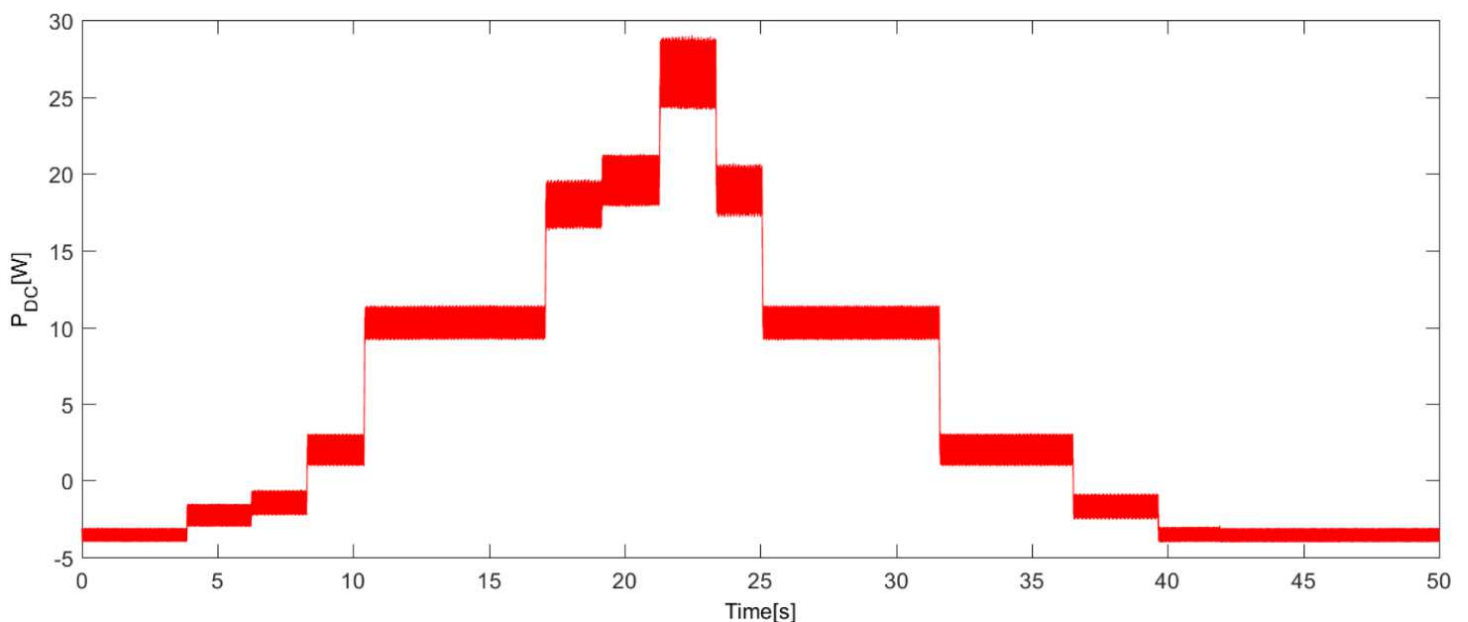


Figure 9.3 Active power exchanged with the battery with a variable reference

As can be seen the power exchange starts from nearly -4W which means that the battery is discharging towards the grid. The next steps lead to lower discharging rates, such as -3 and -2W. This shows how the power exchange is actually controlled through the related slider, and it's not self-discharge. Further increments bring to values like 3W and 10W going towards the maximum value that is 27W. After this value has been reached the reference is decreased and it goes back to, initially nil and after negative values; different steps are undertaken in this phase and eventually the initial situation is reached, that was a discharge rate of -4W. The system is reacting properly and the response is fast. The variations are almost straight lines, thus, the rise time is negligible. However, there is a slight ripple, which is initially low, when the battery is discharging, then increases. The maximum value of the ripple is

$p_{ripple-pk-pk} = 28.8 - 24.5 = 4.3V$  that is  $p_{ripple\%} = \frac{(4.3/2)}{29} * 100\% = 7.41\%$ . This is slightly higher than the desired value which was 5%. The main reason for this is the high ripple of the current, which can be observed hereafter.

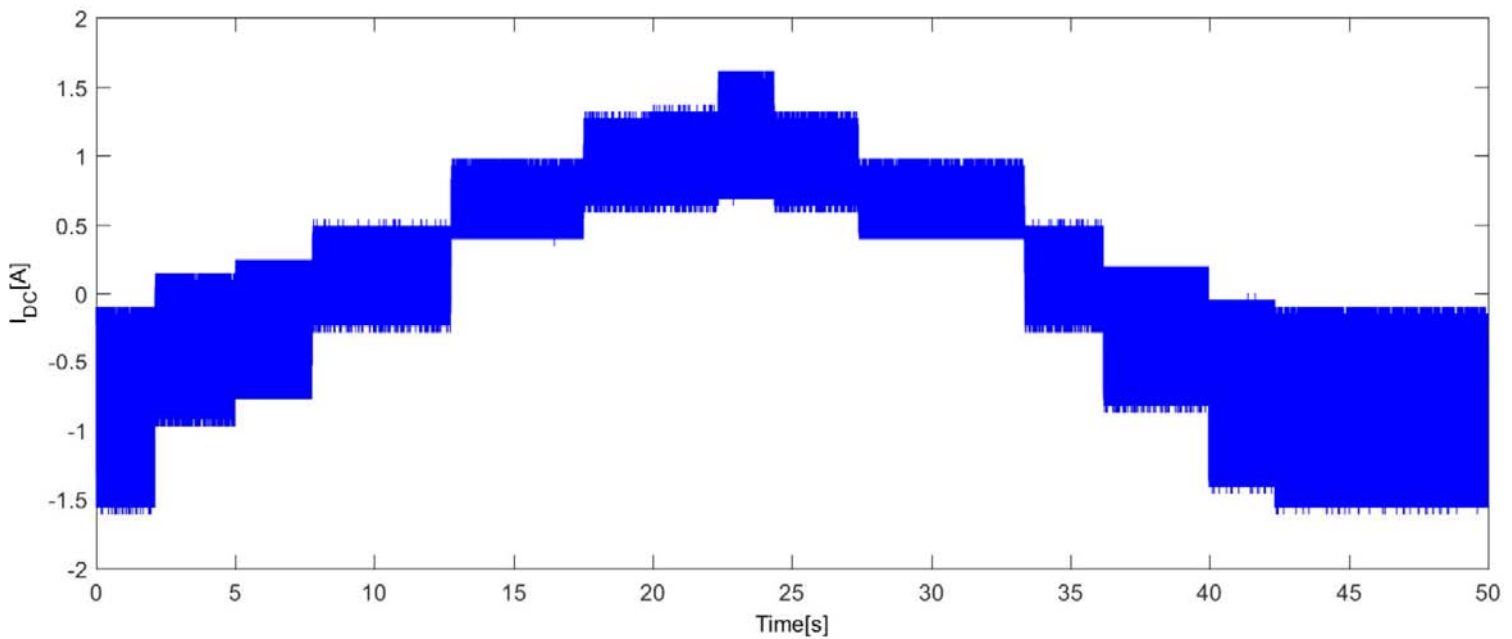


Figure 9.4 DC current exchanged with the battery

As can be seen the current changes with the power reference: when the reference is increased, the average value of the current goes up whereas, when the reference is controlled down, the average value of the DC current decreases. Here, a bigger ripple is observed when the current is negative, and a smaller one when it goes to positive values. Initially the current is completely negative, with the whole waveform, in the next step the average value stays negative, and from the fourth step is positive. This matches the same steps of the power. The maximum ripple for the current is  $i_{ripple-pk-pk} = -(-1.55) - 0.15 = 1.4A$ . The percentage relative current ripple is 43.25% of the maximum value. This is not a correct behaviour, and the reason can be a not enough large inductor or the control method. Higher is the inductance and lower the current ripple is, but, increasing the filter inductor's size means increasing the time constant of the LC circuit that leads to a longer oscillation and a slower system. As far as the control approach is considered, a wrong positioning of the two poles of the controller can cause oscillations and instability. This is done when approximate values have been selected for the constants  $K_p$ ,  $K_i$ ,  $K_D$ , but in order to choose them accurately, the transfer function of the whole system has to be known and this is often impractical. Specifically, in our case, four controllers have been used, in the simulated model, where those referred to the DC/DC control were located after those referred to the AC/DC control. This complicates the entire design procedure.

In the following figure the DC voltage supplied by the converter can be observed: this measurement has been taken at the DC terminals of the converter which corresponds to the terminals of the DC bus capacitor. This means that, the voltage at the terminals of the DC bus capacitor has been measured.

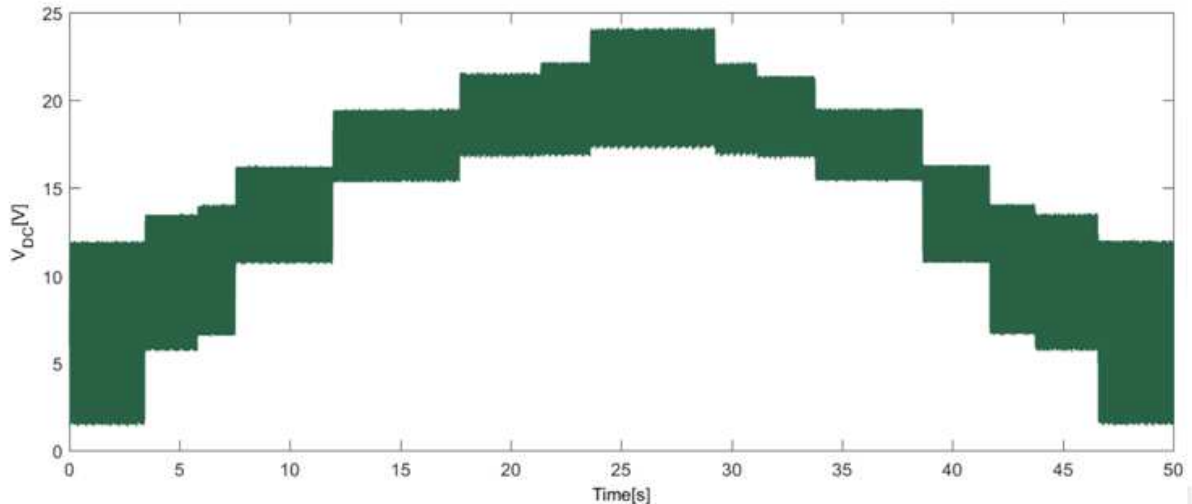


Figure 9.5 DC voltage of the charger

The voltage provided by the controller changes with the power exchange, and this is the main consequence of the absence of a DC/DC controller. In fact, if the voltage changes with the power exchange this affects the stability of the whole system, specifically for the DC side where the battery is located. This is not the ideal situation for operating with a battery. The maximum voltage provided on the DC side was lower than 24V that is quite reasonable, considering that the huge reactor in the AC side causes high power dissipation. Also here a significant ripple is observed, and the maximum value is observed when the power exchange is negative. This might be due to a not enough high size of the DC bus capacitor, that creates instability and doesn't absorb the oscillations, but increasing this value means increasing the current absorbed by the capacitor, which will be initially subtracted by the current provided by the converter, and a longer transient for the charging of the capacitor. The maximum value of the ripple is  $v_{ripple-pk-pk} = 12.8 - 1.5 = 11.3V$ . The percentage relative voltage ripple is 23.5% of the maximum value. This is not acceptable and a larger capacitor is suggested for the DC bus.

## 9.2 Tests with a delay circuit

### 9.2.1 Test with high resistance

During the previous tests, when the battery wasn't protected by any resistor, we experienced a huge current that ultimately burnt some of the IGBTs. This was due to partial short circuits happening when one IGBT has to be switched off and the other, from the same leg, has to be switched on. Because of the dead time required by IGBTs to switch off, for a fraction of the switching period, both the IGBTs of one leg were switched on, and this resulted in a short circuit which led to the huge current. The immediate and not so clever solution was to limit the current somehow and therefore, a power resistor was placed in the output of the DC/DC converter in order to increase the resistance on the DC side. In the previous chapter, a solution for this issue was explained and this was a delay circuit. Basically, we have to delay the firing of one IGBT in order to let the previous one switch off. Another requirement that is as important as the previous, is that, the shutdown of one IGBT doesn't have to be delayed, otherwise the two delays would make each other worthless. With the following circuit this operation is possible and this allows us to operate with the single phase bridge without any problem.

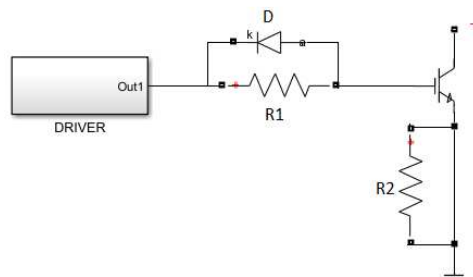


Figure 9.6 the delay circuit

The gate of an IGBT can be considered as a capacitor, that has to be charged in order to allow the current conduction between collector and emitter. The internal capacitance of the IGBTs that have been used was about  $c_{ies} = 2600pF = 2.6nF$ . The resistor connected in series creates along with this capacitance a delay time constant  $RC$ , that depends on the value of the resistance and also how much delay we want to have. A behaviour similar to the charging of a capacitor will be observed, and this waveform will need as much time to reach the steady state value as fixed by the time constant. Now, the falling time of the IGBT is  $t_f=120ns$ , so in order to ensure a correct operation, without short circuits, the delay time constant has to be greater than this value. The resistance that has been chosen is about  $R=1k\Omega$  that causes a total delay time constant of  $RC=2.6\mu s$  which is more than enough to let the previous IGBT switch off. One consequence that needs to be pointed are the losses related to the resistance. The presence of the resistance means losses, hence, the reached steady state value will be lower than the supplied one. This is acceptable if a higher voltage is provided. However, let's not forget about the other requirement, that was an instantaneous switch off. This task is accomplished by the diode which ensures and immediate "discharge" of the "capacity" because the current finds less resistance in its edge, hence the delay time constant isn't involved. The value chosen for the resistance  $R_2$  is  $10k\Omega$ . This circuit has been built before the gate of every IGBT.

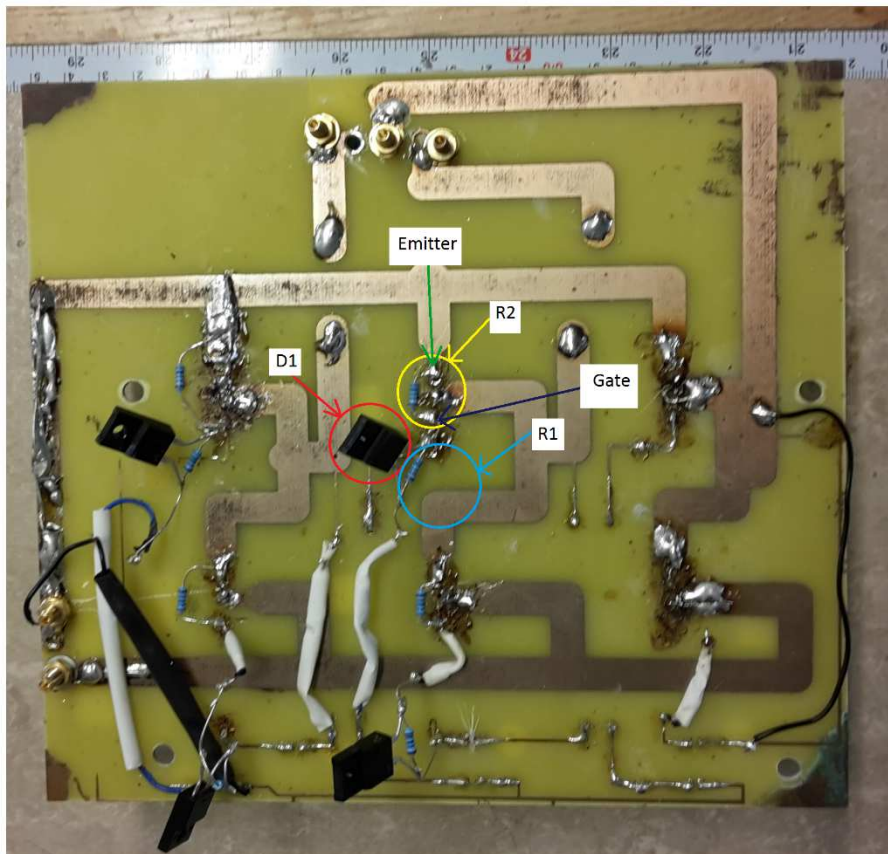


Figure 9.7 The modified board with the delay circuit

The result is observed in the oscilloscope and is the following:

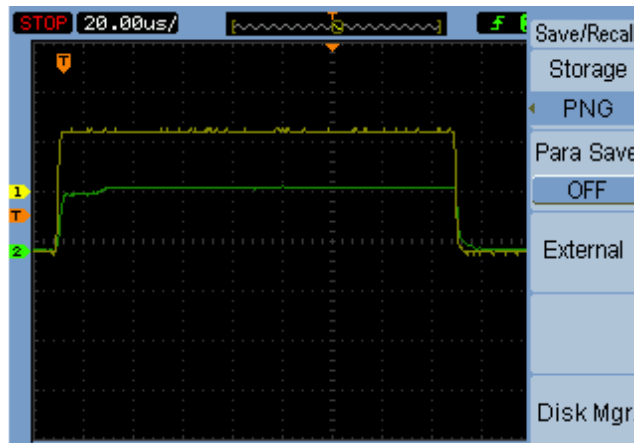


Figure 9.8 Delayed firing signal

The yellow track represents the signal as its supplied by the Driver board, whilst the green signal represents the delayed signal. As can be seen the steady state value is much lower, but a slight delay can already be observed from now on the rising edge whereas in the falling edge no such delay is noticeable. Since the time scale of  $20\mu\text{s}/\text{div}$  is yet large, a zooming of the rising edge is depicted in the following figure with a time scale of  $5\mu\text{s}/\text{div}$ .

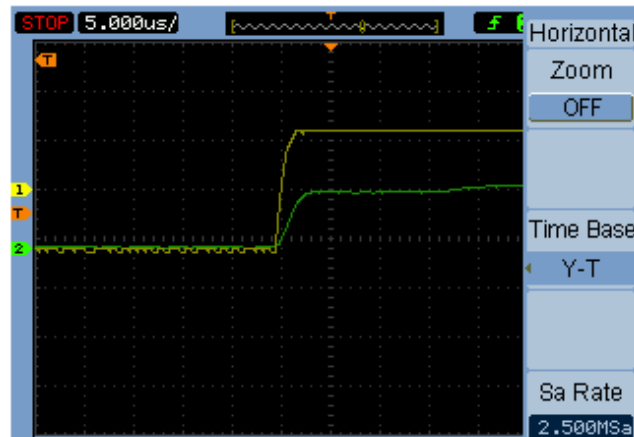


Figure 9.9 Zoom of the delayed firing signal with  $5\mu\text{s}/\text{div}$

If one division represents  $5\mu\text{s}$  then the green track needs roughly half of a division to reach the steady state value; this is nearly a delay of  $2.6\mu\text{s}$ . This delay has been applied to every pulse in the train, in fact, in the following figure some pulses are represented.

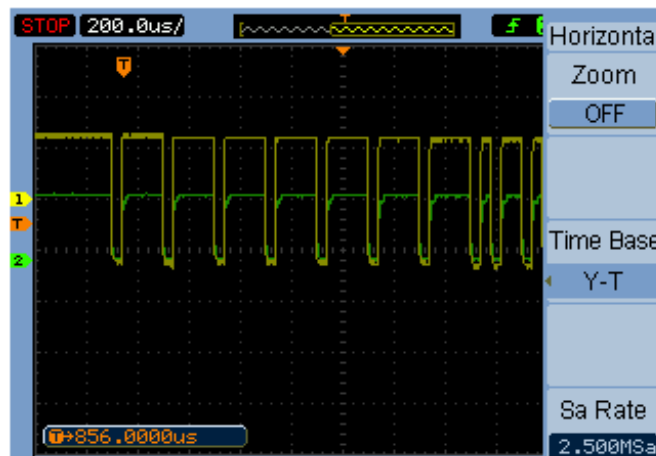


Figure 9.10 Train of delayed pulses

The first thing that is noticed is that the width of the pulses changes from bigger to smaller values: this means the amplitude of the fundamental that underlies this signal is decreasing. This is the SPWM. Despite of the large time scale of  $200\mu\text{s}$  in some pulses the delay is still noticeable.

In the following test, the issue of partial short circuits should have been sorted out, hence, safety measures wouldn't be necessary. However, in order to prevent the IGBTs from burning, because of a high current, in a first instance, the resistance at the DC output has been kept high. Roughly  $100\Omega$  is the value of the power resistor. This means that the current is small and so is the power exchanged. The mean value of the DC power is represented hereafter: the dimension that is depicted, is the average value of the power calculated through a dedicated Discrete Mean Value block, thus, it's free from any ripple.

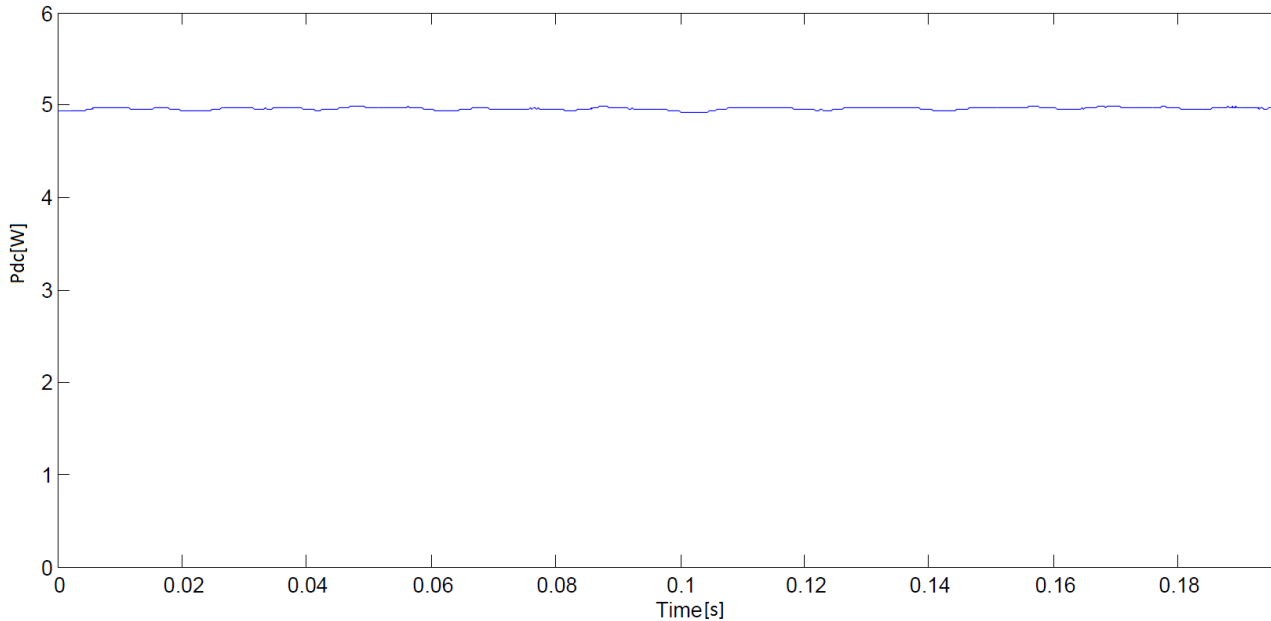


Figure 9.11 Average value of the power exchanged with the battery

As can be seen the power exchange is pretty stable except a shallow oscillation, but this is because the mean value has been represented. The small power exchange is due to the high resistance, in fact, the DC current is really small:

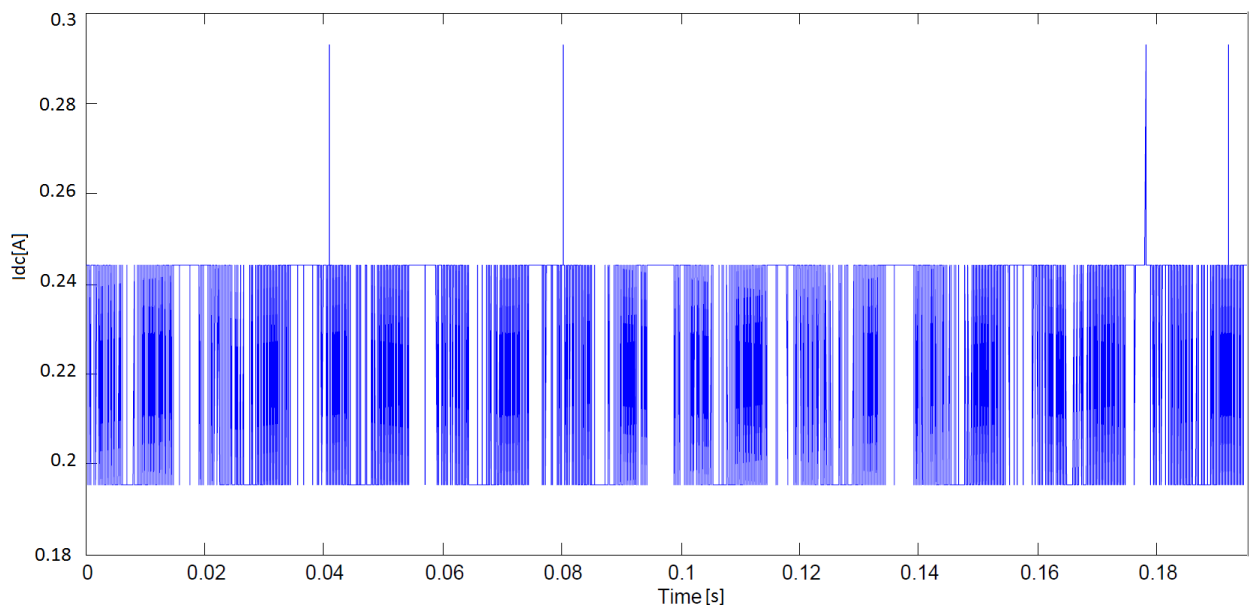


Figure 9.12 DC current feeding the battery



The DC current is small; the average value is approximately 0.22A, whereas the value of the ripple is

$i_{ripple} = \frac{0.245 - 0.195}{2} = 0.025A$  that is roughly 10% of the maximum value. This is acceptable but for a more efficient operation this value should be less than 5%.

Now it's time to have a look at the Battery voltage which is depicted in the next figure. Since there is a positive power exchange, which means the battery is charging supplied from the grid, the voltage of the battery has to increase from the nominal value.

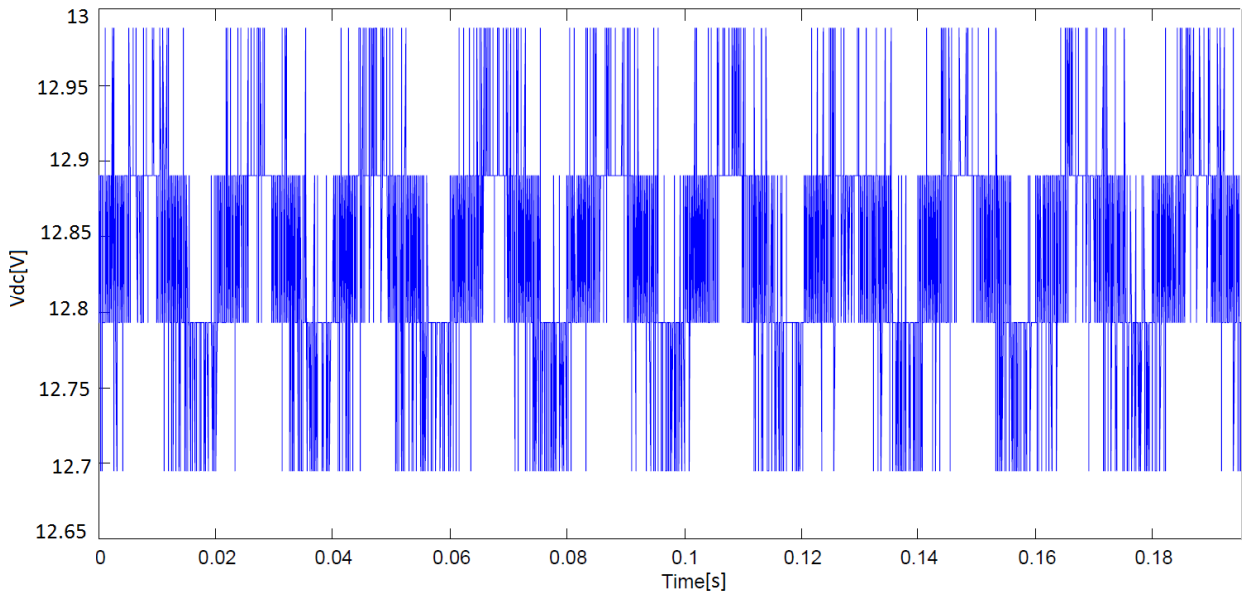


Figure 9.13 Voltage of the battery

And this is exactly what has happened: from a nominal value of 12V, now the voltage of the battery is 12.85V in average, which results in a 0.85V of growth. There is obviously a ripple and the value is:  $v_{ripple} = \frac{12.99 - 12.69}{2} = 0.15V$  that is the 1.15% of the maximum value. This is a reasonable value for the ripple and the reason for such a good shape is the DC filter which has been able to remove the unwanted oscillations. Another feature to be noticed is the periodicity of the waveform: the simulation time was of 200ms, and a periodic oscillation that repeats ten times is observed. This means that, underneath, there is yet the fundamental component of the voltage supplied by the charger.

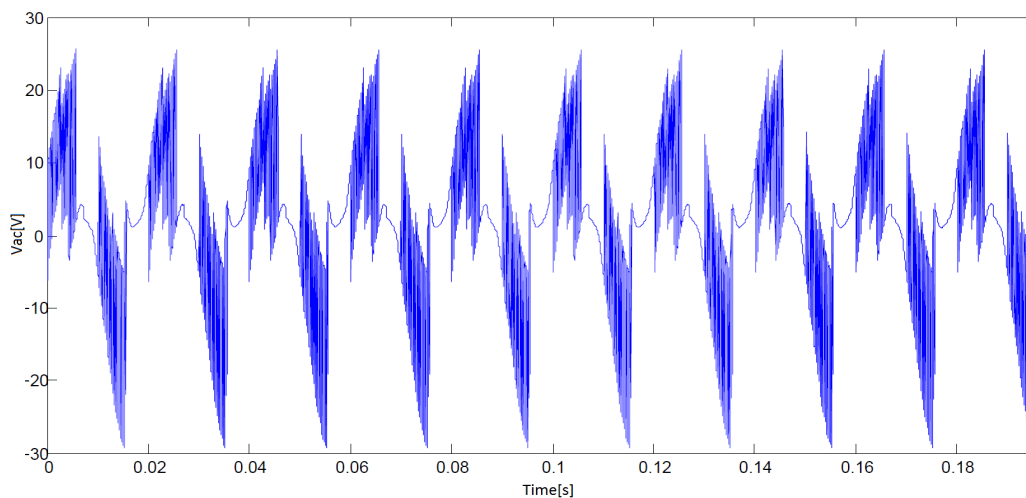


Figure 9.14 AC voltage of the converter

Figure 9.14, in the previous page represents the alternating voltage developed by the charger on the AC side. The periodicity is observed again: there are ten periods in a total frame of 200ms, which means the period is of 20ms. But the main issue with this waveform is the heavy distortion. The waveform is alternating and periodic and the shape reminds the one of the sinusoidal form, but there are a lot of harmonics. In fact, electronic converters introduce harmonics in the grid due to the continuous switching. These increase the  $THD_V$  (Total Harmonic Distortion<sub>VOLTAGE</sub>) provided by the converter.

$$THD_V = 100\% \frac{V_{dis}}{V_1} = 100\% \frac{\sqrt{V_d^2 - V_1^2}}{V_1} = 100\% \sqrt{\sum_{K \neq 1}^{\infty} \left(\frac{V_K}{V_1}\right)^2}; \quad (9.3)$$

Harmonics cause instability in the grid and voltage fluctuation. A solution is represented by an **AC filter** that eliminates or reduces the harmonic introduced towards the grid. This will be explained in the conclusions.

Now, let's conclude this test with the alternating current that flows in the AC link from the grid towards the charger. This current is measured after the reactor, hence, it's the current that feeds the AC/DC converter.

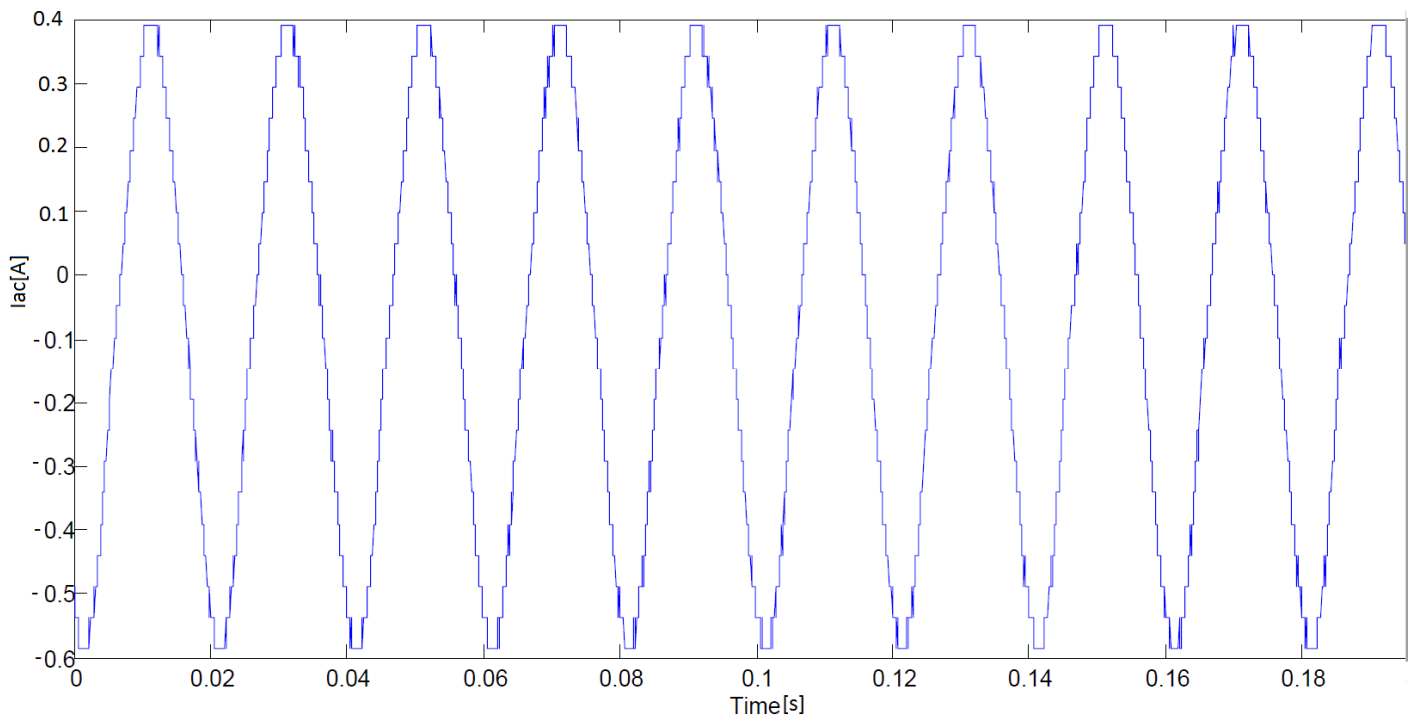


Figure 9.15 AC current feeding the charger

A better shape is seen here, in fact, it's the sinusoidal form; the square shaped variations are only due to a low accuracy of the sampler. This makes us suppose that the  $THD_I$ , which represents the current distortion introduced towards the grid by the AC/DC converter, is low. The expression for the  $THD_I$  doesn't change from the one referred to the voltage: it's the ratio between the RMS value of the distortion contained in the waveform and the RMS value of the fundamental.

$$THD_I = 100\% \frac{I_{dis}}{I_1} = 100\% \frac{\sqrt{I_d^2 - I_1^2}}{I_1} = 100\% \sqrt{\sum_{K \neq 1}^{\infty} \left(\frac{I_K}{I_1}\right)^2}; \quad (9.4)$$

### 9.2.2 Test with low resistance

In this last section, tests with low resistance are reported. With low resistance we refer to the power resistor located at the output of the DC filter. The cursor of the resistor had been dragged to the bottom point, in order to ensure a value of the resistance close to nil. However, the resistor hadn't been taken off from the circuit, again as an extra safety measure; we will assume a nil value.

In this test the power exchange has been controller from a minimum value to a maximum one and brought back to a minimum again. Unlike the experiment without the delay circuit, here, an inversion of the power flow hasn't been archived. In the following figure, the active power exchanged between charger and battery is depicted.

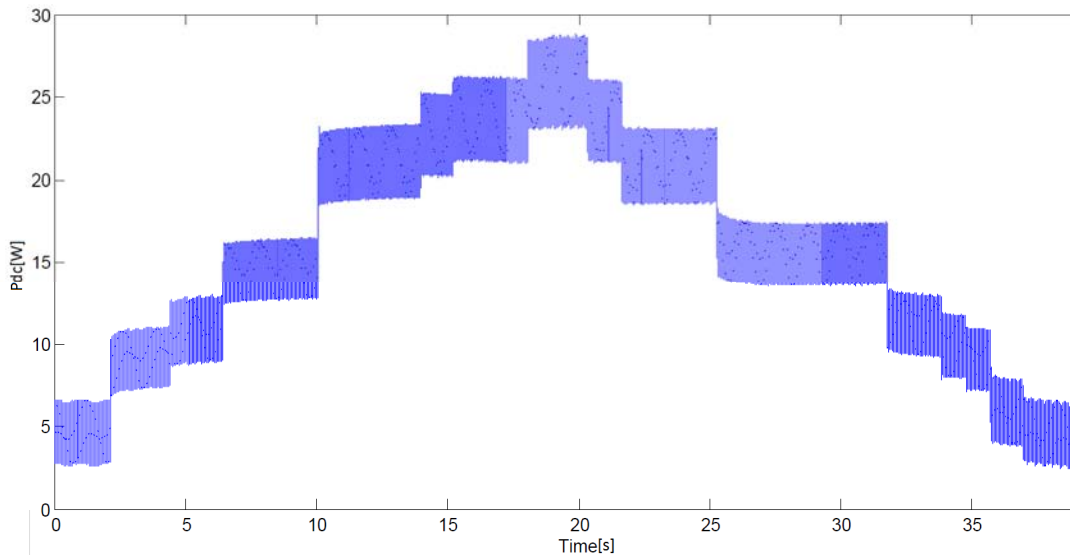


Figure 9.16 Active power exchanged with the battery

The power exchange is controlled, starting from 5W on average to the maximum value of nearly 27W on average. A significant ripple is observed, and it's more evident specifically for high values of power exchange. The maximum value of the ripple is:  $p_{ripple} = \frac{28-22.5}{2} \cong 2.75W$  that is the 9.8% of the maximum value. It's yet not acceptable given that, in the previous case without a delay circuit the percentage ripple was about 7.41%. Again the main reason is the high ripple of the DC current.

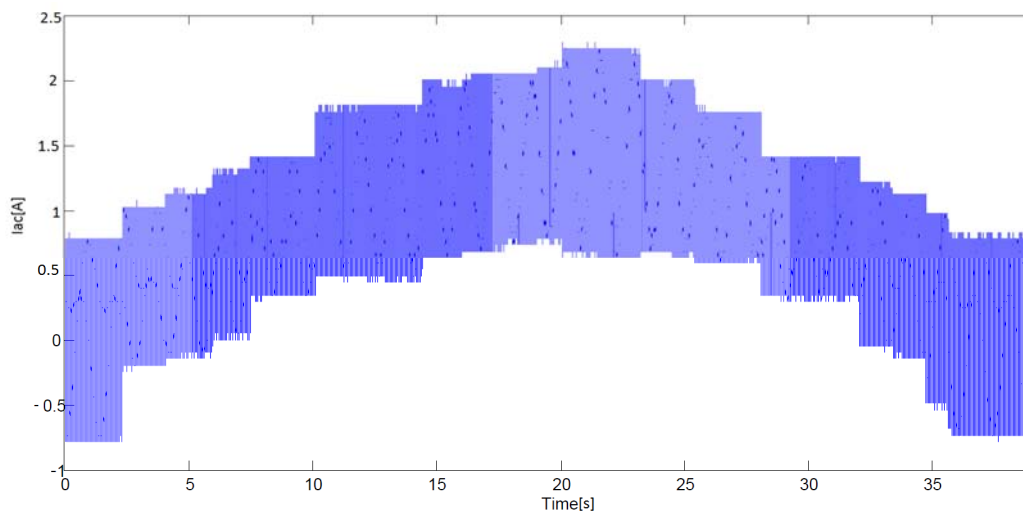
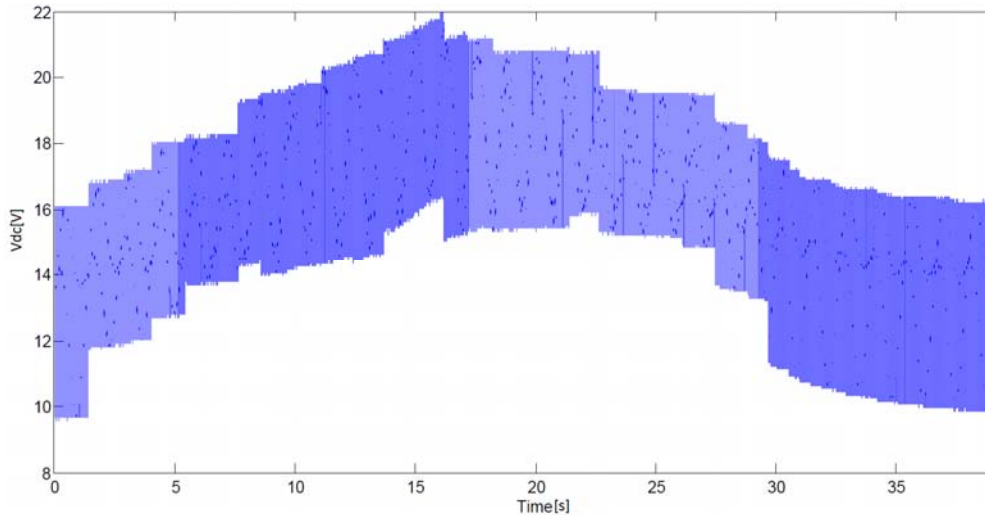


Figure 9.17 DC current feeding the battery

In *Figure 9.17* reported in the previous page the DC current exchanged with the battery is depicted. The current is controlled from a low value to a higher one in order to increase the power exchange and then, again to a low value to decrease the power exchange. The current starts from a positive value on average, though the actual value reaches negative values because of the ripple. The ripple is high initially, and slightly decrease as soon as the current is increased. The value of the ripple is  $i_{ripple} = \frac{0.75 - (-0.75)}{2} = 0.75A$  that represents the 34% of the maximum value reached that is 2.2A. This is absolutely not acceptable, hence, as a first action the size of the filter inductor has to be increased.

In the following figure the DC voltage supplied by the converter is represented: this is the voltage at the DC Bus so the DC Bus capacitor's voltage.



*Figure 9.18 DC voltage of the charger*

Again the lack of a DC/DC controller is felt: with the power exchange, the voltage at the DC bus is seen changing and this affects the power exchange. We want a stable value that will buffer any oscillation. The voltage is seen increasing with the power exchange and a high ripple is observed. The ripple is bigger at the minimum values of the voltage and decreases as soon as the voltage increases. The value of the voltage ripple is  $v_{ripple} = \frac{16-9}{2} \cong 3.5V$  that is nearly the 16% of the maximum value reached which is 22V. This will harm the health of the battery both in terms of SOH and internal resistance. A DC/DC controller is strongly recommended as well as a larger capacitor for the DC bus.

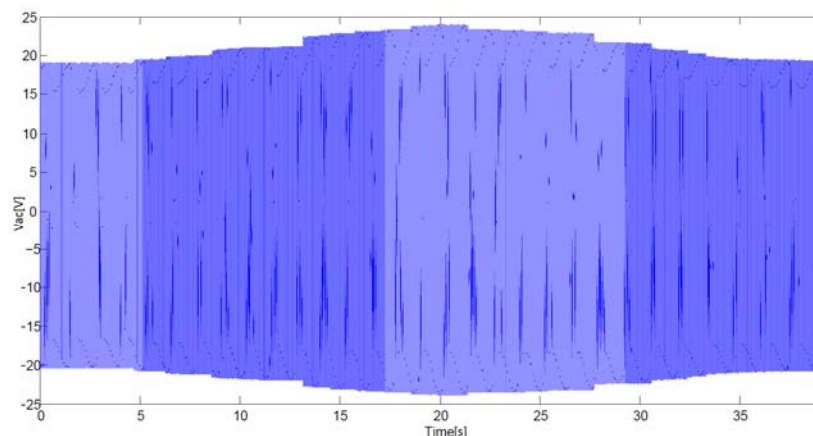


*Figure 9.19 AC voltage of the charger*

In the last figure the alternating voltage on the AC side of the converter is represented. The peak value of this voltage increases with the power exchange up to 24V. This is an alternating voltage, in fact the behaviour is symmetric in regards of the zero line.

## Conclusions

The realization of a bidirectional charger has been conducted in the dissertation, both from a theoretical and practical point of view. The charger has been designed, simulated, practically realized and tested. The initial framing explained what the current technologies regarding V2G are and where the work that has been produced, can be collocated. The location is after the smart high level charger, which provides the references after the optimization process. After this stage, the presented controller imposes the predefined references and makes the charger establish the right power exchange between grid and battery. The control approach has been designed and tailored to the design specifications. The Simulink model has been designed which consists of the grid model, the AC/DC converter, the DC/DC converter, the DC bus capacitor, the LC filter and the battery model. The design of the single elements has been conducted. Simulations initially against a fixed reference and after a variable reference have been done and the results have shown that the charger is able to chase predefined references.

A physical bidirectional charger that consists of only an AC/DC converter has been built and tested. Extra components such as DC bus capacitor and the LC filter have been designed and connected, along with a reactor and for some of the tests, a delay circuit. The device successfully interacted with the dSPACE board which supplied the firing signals. A satisfyingly accurate firing signal, result of the SPWM, has been supplied to the IGBTs. The power exchange between the charger and the battery has been monitored and reversed in order to prove the concept of V2G. This work has proven how a low level controller can actually be implemented and included in V2G operations in order to support the grid by establishing bidirectional power flow.

An improved control strategy is the next step: a prediction about the transfer function of the whole system is necessary in order to apply the proper controller, and not empirically assigning the constants of a PID controller. This will allow a more effective power transmission, without the significant ripples that have been noticed. A deeper study on the DC bus capacitor and its size as well as the LC filter is also necessary. The addition of an AC filter will eliminate the harmonics introduced by the charger towards the grid, hence, further studies on this topic need to be conducted, both for the simulations and for the practical tests.

In practical, the lack of a DC/DC converter has been perceived because no reactive power exchange has been registered. The next step will be, to include a converter that regulates the voltage of the DC bus in order to make the reactive power exchange independent from the active power exchange. More investigations on the delay circuit are necessary.

The V2G operation is an innovative technology and research on this topic have just started. Though, studies on how to mitigate the effect of an uncontrolled charging of EVs are not strictly urgent in the current situation, the realistic prediction of a huge deployment of EVs in the next future makes this a hot topic and the urgency is therefore felt. This study has proven how a possible V2G architecture might imply huge investments, in order to install the required information network, but it's absolutely necessary in order to prevent electrical disasters in the grid once the EVs will be highly deployed. The innovative idea of the efficient distribution of Renewable Energies' productions with the help of V2G has also be mentioned.

V2G represents innovation, efficiency, sustainability and because of all these reasons is the future.

## References

- [1] N. Mohan, T.M. Undeland, W. P. Robbins, "Elettronica di potenza", HOEPLI, 3<sup>rd</sup> Edition, 2014;
- [2] T. Jiang, G. Putrus, Z Gao, M. Conti, S. McDonald, G. Lacey, "Development of a decentralized smart charge controller for electric vehicles", Elsevier, "ELECTRICAL POWER & ENERGY SYSTEMS", April 2014;
- [3] M. Andriollo, "Inverter DC/AC a commutazione: DC-AC sinusoidale", 2014;
- [4] M. Andriollo, "Convertitori DC-DC a commutazione", 2014;
- [5] M. Andriollo, "Applicazioni per le reti elettriche", 2015;
- [6] G. Buja, "Hybrid Electric Vehicles", 2014;
- [7] B. Yagcitezkin, M. Uzunoglu, "A double-layer smart charging strategy of electric vehicles taking routing and charge scheduling into account", Elsevier, "Applied Energy", September 2015;
- [8] S. Habib, M. Kamran, U. Rashid, "Impact analysis of vehicle-to-grid technology and charging strategies of electric vehicles on distribution networks- A review", Elsevier, "Journal of POWER SOURCES", December 2014;
- [9] J. Garcia-Villalobos, I. Zamora, J.I. San Martín, F.J. Asensio, V. Apperibay, "Plug-in electric vehicles in electric distribution networks: A review of smart charging approaches", Elsevier, "Renewable and Sustainable Energy Reviews", July 2014;
- [10] A. Dinger, R. Martin, X. Mosquet, M. Rabl, D. Rizoulis, M. Russo, G. Sticher, "Batteries for Electric Cars- Challenge, Opportunities, and the Outlook to 2020", The Boston Consulting Group, 2010;
- [11] D. Sbordone, I. Bertini, B. Di Pietra, M.C. Falvo, A. Genovese, L. Martirano, "EV fast charging stations and energy storage technologies: A real implementation in the smart micro grid paradigm", Elsevier, "ELECTRIC POWER SYSTEM RESEARCH", August 2014;
- [12] K. De Branbadere, J. Van den Keybus, R. Belmans, "A Voltage and Frequency Droop Control Method for Parallel Inverters", IEEE TRANSACTIONS ON POWER ELECTRONICS, VOL. 22, NO. 4, July 2007;
- [13] F. Musavi, W. G. Dunford, "Evaluation and Efficiency Comparison of Front End AC-DC Plug-in Hybrid Charger Topologies", IEEE TRANSACTIONS ON SMART GRID, VOL. 3, NO. 1, March 2012;
- [14] L. Jian, X Zhu, Z. Shao, S. Niu, C.C. Chan, "A scenario of vehicle-to-grid implementation and its double-layer optimal charging strategy for minimizing load variance within regional smart grids", Elsevier, "Energy Conversion AND Management", December 2013;
- [15] Y. Ota, H Taniguchi, J. Baba, A. Yokoyama, "Implementation of autonomous distributed V2G to electric vehicle and DC charging system", Elsevier, "ELECTRIC POWER SYSTEM RESEARCH", June 2014;
- [16] J. Y. Yong, V. K. Ramachandranurthy, K. M. Tan, N. Mithulananthan, "Bi-directional electric vehicle fast charging station with novel reactive power compensation for voltage regulation", Elsevier, "ELECTRICAL POWER & ENERGY SYSTEMS", August 2014;
- [17] Y. Luo, T. Zhu, S. Wan, S. Zhang, K. Li, "Optimal charging scheduling for large-scale EV (electric vehicle) deployment based on the interaction of the smart-grid and intelligent-transport systems", Elsevier, "ENERGY-The International Journal", January 2016
- [18] A. Dubey, S. Santoso, M. P. Cloud, "Average-Value Model of Electric Vehicle Chargers", IEEE TRANSACTIONS ON SMART GRID, VOL. 4, NO. 3, September 2013;
- [19] M. Andriollo, "Panoramica sui dispositivi semiconduttori di potenza", 2015